Wildfire modelling and impacts on carbon cycle, climate, and vegetation distribution induced by climate change

Submitted by Chao Wu to the University of Exeter
as a thesis for the degree of
Doctor of Philosophy in Geography
In April 2019, to be jointly awarded by the University of Exeter and Tsinghua University

I certify that all material in this thesis which is not my own work has been identified and that no material has previously been submitted and approved for the award of a degree by this or any other University.

Signature: ……..

Abstract

Wildfire is a natural and unavoidable feature of the environment in many terrestrial ecosystems and has a strong influence on global ecosystem patterns and processes, including vegetation distribution and structure, the carbon cycle, and climate. However, as illustrated in recent studies, fire is a risk to human societies, emits atmospheric pollutants, and causes death and damage to homes and businesses. Fire regimes have been altered by complex interactions among climate change, anthropogenic activities, and biome community changes and are predicted to change further with global warming, population growth, and urbanization. Therefore, the frequency and spatial distribution of wildfires, along with their drivers of recent trends, requires better understanding to enable robust future predictions. Many studies have had a central focus on the interactions between the carbon cycle and climate. However, as an important component in modulating future climate change, the climate-carbon feedback derived from changing fires is poorly understood.

Here, we develop a fully coupled climate-vegetation-carbon-fire framework and perform simulations to investigate global Burnt Area (BA) trends and their drivers, climate-carbon feedbacks derived from changing fires, and the role of fire on the global carbon cycle. Meanwhile, the individual contribution of fire and climate on regional vegetation distribution is assessed using models, remote sensing technology and statistics.

The main results and conclusions are provided below:

(1) Global BA has decreased, and this is reproduced well in our simulation framework, capturing recent climate and human limits of change. Global BA will increase under climate change, rapid population growth and urbanization, and

this is especially through high latitude warming and increases in human-induced fires over the tropics and subtropics. However, urbanization will also offset the potential future large increases in BA by enhancing fire suppression capacities and management.

(2) Over the period 2005-2014, the carbon-cycle effect (i.e., caused via release of extra carbon into the atmosphere) of fire has increased the additional mean annual global land temperature by ~0.16 °C yr^{-1} relative to a world without fires. Future mean annual global fire carbon emissions will be sensitive to anthropogenic CO_2 emissions and human behaviour (2.2 to 3.0 PgC yr^{-1}), providing an approximate increasing mean annual atmospheric CO_2 concentration of 15-22 ppm yr^{-1} and global land-mean warming of 0.13 to 0.18 °C yr^{-1} over the period 2081-2100, with warming being greatest at high latitudes. However, although the largest impact of fire on atmospheric CO_2 concentrations is associated with the more severe anthropogenic emissions scenarios, the associated fire-climate feedbacks on enhanced warming are the lowest under these scenarios.

(3) The vegetation distribution for the present day is mainly determined directly by climate (35%) rather than fire (1%-10.9%). However, global warming will change the balance between fire and climate in driving variations of boreal forest distribution under four global warming scenarios. With a future global warming of 1.5 °C, the fire control on local vegetation composition will grow to exceed that of climate (36.3% > 29.3%). Above a 1.5 °C warming, temperature will be more important than fires in regulating vegetation distribution, although other factors like precipitation will also contribute.

Our analysis will help to develop wildfire management strategies in conditions of different possible future socioeconomic development pathways, to

assess future ecological changes, and to help inform adaptation and mitigation options to global climate change.

Acknowledgements

As a dual degree student between University of Exeter and Tsinghua University, I thank my amazing and distinguished supervisors, Professors Stephen Sitch, Lina M. Mercado, and Sergey Venevsky (Tsinghua University), from the deepest of my heart.

My Ph.D. study in University of Exeter under the supervision of Stephen and Lina really improves my research capacity, broadens my horizon, and lets me know what the best science is, although there is still long distance for me to get there. I really enjoy a lot working with them. Stephen not only helps me to conceive a bigger research topic, but only can help me coding hand by hand. After meeting with him, I always think that I leaned more than yesterday and really excited with that, he also creates all possibilities for me to improve my research, e.g., introduced me to the FireMIP group. After working with him, I have decided my future goal, that is to become a distinguished professor in my field. I really thank for him and my precious experience in UK. Similar to Stephen, Lina helps me a lot as well, I still remember that it is she that gives me the first Python mapping script, and based on that, I develop my Python coding skills and now I can plot any beautiful figures. It is not only for the science, Stephen and Lina always care me and help me a lot in the life. When I first came to Exeter, Stephen sent me many emails, what surprised me is that they are not about science but reminding me that there is a second-bicycle selling activity in the forum. I almost cannot believe such a great professor cares my life so much. During the Christmas, Stephen and Lina also invite me to their house to celebrate the Christmas with them, I really thank for that and do not feel lonely in the UK.

Surely, my opportunity to study in Exeter comes from Sergey, who brought me to Tsinghua University in the summer of 2013. Since then, luck and kindness from him accompany with me all the time. I cannot use simple words, especially in English to describe how he is important and amazing for me during my Ph.D. study in Tsinghua. He is the real supervisor who really cares my future. He provides me many first time in my life, e.g., first time going abroad, first time publication, even first time getting on the plane. During working with him, he just like my parents, and I learned what is carness and responsibility. And the most impressive things he told me are that never say you are not interested in something and never use emotion as a man. As his first Ph.D. student in China, I know he puts much time and expectation on me. He provides me every opportunity and chance for me if I like. For example, he threw me to UK and got the opportunity of working with Stephen.

I really thank Chris Huntingford very much, who helps me a lot on my recent interesting studies. As a famous scientist, not only he provides many important suggestions and knowledge on the bigger study, but he also teaches me many details, e.g., he told me how to write a good cover letter and a powerful response. I am so lucky to have the amazing study experiences with him.

I thank my colleagues in Tsinghua and Exeter. Felix Leung, who helps me a lot when I was in Exeter and shared me a lot both in science and in life. Menghui Wang and Hongshuai Chu are my most believable and reliable colleagues and friends. I have no any concerns if somethings come to them. We have many unbelievable memories both in research and life. I thank Chenxi Lu and Yukun Qian, these talented group colleagues. I also need to thank Wenyan Yang, who contributes much to the Tsinghua-Exeter dual degree programme.

I thank the funding from National Natural Science Foundation of China (31570475), China Scholarship Council, and College of Life and Environmental Sciences, University of Exeter.

Finally, I must thank my families. My dear parents from the deepest of my heart, who gave me extremely strong supports, providing me comfortable life, and warm and lovable home. They are the best, I hope them healthy, happy and accompany with me all the time. I thank my loved girlfriend from Peking University, Hongyan Zhan, who gave me continuous encouragement, strong support and unconditional trust. We have many unbelievable and wonderful memories. Hope that we will have a very bright future.

List of Contents

List of Tables

List of Figures

Abbreviations

BA	Burnt Area
CLM	Community Land Model
CMIP5	Coupled Model Intercomparison Project Phase 5
CO_2	Carbon dioxide
CRU	University of East Anglia Climate Research Unit
CTEM	Canadian Terrestrial Ecosystem Model
DGVM	Dynamic Global Vegetation Model
ESM	Earth System Model
FINAL	Fire Including Natural & Agricultural Lands model
FireMIP	Fire Model Intercomparison Project
GCM	General Circulation Model
GFED3	The third version of Global Fire Emissions Database
GFED4s	Global Fire Emissions Database version 4 product that includes small fires
GHGs	GreenHouse Gases
GLC2000	Global Land Cover 2000 Project
Glob-FIRM	GLOBal FIRe Model
GPP	Gross Primary Production
IMOGEN	Integrated Model Of Global Effects of climatic aNomalies
IPCC AR5	Intergovernmental Panel on Climate Change Fifth Assessment Report
JSBACH	Jena Scheme for Biosphere-Atmosphere Coupling in Hamburg
LMfire	Lausanne–Mainz fire model
LPJ	Lund–Potsdam–Jena
LPJ-GUESS	Lund–Potsdam–Jena General Ecosystem Simulator
MC-FIRE	MAPSS-CENTURY fire module
MEM	Moran's Eigenvector Map
Mha	Million hectare
NCAR	National Center for Atmospheric Research
NCEP	National Centers for Environmental Prediction

NEP	Net Ecosystem Production
NPP	Net Primary Production
O_3	ozone
ORCHIDEE	ORganizing Carbon and Hydrology In Dynamic EcosystEms
PCA	Principal Component Analysis
PFT	Plant Function Type
PFTC	Plant Function Types Coverages
PgC	Petagram of Carbon
ppm	parts per million
RCPs	Representative Concentration Pathways
RDA	Redundancy Analysis
REDD+	Reducing Emissions from Deforestation and. Degradation, plus the conservation and sustainable management of forests and enhancement of forest carbon stock (+)
Reg-FIRM	Regional FIRe Model
RH	Heterotrophic Respiration
SEVER-FIRE	Socio-Economic and natural Vegetation ExpeRimental global fire model
SIMFIRE	SIMple global fire model
SPITFIRE	SPread and InTensity of FIRE
SSPs	Shared Socioeconomic Pathways
VIF	Variance Inflation Factors
WDI	World Bank World Development Indicators

Chapter 1 Introduction

1.1 Background: fire in the Earth system

Earth is an intrinsically flammable planet because of its cover of carbon-rich vegetation (providing potential fuel load during burning), seasonal drought, abundant atmospheric oxygen, and globally distributed lightning and volcano ignitions (Bowman et al., 2009). Wildfire (or fire), defined as a fire in an area of flammable biome or ecosystem occurring in natural land, including multiple types, e.g., forest fire, grass fire, peatland fire, and it is a natural and unavoidable feature of the environment in many terrestrial ecosystems and has a strong influence on global ecosystem patterns and processes, including vegetation distribution and structure, the carbon cycle, and climate (Bowman et al., 2009, Veraverbeke et al., 2017).

Naturally burning fires are necessary for vegetation growth and regeneration, especially in savanna ecosystems (Bond and Keeley, 2005). Wildfire regulates vegetation patterns by controlling vegetation height, biomass accumulation and ecosystem function. However, as illustrated in recent studies, fire is a risk to human societies, emits atmospheric pollutants (van der Werf et al., 2017), and causes death and damage to homes and businesses (Bowman et al., 2009, Moritz et al., 2014). For example, wildfires occurred in many parts of the world in 2017, with extensive and severe fires occurring in Chile, the Mediterranean, Russia, the US, and Canada. Furthermore, the ‘camp fire’, the deadliest and most destructive wildfire in California history to date, occurred in the year 2018, causing extremely large economic losses and massive threats to human health. Therefore, it is of great practical importance to reproduce historical fire regimes,

investigate their drivers, evaluate their influences on ecosystems and feedback to climate system, and better predict future fire dynamics.

Satellite records show that the global Burnt Area (BA) from wildfires has declined significantly, by 24.3 ± 8.8%, over the past 18 years (Andela et al., 2017). However, large uncertainties exist in projecting future global BA trends and their spatial patterns (Moritz et al., 2012). Although multiple studies predict that indices of climatic fire risk and fire activity will increase in a warmer and often drier world (Kloster and Lasslop, 2017, Krawchuk et al., 2009, Pechony and Shindell, 2010), global BA is projected to decline under a moderate emission scenario when additional human influences are considered (Knorr et al., 2016). Better understanding of how both climate and direct human effects interact is required to provide improved projections of future BA. Currently, average global mean fire-induced carbon emissions were 2.2 PgC yr^{-1} during 1997–2016 based on satellite observation (van der Werf et al., 2017). However, fire regimes have been altered by complex interactions and uncertainties among climate change, anthropogenic activities, and biome community changes (Andela et al., 2017, Knorr et al., 2016), and are predicted to change further as global warming continues, populations grow, and urbanization progresses (Knorr et al., 2016, Pellegrini et al., 2018). Therefore, better understanding the future fire regimes, specific to fire emitted carbon will be essential to the future of global carbon cycle and the resulting feedback to climate.

Boreal forest, as one of the important flammable ecosystems in the world, occupies 30% of the global forest area (Gauthier et al., 2015). The vegetation structure and distribution are influenced by many factors. Climate is well known to be an important determinant of biogeography. Although climate is directly important for vegetation composition in boreal forests, these ecosystems are

strongly sensitive to indirect effects of climate via fire disturbances. However, the balance between fire disturbance and climate in driving composition is poorly understood. It is widely considered that climate, especially temperature and precipitation, directly controls the composition and distribution of vegetation (Scheiter and Higgins, 2009), hence vegetation classifications are mainly based on such climate variables (e.g., Holdridge Life Zones; Holdridge, 1947). Temperature impacts vegetation growth and distributions by changing the rates of photosynthesis and respiration, and regulating phenology, tissue growth, and regeneration and mortality processes (e.g., frost damage). Precipitation controls vegetation distributions by changing the water balance of the ecosystem (Stephenson, 1990). Although climate is undoubtedly an important driver in regulating vegetation structure, within a single climate zone, different combination of species can exist together, suggesting a decoupling of climate and vegetation, which means that other controls, e.g., fire in flammable ecosystems, are also important in determining the local vegetation composition within any biome (Murphy and Bowman, 2012, Scheffer et al., 2012). However, the relative individual contributions of fire and climate to the vegetation distribution and how the balance between these drivers might change with climate change remain unclear.

1.2 Fire regime modelling

1.2.1 Definition of fire regime

Fires burn with different intensities and frequencies, resulting in a wide variety of ecological effects (Bowman et al., 2009). To better describe this difference, the concept of ‘fire regime’ was introduced by ecologists on the basis of a range of variables, including fuel consumption and fire spread, as well as

frequency, fire season, intensity, and severity, (Bond and Keeley, 2005, Bowman et al., 2009). Different types of fire consume diverse fuel types. For example, surface fires mainly consume fuels which are close to the ground, such as grass or dead leaf and stem material, ground fires burn soil organic matter in the soil, and crown fires burn in the canopies of shrubs and trees (Bond and Keeley, 2005). Fire frequency is always described as fire rotation interval (the time required to burn the equivalent of a specified area) and fire return interval (the time interval between fires at any one site) (Bond and Keeley, 2005). Fire season is usually the driest time of the year, but this has been altered by human activities. Fire intensity describes the energy release, (e.g., fireline intensity) but is not easily quantified relative to fire severity. The latter is more important for determining the impact of fire on ecosystems, e.g., BA from fires and fire-emitted carbon to the atmosphere (Thonicke et al., 2010, Venevsky et al., 2002).

1.2.2 Global fire models

Fire plays an important role in the Earth system, and there is increasing concern about how fire regimes will change in response to projected climate changes in the 21st century (Hantson et al., 2016). Our capacity to predict future fire regimes and their interactions and feedbacks with vegetation, human societies and climate rely on fire models, using either well-founded empirical relationships or process-based descriptions (Hantson et al., 2016).

Dynamic Global Vegetation Models (DGVMs) and Earth System Models (ESMs) simulate vegetation dynamics at global scale. Fire is included as an explicit disturbance in some of these models (Arora and Boer, 2005, Li et al., 2013, Rabin et al., 2018, Thonicke et al., 2010, Thonicke et al., 2001, Venevsky et al., 2002, Yue et al., 2014). Given the importance of fires and their dependence on various model inputs or simulated processes, the development of fire modules

is of great importance and interest to better understand and evaluate fire-related couplings and feedbacks.

In order to comprehensively compare and evaluate existing global fire models against benchmark data sets for present-day and historical conditions, eleven state-of-the-art global fire models participated in the Fire Model Intercomparison Project (FireMIP), as summarized by Hantson et al. (2016). They divided the global fire models into four categories depending on the complexity of processes included in the models: (1) Simple statistically-based models that relate burnt areas with climate, vegetation (Glob-FIRM (Thonicke et al., 2001)), and/or human activities (Knorr et al., 2014); (2) Models estimating statistically number and expected size of fires (Pechony and Shindell, 2009). (3) Process-based quasi-mechanistic models that use functional relationships between climate, vegetation and socio-economic drivers of wildfires (MC-FIRE (Lenihan and Bachelet, 2015), CTEM fire module (Arora and Boer, 2005), CLM-fire module (Li et al., 2013), LM3-FINAL (Rabin et al., 2018) etc.). This approach was originally introduced by Reg-FIRM (Venevsky et al., 2002) and further developed in the follow-up model SPITFIRE (Thonicke et al., 2010) and its derivatives (JSBACH-SPITFIRE (Lasslop et al., 2014), LPJ-LMfire (Pfeiffer et al., 2013), LPJ-GUESS-SPITFIRE (Lehsten et al., 2009), and ORCHIDEE-SPITFIRE (Yue et al., 2014); and (4) Complete representation of all processes in space and time (first-principle approach model).

Although existing global fire models have been considered as the important tools to reproduce and predict the future potential fire dynamics, complete representation of all processes that determine wildfire dynamics in space and time remain a work in progress.

1.3 Drivers and limiting factors on fire dynamics

Fire dynamics is controlled by multiple factors. Climate, particularly temperature (T; °C) and precipitation (P; mm), is an important driver of fire activity, regulating vegetation productivity and fuel moisture (Bond and Keeley, 2005). Wind speed (W; m s^{-1}) also plays a key role in fire spread (Venevsky et al., 2002). However, in many cases, high climate-induced wildfire risks do not automatically lead to frequent fire occurrence (Knorr et al., 2016), indicating that other drivers should be considered. Currently, human activity is reported to be the primary source of ignitions in tropical forests, savannas, and agricultural regions (Aragão et al., 2008, Archibald et al., 2009). Human impacts on fire dynamics mainly depend on (1) population density (POP), and thus number of anthropogenic ignitions, (2) socioeconomic development (e.g., urbanization, described as the percentage of rural population to the total, RUR, as rural populations are major sources of pyrogenic activity and have more contact with flammable vegetation), and (3) fire suppression (determined by the distance to human settlements (cities), DIS; Andela et al., 2017, Venevsky et al., 2002). Continued global population growth could potentially lead to a similar increase in anthropogenic ignitions (Bistinas et al., 2014), but at the same time a greater concentration of people in cities and reduced rural population acts to decrease anthropogenic pyrogenic activity in both space and time. Urbanization increases the proximity of human settlements to potential wildfires and raises the requirements for wildfire suppression to avoid damage to the inhabitant's health and wealth. Better accessibility of natural vegetation due to the development of urbanized infrastructure results in an increase in potential human ignitions, but to a much smaller extent. Thus, population growth and urbanization are counteracting drivers for wildfires, and the overall effect of these human factors

on BA varies regionally and temporally. However, the dominant driver of change in fire dynamics, e.g., prediction of trends in future global BA, whether climate (Pechony and Shindell, 2010) or human driven (Knorr et al., 2016) or a combination is uncertain and controversial.

In addition, it is a challenging to project fire dynamics owing to the complex interactions among human societies, climate and vegetation (Andela et al., 2017, Wu et al., 2017). Given the interactions between climatic conditions and anthropogenic activities, a dominant limiting factor is defined as the factor that most limits changes in BA in a given location. For example, precipitation is an important driver of wildfire (generally, a driver is considered as an independent variable), regulating fuel moisture, and reduced precipitation implies an increase in fire risk, but this increase may not be realized without an ignition source (limiting factor). Therefore, to project future BA, the dominant drivers of wildfire (independent) and limiting factors (including interactive effects) on wildfire and their spatial patterns must be better understood, e.g., how these might alter under climate change and in parallel to any direct human intervention on fire ignition and/or suppression.

Other factors like lightning (Veraverbeke et al., 2017), CO_2 fertilization effects (Knorr et al., 2016), atmosphere, vegetation and fire regime interactions (e.g., vegetation with different susceptibility to fires impacts the local fire regime (Thonicke et al., 2001), while fire also helps to shape biome composition in flammable ecosystems (Wu et al., 2017), and feedbacks (e.g., aerosol feedback; Randerson et al., 2006) also contribute to the fire dynamics. Therefore, the drivers and controls of fire regimes require better understanding to enable robust future predictions.

1.4 Fire, carbon, and climate

Fire is an important component in the global carbon cycle and feedback to the climate system (Bowman et al., 2009). For example, Yue and Unger (2018) use multiple models and field measurement datasets to quantify the impact of fire, via O_3 damage and aerosol diffuse fertilization influence on the global land carbon storage (e.g., GPP), suggesting that fire-induced pollution decreased GPP at a rate of 0.86 (± 0.74) Pg C yr^{-1} during the period of 2002-2011. From data at 48 global sites, including broad leaved, needle leaved and savanna ecosystems which are frequently fire disturbed and DGVM simulations, Pellegrini et al. (2018) revealed that fire frequency determines long-term changes in soil carbon and nitrogen limitation and thus alters the carbon storage capacity of terrestrial ecosystems. Similarly, a recent study showed that the impacts of fire disturbances on soil composition are longer-lived than suggested by previous evaluations (Bowd et al., 2019). However, the influence of climate-change-induced changes in fire activity on the global carbon cycle needs to be better understood.

Many studies centrally focus on interactions between the carbon cycle and climate (Arneth et al., 2010, Sitch et al., 2008). However, as an important component in modulating future climate change (Arneth et al., 2010, Bowman et al., 2009, Heinze et al., 2018), the climate-carbon feedback derived from changing fires is poorly understood. From a biogeochemical perspective, fire impacts the climate system via the release of carbon (Bowman et al., 2009). This always exerts a warming effect (Harrison et al., 2018), referred to as 'carbon-cycle effects' (Bala et al., 2007). Fire also influences climate via biophysical effects, e.g., releasing atmospheric aerosols and changing surface albedo (Bowman et al., 2009). However, the existence of climatic cooling or warming

induced by fire physical effects is controversial (Arneth et al., 2010, Harrison et al., 2018, Ward et al., 2012), and this is particularly strong in the high latitude regions in the Northern Hemisphere (Liu et al., 2019, Randerson et al., 2006). In addition, aerosol and surface albedo effects could even cancel each other (Bowman et al., 2009, Randerson et al., 2006). Therefore, I focus on investigating carbon-cycle effects of fire on climate.

Past studies have investigated the effects of fire on climate-carbon feedback by using simple (Harrison et al., 2018) and single models (Ward et al., 2012), specific regional field measurements (Randerson et al., 2006), and time-limited remote sensing observations (Liu et al., 2019). Here, we update the Lund-Potsdam-Jena dynamic global vegetation model (LPJ-DGVM) (Sitch et al., 2003) by coupling it with a process-based SEVER-FIRE (Socio-Economic and natural Vegetation ExpeRimental global fire model) (Venevsky et al., 2019). The coupled system is then forced by Integrated Model Of Global Effects of climatic aNomalies (IMOGEN), which emulates 34 General Circulation Models (GCMs) from the Coupled Model Intercomparison Project Phase 5 (CMIP5), composing a fully coupled model framework (IMOGEN-LPJ-SEVER). Our study investigates the fire dynamics and possible drivers, carbon-cycle effects of fire on global carbon cycle, and the climate-carbon feedbacks derived from changing fires and their uncertainties over the period of 1860-2100. This is performed in a fully coupled model that incorporates complex sub-models of vegetation dynamics and terrestrial and oceanic feedbacks to the atmosphere under multiple scenarios of emissions-dependent global warming and human demography. Our analysis will help to develop wildfire management strategies suitable for different possible future socioeconomic development pathways, to assess future changes in the

global carbon cycle, and to help inform adaptation and mitigation options to global climate change

1.5 Balance between fire and climate in driving vegetation distribution

Dynamic Global Vegetation Models (DGVMs) are important tools to simulate potential vegetation and carbon cycles in the terrestrial ecosystems. In particular, when fire models are incorporated into DGVMs, fire regime and vegetation-fire interactions can be represented (Bachelet et al., 2015, Scheiter et al., 2015, Scheiter et al., 2013, Wu et al., 2015). According to DGVM simulations, forest cover (around 80-100% of tree cover) would more than double from 26.9% to 56.4% in a world without fire (Bond and Keeley, 2005). Existing research has revealed that some flammable ecosystems (including boreal forests, eucalypt woodlands, shrub lands, grasslands and savannas) are actually determined by fires (Bond et al., 2005). However, there is difficulty in isolating the controls from climate and fires on vegetation distributions (Mills et al., 2006) and few studies have focused on analysing the balance of drivers between fire disturbances and climate on boreal forests. Especially, this balance may change significantly under climate change. And my study will fill the mentioned gap.

1.6 Research aims, objectives, key findings, and significance

1.6.1 Research aims and objectives

This thesis is divided into three main parts: (a) coupling a new global process-based fire model, SEVER-FIRE to multiple GCMs to investigate the trends in global BA and its drivers, (b) using this fully coupled model to explore the climate-carbon feedbacks derived from changing fires, and (c) a

comprehensive application using models, remote sensing technology, and statistics to quantitatively analyse the individual contribution of fire and climate for the boreal forests of the Heilongjiang province, China and their response to climate change. The specific objectives and their technical routes are described below.

(1) Reproduce historical global BA trends and predict future BA trends and their drivers with global warming and human demography.

I use the LPJ-DGVM (Sitch et al., 2003) modified to include SEVER-FIRE (mainly implementation of pyrogenic behaviour of human, e.g., the timing of their activities and their willingness/necessity to ignite or suppress fire) to project global trends of BA in response to climate change and human alterations to the Earth system. I used outputs from a climate impacts system called IMOGEN (Huntingford et al., 2010). This system is based on pattern scaling of climate model output and estimates surface meteorology for altered atmospheric gas composition and thus global radiative forcing (Huntingford et al., 2010). Therefore, wildfire-induced changes in the terrestrial carbon storage give feedback on climate itself, via augmented atmospheric CO_2 concentration. In this study, I used IMOGEN to emulate 34 General Circulation Models (GCMs) from the CMIP5 to drive LPJ-DGVM. I performed coupled model runs under four different CO_2-socioeconomic scenarios. These were based on four standard Intergovernmental Panel on Climate Change Fifth Assessment Report (IPCC AR5) Representative Concentration Pathways (RCPs) (Moss et al., 2010) describing potential scenarios of atmospheric greenhouse gas emissions in combination with three demographic Shared Socioeconomic Pathways (SSPs) (Riahi et al., 2017). Model forcings are common among all simulations for the historical period, then diverge from the present day to the end of the 21st century.

I first evaluated the model's ability to reproduce the global BA trend for the recent historical period (1997-2013) against the Global Fire Emissions Database version 4 product that includes small fires (GFED4s) (van der Werf et al., 2017). I explored the dominant limiting factors (including interactive effects) on the present-day BA trend for the period 1987-2016 using model factorial simulations by fixing either one climatic forcing variable (T, P, and W) or one of the socioeconomic forcing variables (POP, RUR, and DIS) through six factorial historical runs and quantified the fraction of the global burnt land grid cells associated with each limiting factor, i.e., sum of number of grid cells with the same dominant limiting factor divided by the total number of global burnt land grid cells. I then projected the future global BA trends over the period 2014-2100, and analysed its spatial pattern and drivers (independent) using a partial derivatives approach by varying one driver (either climatic (T, P, and W) or socioeconomic (POP, RUR, and DIS)) at a time during six runs over the last 30 years of the 21st century.

(2) Investigate climate-carbon feedback derived from changing fires with global warming and human demography.

Using the same coupled framework as in objective (1), here I mainly investigated fire dynamics and their possible drivers, the carbon-cycle effects of fire on the global carbon cycle, and climate-carbon feedbacks derived from changing fires and their uncertainties over the period of 1860-2100. This was performed in a fully coupled model that incorporates complex sub-models of vegetation dynamics and terrestrial and oceanic feedbacks to the atmosphere under multiple pathways of emissions-dependent global warming and human demography. Especially under mitigation scenario (RCP2.6), in order to explore

the uncertainties among human changes, I tried all of the possible socioeconomic pathways involving different levels of population growth and urbanization rates.

(3) Quantify the individual contribution of climate and fires to vegetation composition in the boreal forest of China in present day and future.

This study employed the statistical methods of Redundancy Analysis (RDA) and variation partitioning combined with simulation results from a dynamic global vegetation model, SEVER-DGVM, and remote sensing datasets of global land cover (GLC2000) and the Global Fire Emissions Database (GFED3) to investigate the respective individual contributions of climate and fires to vegetation composition in the present-day boreal forest of China and in future scenarios under four global warming targets (global temperature increasing 1.5, 2.0, 3.0, and 4.0 °C relative to pre-industrial).

1.6.2 Thesis structure and key findings

The thesis comprises 5 chapters. A summary and key findings of each chapter are shown below.

Chapter 1, the introduction, presents the background to this thesis: fire in the earth system, and particularly focuses on an overview of the role of fire in the Earth system, i.e., global fire regime changes, the impacts of fire on global carbon cycles and feedbacks to climate, and the role of fire on regional vegetation distribution. Then it defines fire regime and describes the state of art modelling technology on fire regime changes, specifically, to investigate global BA trends and their drivers. Furthermore, it presents the role of fire on carbon cycles and feedbacks to climate systems, focusing on the carbon-cycle effects of fire on climate. Next, it analyses the influence of fire on the regional vegetation distribution and the driving balance in regulating biome composition with climate.

Finally, it summarizes the research objectives, methodology and significance of this thesis.

Chapter 2 describes the global burnt area trends from wildfires simulation using a fully coupled model framework driven by 34 GCMs and analysing their potential drivers and limiting factors. I show that global burnt area will increase under climate change and rapid population growth and urbanization and this is especially in high latitudes, through high latitude warming (polar amplification) and increases in human-induced fires over the tropics and subtropics. However, expected rapid urbanization also limits strongly burnt area by enhanced fire suppression and management. Averaged globally, this effect is sufficient to offset the potential large future rises in burnt area.

Chapter 3 aims to comprehensively evaluate associated climate-carbon feedbacks derived from changing fires at a global scale with global warming and human demography. Using similar methods to the previous chapter, I find that fire increases global-mean temperature by around 0.16 °C yr^{-1} owing to carbon-cycle effects over the period 2005-2014. Future global fire carbon emissions depend dramatically on anthropogenic CO_2 emissions and human controls (2.0 to 3.1 PgC yr^{-1}), providing approximate increasing atmospheric CO_2 concentration by around 15–22 ppm and global-mean warming by around 0.13 to 0.18 °C yr^{-1}, especially in high latitudes. This study will be submitted in the very near future.

Chapter 4 investigates the impact of fires on regional vegetation distribution and analyses the balance of drivers between fire and climate on the biome composition in a boreal forest ecosystem of China. This study employs statistical methods combined with simulations and remote sensing technology. I find that the regional vegetation distribution is mainly determined directly by climate rather

than fire in the recent period. However, climate warming will change this balance. For example, with a future global warming of 1.5 °C, local vegetation composition will be determined more by fires than by climate. This chapter is largely based on a study published in Ecosphere in 2017 (Wu et al., 2017).

Chapter 5 presents the summary and opportunities for further development, including summary and limitations of this thesis.

1.6.3 Significance

The newly developed SEVER-FIRE aims to get a step further toward creating a first-principle global mechanistic fire model. SEVER-FIRE extends from the earlier version of the fire model, Reg-FIRM, by (1) calculating lightning-induced fires using atmospheric convective activity, (2) distinguishing human-induced fires from urban and rural populations, and (3) better estimating fire duration through anthropogenic suppression and weather, limiting the maximum fire duration globally to two days. One of the most innovative features implemented in SEVER-FIRE is the inclusion of human pyrogenic behaviour to improve simulations of fire dynamics (Venevsky et al., 2019). Based on the newly-developed SEVER-FIRE coupled with LPJ DGVM as forced output from 34 GCMs, I reproduced the historical global BA trends and predicted future changes in fire regimes under global warming and changes in human demography. The result of this work will help humans to better coexist with fires and help to develop wildfire management strategies in conditions of different possible future socioeconomic development pathways, to assess future ecological changes. Investigation of the balance of drivers between fire and climate in regulating the boreal forest of China will help to develop local forest and fire management policies and prevent the occurrence of uncontrolled severe fire events in Northeast China. My findings regarding climate-carbon feedbacks derived from

changing fires suggest that controlling wildfire would be clearly beneficial in mitigating global-scale warming. This conclusion helps to inform adaptation and mitigation options to better cope with the challenges of destructive wildfires and climate change, especially when the world has been significantly disturbed by human activities.

1.7 Contribution to co-authored papers

I led three papers and co-authored another one which are quite relevant to my Ph.D. thesis, including:

1. **Wu, C.**, S. Venevsky, S. Sitch, L. M. Mercado, and C. Huntingford. 2019. Understanding global burnt area trends from wildfires with changing climate and human demography. In review.
2. Venevsky, S., Y. Le Page, J. M. Pereira, and **C. Wu**. 2019. Analysis fire patterns and drivers with a global SEVER-FIRE v1.0 model incorporated into dynamic global vegetation model and satellite and on-ground observations, Geoscientific Model Development 12(1):89-110, doi:10.5194/gmd-2018-178.
3. **Wu, C.**, S. Sitch, C. Huntingford, L. M. Mercado, and S. Venevsky. 2019. Climate-carbon feedback derived from changing fires with global warming and human demography. Ready for submission.
4. **Wu, C.**, S. Venevsky, S. Sitch, Y. Yang, M. Wang, L. Wang, and Y. Gao. 2017. Present-day and future contribution of climate and fires to vegetation composition in the boreal forest of China. Ecosphere 8(8):e01917, doi:10.1002/ecs2.1917.

Paper 1 is contained in Chapter 2 (Global burnt area trends, drivers, and climate change) in this thesis. This study was mainly designed by Stephen Sitch, Sergey Venevsky and myself with important suggestions from Lina M. Mercado and Chris Huntingford. I performed the simulations and wrote the draft and all the other co-authors contributed to analysing the results and revise the paper. The description of SEVER-FIRE in Chapter 2 is mainly from my co-authored paper 2. I mainly worked on the

codes and contributed to the writing of this paper. Results from paper 3 is the main part of Chapter 3 (Climate-carbon feedbacks derived from changing fires). Stephen Sitch, Chris Huntingford, Sergey Venevsky, and myself mainly designed this study with important help from Lina M. Mercado. Similarly, I performed the simulations and prepared for the draft. All the co-authors interpreted the results and contributed to the revisions. Finally, paper 4 is my Chapter 4 (Impact of fire on regional vegetation distribution). This was designed by Sergey Venevsky and myself. I performed the simulations and analysed the results. Stephen Sitch contributed revise the manuscript.

I also led one and co-authored one other paper during my Ph.D. study. However, they are partly beyond the scope of my thesis. Therefore, I do not include in my thesis. They are:

1. **Wu, C.**, M. Wang, C. Lu, S. Venevsky, V. Sorokina, V. Kulygin, and S. Berdnikov. 2018. Climate-induced fire regimes in the Russian biodiversity hotspots, Global Ecology and Conservation, 16:e00495, doi:10.1016/j.gecco.2018.e00495.
2. Chu, H., S. Venevsky, **C. Wu**, and M. Wang. 2019. NDVI-based vegetation dynamics and its response to climate changes at Amur-Heilongjiang River Basin from 1982 to 2015. Science of the Total Environment, 650, 2051-2062.

Chapter 2 Global burnt area trends, drivers, and climate change

2.1 Introduction

Wildfire is an important natural disturbance influencing the global biome distribution and the structure of fire-prone communities, yet is a risk to human safety. The frequency and spatial distribution of wildfires, along with their limiting factors and the drivers of recent trends, must be understood to enable robust future predictions. I enhance the Lund–Potsdam–Jena (LPJ) dynamic global vegetation model to describe Burnt Area (BA) and its responses to changing climate and human demographics. LPJ is placed within a coupled climate-carbon system that emulates 34 climate models from the Coupled Model Intercomparison Project Phase 5 (CMIP5) database. In this chapter, I aim to investigate the global bunt area trends from wildfires with climate change and human demography and quantify the dominant drivers of recent and future BA trends through factorial analysis. The results will help to develop wildfire strategies and inform the climate change adaption and mitigation.

2.2 Methods

2.2.1 Fully coupled model framework

LPJ DGVM - SEVER FIRE (LPJ-SEVER) model. SEVER-FIRE (Socio-Economic and natural Vegetation ExpeRimental global fire model; abbreviated as SEVER-FIRE in the following text) has been incorporated into LPJ-DGVM (Sitch et al., 2003). DGVMs are important tools to simulate potential vegetation and carbon cycle dynamics in terrestrial ecosystems (Sitch et al., 2015). DGVMs

integrate biophysical, physiological, and ecological processes on a large scale, including vegetation physiology, phenology, vegetation dynamics, and competition (Sitch et al., 2008, Sitch et al., 2003). SEVER-FIRE is a quasi-mechanistic global model, built on the earlier Reg-FIRM (Venevsky et al., 2002), with several new features aiming to approach complete representation of wildfire processes. SEVER-FIRE extends from the earlier algorithms of Reg-FIRM and introduce new functionality with respect to: 1) estimating the numbers of lightning fires from data on convective activity in the atmosphere; 2) estimating numbers of human fires separately for urban and rural populations (the timing of their appearance in natural landscapes and their ratio) as well as regional wealth index; and 3) estimating more realistic fire durations, which in the new model depend on human suppression and weather situation and can last for up to two days.

One of the main novelties of SEVER-FIRE model is its implementation of human pyrogenic behaviours (e.g., the timing of their activities and their willingness/necessity to ignite or suppress fire), related to socioeconomic and demographic conditions in the geographical domain of the model application (Venevsky et al., 2019). Based on climate forcing, external anthropogenic drivers and LPJ-DGVM derived vegetation (e.g., fuel state set by vegetation dynamics), SEVER-FIRE provides a mechanistic description of major fire characteristics at the global scale, namely number of fires, area burnt and carbon emissions, which are separated into human-induced and lightning-induced fires according to their ignition sources. Post-fire conditions then regulate vegetation and ecosystem regeneration, which act as a feedback to burning by modulating new fuel load accumulation and differences in flammability among Plant Functional Types (PFTs) in the DGVM. BA has been widely used in assessing the effects of fire (Bond and Keeley, 2005, Bowman et al., 2009, Hantson et al., 2016).

SEVER-FIRE includes six components, including estimation of fire weather danger index and fire probability, simulation of lightning ignition events and number of lightning fires, simulation of human ignition events and number of human fires, simulation of fire spread after ignition, fire termination, and estimation of fire effects (areas burnt, pyrogenic emissions, number of individuals killed in each PFT). More details of the description of SEVER-FIRE have been provided by Venevsky et al. (2019).

The IMOGEN climate-carbon cycle system. LPJ-SEVER is forced by a common base climatology plus patterns of changing meteorological conditions fitted against multiple CMIP5 GCMs. 'Pattern scale' that approximate linear relationships are found between local and seasonal meteorological variations and the amount of global average warming over land (Huntingford and Cox, 2000), is used to calculate climate change (Huntingford et al., 2017, Huntingford et al., 2010, Huntingford et al., 2013). An energy balance model calculates global warming amounts by changes in atmospheric greenhouse gases (GHGs), also fitted to the CMIP5 ensemble. This component is coupled to the LPJ-SEVER with vegetation dynamics, which provides land-atmosphere feedback via Net Ecosystem Production (NEP). NEP is calculated as net primary production minus heterotrophic respiration and fire emitted carbon. A simple global oceanic model is used to estimate ocean feedbacks to the atmosphere associated with the oceanic drawdown of CO_2 (Huntingford et al., 2010).This combined impact system, IMOGEN, is operated online with a closed carbon cycle and forced with anthropogenic CO_2 emissions. Annual CO_2 concentrations are updated at the end of each year based on annual CO_2 emissions and changes in global land and ocean carbon fluxes from LPJ-SEVER and the global ocean model, respectively (Sitch et al., 2008). Non-CO_2 GHG emissions are not considered in

this study. The flowchart of the fully coupled framework is shown in Figure 2.1.

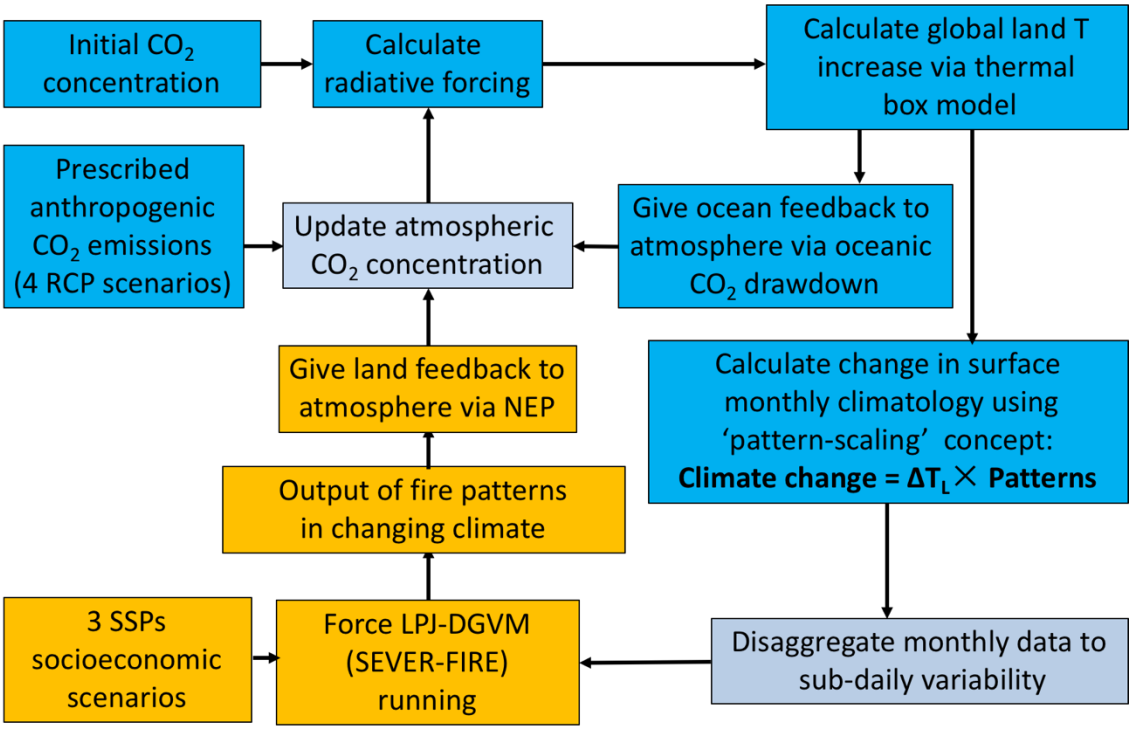

Figure 2.1 Flowchart of IMOGEN-LPJ-SEVER fully coupled framework. The boxes with blue background are IMOGEN process, the boxes with orange background are LPJ-SEVER process, and the boxes with grey background are coupler.

2.2.2 Datasets and experimental design

Atmospheric composition and climate datasets. For the offline historical simulations, we use observed monthly climatology for the period 1950–2016 from the University of East Anglia Climate Research Unit (CRU) gridded dataset (Harris et al., 2013), supplemented by variables from the NCEP/NCAR Reanalysis (Kalnay et al., 1996) (e.g., precipitation, convective precipitation, and wind speed). These climate datasets were aggregated to a resolution of 3.75° longitude × 2.5° latitude, in keeping with the resolution of the climate patterns of GCMs used in IMOGEN. We also use observed annual global atmospheric CO_2 concentrations for the period 1950–2016 in conducting the offline historical simulation (Sitch et al., 2008).

For the fully coupled online carbon cycle simulation, IMOGEN requires prescribed fossil fuel and/or non-fossil fuel CO_2 emissions, which are based on

historical records for the period 1860-2005 (Meinshausen et al., 2011). RCP2.6, RCP4.5, RCP6.0, and RCP8.5 emissions scenarios are then used for the period 2006-2100. Interannual-varying climate is necessary for LPJ-SEVER to simulate realistic fire dynamics (Sitch et al., 2008). Therefore, 34 patterns from GCMs are added to a random sequence of years between 1901 and 1930 from the CRU dataset (New et al., 2000). Hourly surface climate is derived by temporal disaggregation of the monthly means, including temperature at 1.5m, diurnal temperature range, precipitation and wind speed. In this way, monthly temperature, maximum/minimum temperature, precipitation, convective precipitation and wind speed are used to force LPJ-SEVER (Huntingford et al., 2010). However, we assume that cloudiness fluctuation would not change with time and the constant long-term means are used to force the model in this study (Sitch et al., 2003). All data used in the simulation (including the socioeconomic variables in the next section) are prepared at a spatial resolution of 3.75° longitude × 2.5° latitude, in keeping with associated patterns of GCMs. Nearest neighbour interpolation is used when needed.

Socioeconomic scenarios. SEVER-FIRE is also forced by socioeconomic variables, mainly including population density (POP), the ratio of rural to total population (RUR), and average distance from the nearest city (DIS). Common global gridded (urban) population density base maps over the period 1950-1960 were derived from United Nations Population Division. Population density is then obtained by multiplying this common base map by the annual average population growth rate. The annual average (urban) population growth rates (%) have been extracted from the SSPs database (Riahi et al., 2017), which describes the world different levels of challenges to climate mitigation and adaptation (Knorr et al., 2016). SSP2 represents an intermediate scenario with moderate population

density growth and moderate urbanization; SSP3 reflects rapid population growth and slow urbanization, leading to greater challenges to mitigation and adaptation; SSP5 describes a world with conventional economic growth and fossil fuel consumption leading to rapid urbanization but with slower population growth (Knorr et al., 2016). World Bank World Development Indicators (WDI) historical population annual average growth rates are used for the period 1960-2005. For the period 2006-2100, the SSP2, SSP3 and SSP5 scenarios as provided by the National Center for Atmospheric Research (NCAR) are selected to project the potential growth rates of population density in five different regions with different development levels (Riahi et al., 2017). Similarly, projections of RUR for the period 1950-2100 are prepared according to the urban population density baseline and the rate of urbanization. Historical records are taken from the World Urbanization Prospects (WUP2009).

DIS determines fire management strategies to some degree, and it is strongly related to urbanization. Generally, global urban areas are expanding on average twice as fast as their populations (Seto et al., 2012). However, the ratio of urban area growth rate to urban population growth rate (*coef*) differs among regions with different levels of development (Angel et al., 2011). We assume that the distance from a city changes at the same rate as the growth of urban areas. The base DIS for a grid cell (3.75° × 2.5°) was calculated as a distance from the grid cell to the nearest grid cell with a population density exceeding 400 per/km^2, which defines the threshold for an urban area (Liu and Phinn, 2003, Millward, 2005). Based on the low projection scenario outlined in Tables 6.1 and 6.2 of Angel et al. (2011), we calculate the ratios of urban area growth rate to urban population growth rate in five regions corresponding to the development zones defined in the SSPs, thus obtaining the rate of change in DIS for the period 1950-

2100.

Model initialization. The fully coupled IMOGEN-LPJ-SEVER simulation was started from ‘bare ground’ conditions (no plant biomass present) and ‘spun up’ 1000 years until approximate equilibrium of carbon pools and vegetation cover was reached (Sitch et al., 2003). A random sequence of years between 1901 and 1930 from the CRU dataset and the socioeconomic forcing data in the year 1950 were used to force the coupled model. CO_2 emissions were ‘switched off’ and no feedbacks from land and ocean to atmosphere were allowed during the model initialization.

Offline historical LPJ-SEVER simulation. In the first set of experiments, LPJ-SEVER was run from its preindustrial equilibrium over the historical period 1950–2016 using observed fields of monthly climatology CRU datasets, NCEP/NCAR Reanalysis datasets, and annual global atmospheric CO_2 concentration at the GCM grid resolution of 3.75° longitude × 2.5° latitude. The input soil texture data was specified as in Sitch et al. (2003). No land or ocean carbon cycle feedbacks were included at this stage (Sitch et al., 2008).

Fully coupled IMOGEN-LPJ-SEVER simulation. LPJ-SEVER was run from its preindustrial equilibrium at 1860 over the historical and future period 1860-2100 at the spatial resolution of the GCM patterns. Once the equilibrium state was reached, LPJ-SEVER was run in transient mode forced by the IMOGEN framework using climate anomalies from 34 GCMs. Climate anomalies were added to a random sequence of 30 years baseline climatology. This was undertaken for four IPCC AR5 RCP fossil fuel and non-fossil fuel CO_2 emissions scenarios (RCP2.6, RCP4.5, RCP6.0, and RCP8.5). Three external anthropogenic SSPs (SSP2, SSP3, and SSP5) were added in the fully coupled simulation (with socioeconomic data for the year 1950 used for the period 1860-

1949 of the transient phase). Details of the experiment scenarios are listed in Table 2.1.

Table 2.1 Experimental scenarios. Overview of the experimental climate and socioeconomic scenarios used in this study

Scenarios	CO_2 emissions	Socioeconomic scenarios		
		POP	RUR	DIS
S1	RCP2.6	SSP2(middle†)	SSP3(slow)	SSP3(slow)*coef‡
S2	RCP4.5	SSP5(slow)	SSP2(middle)	SSP2(middle)*coef
S3	RCP6.0	SSP2(middle)	SSP2(middle)	SSP2(middle)*coef
S4	RCP8.5	SSP3(rapid)	SSP5(rapid)	SSP5(rapid)*coef

† 'Slow', 'middle', and 'rapid' in 'POP' refer to the general levels of population growth rate while in 'RUR' and 'DIS', they refer to urbanization rate.
‡ '*coef*' refers to the ratios of urban areas growth rate to urban population growth rate.

2.2.3 Analysis

Present-day and future BA trends projection. Based on the offline historical and fully coupled IMOGEN-LPJ-SEVER simulations (corresponding to the full set of 34 GCMS emulated), the present-day (the period 2000-2013) global BA and its trend are reproduced and evaluated against the observed long-term BA from GFED4s. The simulated spatial pattern of present-day BA trend is also compared with that inferred from GFED4s. Nearest neighbour interpolation is used to remap the GFED4s dataset from the resolution of 0.5° × 0.5° to 3.75° × 2.5°. The correlation of simulated against observed temporal BA dynamics is evaluated via a Pearson correlation analysis. Future global BA trends are then projected for four different scenarios S1-S4 (see Table 2.1) covering the period 2014-2100. We also project the spatial patterns of BA trends for the last 30 years of the 21st century under different scenarios to explore the spatial differences of BA trends under different emissions and demographic forcings. The spatial pattern of global BA trend is tested using the Mann-Kendall test at the 5% significance level.

Limiting factors of present-day BA trend. Human and climatic effects are

generally considered as the main factors influencing BA trends (Andela et al., 2017, Knorr et al., 2016). However, we define limiting factors and drivers differently in this study. The dominant limiting factors are defined as these factors that most limit the magnitude of the BA trend in each grid cell, including interactive effects among different factors (i.e., we consider interactions between climatic and human factors). We perform six factorial experiments in an 'offline' scenario (see Table 2.1) to evaluate the dominant limiting factors, namely, T, P, W, POP, RUR, and DIS, on present-day BA trends: (F1) fixed T using non-varying temperatures from the year 1950, (F2) fixed P using non-varying precipitation from the year 1950, (F3) fixed W using non-varying wind speeds from the year 1950, (F4) fixed POP using non-varying POP values from the year 1950, (F5) fixed RUR using non-varying RUR values from the year 1950, and (F6) fixed DIS using non-varying DIS values from the year 1950. The F0 simulation is the 'All varying' scenario with all factors allowed to vary. Six formulas (F0 - F1, F0 - F2, F0 - F3, F0 - F4, F0 - F5, and F0 - F6) are then used to evaluate the effects of T, P, W, POP, RUR, and DIS in limiting the BA change. The limiting factors on changes in present-day BA are explored using offline simulations covering the period 1987-2016.

Factorial analysis on long-term BA limiting factors. Factorial analysis on long-term BA limiting factors is conducted similarly to the factorial experiments F1-F6 in the last section. A second set of factorial analysis is performed to explore the roles of different limiting factors on long-term global BA dynamics over the period 1860-2100 using the fully coupled framework under the S3 scenario (see Table 2.1). Here, the baseline CRU climatology is used to replace 'the climate of the year 1950' in the F1-F3 runs to represent the fixed climate experiments. The simulations are forced by three GCMs: IPSL-CM5A-MR, CSIRO-Mk3-6-0, and

MIROC-ESM which project maximum, minimum, and mid-range changes in precipitation by the year 2100, respectively (Figure 2.2).

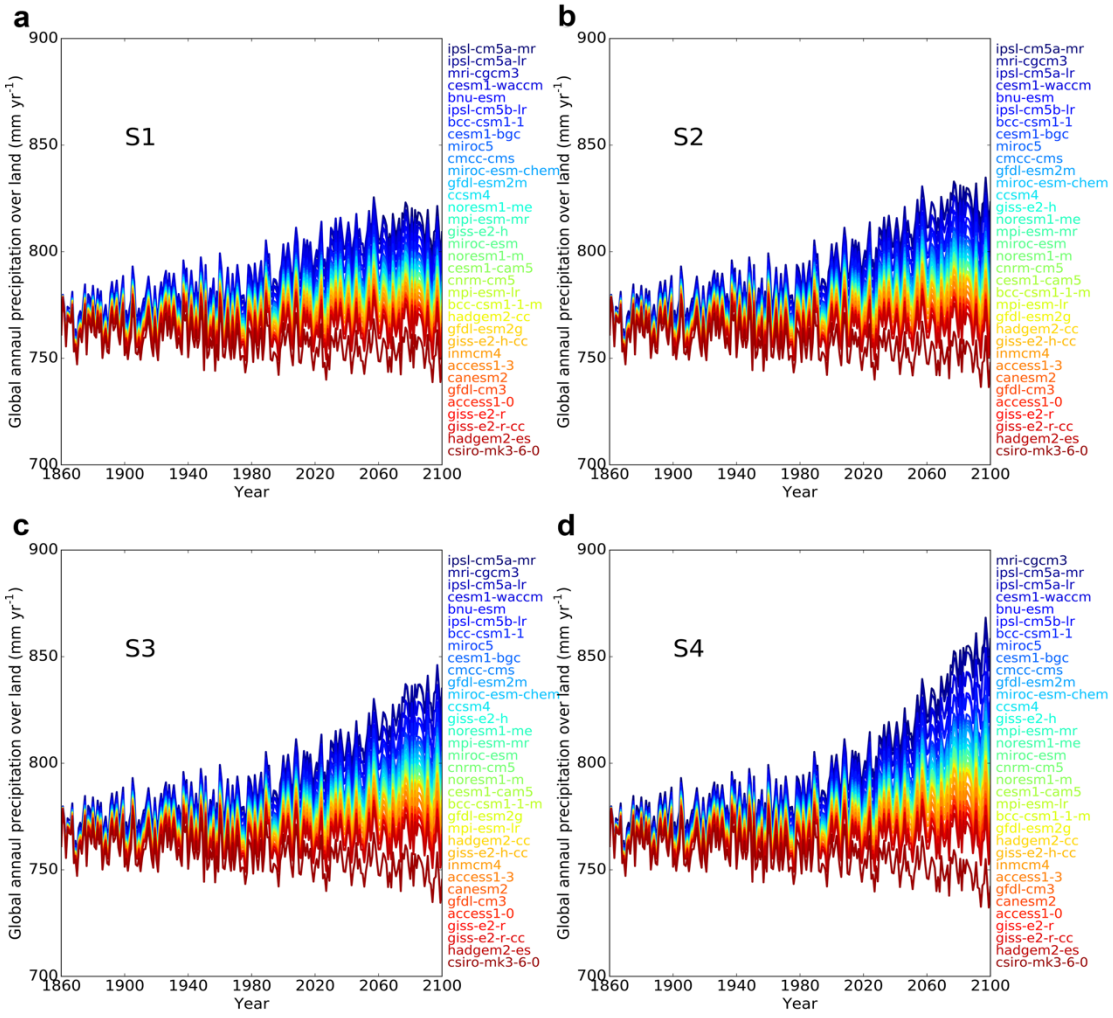

Figure 2.2 Global precipitation changes during the period 1860-2100 using 34 GCMs. Panels are (a) S1, (b) S2, (c) S3, and (d) S4

Human impacts on BA dynamics. Population growth and urbanization are the important factors in determining BA dynamics. However, our study is based on only four experimental scenarios, each representing a specific combination of future demographic changes and changes in CO_2 emissions (Table 2.1). To better understand and clarify the priority in sequence of human impacts on global BA dynamics, a sensitivity analysis using the intermediate CO_2 emissions scenario (RCP6.0) is performed exploring all combinations of population growth and urbanization rates within the various SSPs. This yields 9 combinations (3

population growth rates × 3 urbanization rates) with different levels (slow, middle, and rapid in Table 2.1) of population growth and urbanization.

Drivers of future BA trend. To supplementary identification of limiting factors, the dominant drivers of BA trends are defined as the independent driving factors that contribute most to the increase (or decrease) in BA trends in each grid cell excluding any interactive effects among factors. We perform a second set of factorial analysis (including six runs): (M1) varying T only, (M2) varying P only, (M3) varying W only, (M4) varying POP only, (M5) varying RUR only, and (M6) varying DIS only. M0 is a 'control experiment' with socioeconomic factors prescribed as values from the year 1950 and climatic factors as constant values from the baseline CRU climatology. The six formulas (M1-M0, M2-M0, M3-M0, M4-M0, M5-M0, and M6-M0) are used to evaluate the drivers of T, P, W, POP, RUR and DIS on changes in BA. The fraction of global burnt land grid cells (%) where a change in BA is attributed to a given dominant driver is obtained by summing the number of grid cells with the same dominant driver and dividing by the total number of global burnt land grid cells. Burnt land grid cells are defined as land grid cells with simulated annual mean BA larger than 0. The projected drivers of future BA trends are based on the GISS-E2-R-CC GCM simulation (Table 2.2) over the last 30 years of the 21st century. The results are qualitatively insensitive to the selection of the GCM used here (Figure 2.3).

Table 2.2 The information of 34 GCMs used in this study

No.	Model Institution	Model name
1	BCC	bcc-csm1-1
2	BCC	bcc-csm1-1-m
3	BNU	BNU-ESM
4	CCCma	CanESM2
5	CMCC	CMCC-CMS
6	CNRM-CERFACS	CNRM-CM5

Continued Table 2.2 The information of 34 GCMs used in this study

7	CSIRO-BOM	ACCESS1-0
8	CSIRO-BOM	ACCESS1-3
9	CSIRO-QCCCE	CSIRO-Mk3-6-0
10	INM	inmcm4
11	IPSL	IPSL-CM5A-LR
12	IPSL	IPSL-CM5A-MR
13	IPSL	IPSL-CM5B-LR
14	MIROC	MIROC5
15	MIROC	MIROC-ESM
16	MIROC	MIROC-ESM-CHEM
17	MOHC	HadGEM2-CC
18	MOHC	HadGEM2-ES
19	MPI-M	MPI-ESM-LR
20	MPI-M	MPI-ESM-MR
21	MRI	MRI-CGCM3
22	NASA-GISS	GISS-E2-H
23	NASA-GISS	GISS-E2-H-CC
24	NASA-GISS	GISS-E2-R
25	NASA-GISS	GISS-E2-R-CC
26	NCAR	CCSM4
27	NCC	NorESM1-M
28	NCC	NorESM1-ME
29	NOAA-GFDL	GFDL-CM3
30	NOAA-GFDL	GFDL-ESM2G
31	NOAA-GFDL	GFDL-ESM2M
32	NSF-DOE-NCAR	CESM1-BGC
33	NSF-DOE-NCAR	CESM1-CAM5
34	NSF-DOE-NCAR	CESM1-WACCM

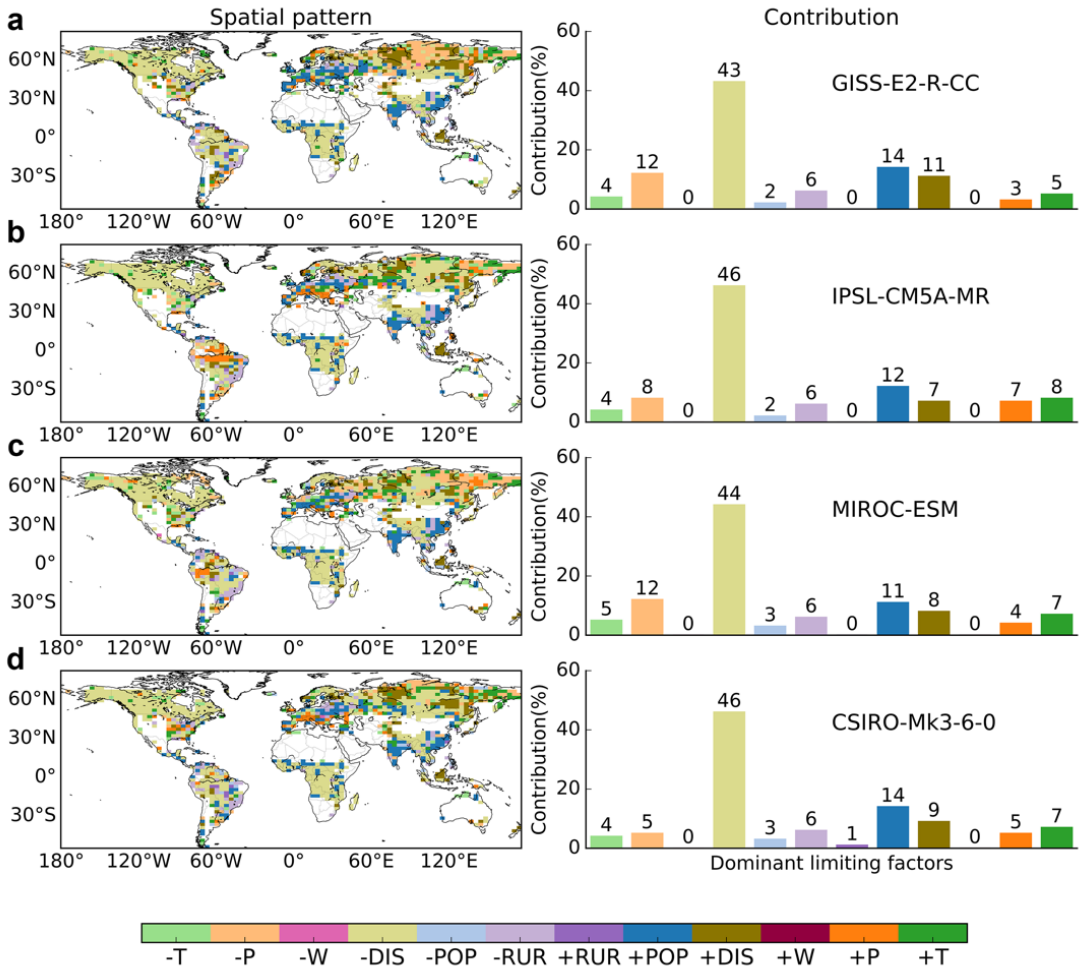

Figure 2.3 Spatial patterns of dominant limiting factors of present-day BA trend over the period 1987-2016. Shown are using four GCMs: GISS-E2-R-CC (a), IPSL-CM5A-MR (b), MIROC-ESM (c), and CSIRO-Mk3-6-0 (d)

2.3 Results

2.3.1 Present-day global BA trend

We compare the mean values and trends inferred from satellite-based (GFED4s) BA with those simulated by SEVER-FIRE, as driven by (1) the 'offline' observed Climate Research Unit (CRU)/National Centers Environmental Prediction (NCEP) climatology (Harris et al., 2013, Kalnay et al., 1996) and (2) climate forcings based on 34 GCM simulations of the period 2000-2013. We first validate the simulated fire dynamics against observations. Temporal trends in

global BA (see Figure 2.4a) are captured well by both simulations (Pearson correlation r = 0.88 for the offline simulation and r = 0.46 for the GCM framework simulation; both statistically significant). Overall, SEVER-FIRE successfully reproduces the observed GFED4s global decreasing BA trend at a rate of -6.18 Mha yr^{-1} over the period 2000-2013 (Figure 2.4a) when driven by (1) observed climatology at a rate of -4.85 Mha yr^{-1} ($P < 0.05$) and by (2) the 34 GCM-ensemble-mean at a rate of -2.01 Mha yr^{-1} ($P < 0.05$). The simulated global absolute BA trend based on GCM outputs is lower than observed owing to the inability of GCMs to reproduce recent decadal climate variability (Meehl et al., 2014). The simulated spatial pattern of BA trends agrees well between satellite data, offline simulations forced by observed climate, and the GCM-ensemble mean (Figure 2.4b-d). Both sets of simulations capture observed decreasing trends across the Amazon and Central Africa. However, over large boreal regions such as northern Eurasia, the satellite and GCM-ensemble mean trends show different magnitudes and even signs. The most common fires in these regions are lower-intensity small surface fires (Rogers et al., 2015). These have been included in GFED4s but are evidently not well represented by the SEVER-FIRE in boreal regions. Generally, the offline simulations capture BA trends well around Africa, the Amazon, Canada, and some parts of northern Eurasia, while failing to simulate the trends in the USA and Europe (Figure 2.4e).

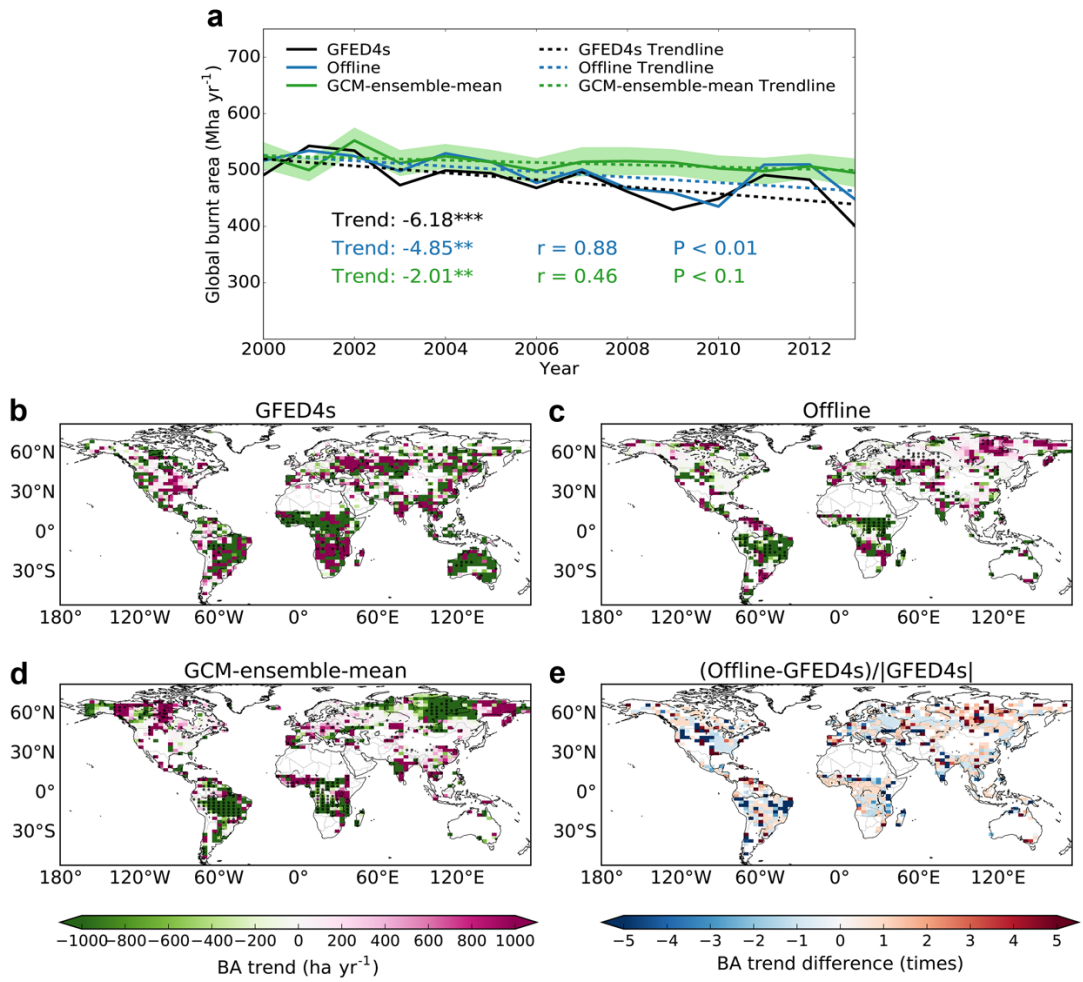

Figure 2.4 Present-day global BA trends. (a) Global BA and BA trends over the period 2000-2013. Offline: the global BA driven by CRU/NCEP observed climatology. GCM-ensemble mean: the mean of global BA simulated by SEVER-FIRE across the 34 GCMs emulated. The shaded areas in this and subsequent figures represent the standard deviation for the results of 34 runs. r and P in this and subsequent figures represent the Pearson correlation coefficient and the p-value, respectively. The asterisks in this and subsequent figures indicate whether the trend is statistically significant (Mann–Kendall test; ***p<0.01, ** p<0.05, * p<0.1). Spatial patterns of BA trends over the period 2000-2013 observed from (b) GFED4s, simulated by (c) SEVER-FIRE (Offline), and (d) SEVER-FIRE (mean across the 34 GCMs emulated). Regions labelled with black dots in this and subsequent figures indicate trends that are statistically significant (Mann–Kendall test; p<0.05). (e) Spatial patterns of relative difference of BA trends between the Offline simulation and GFED4s

2.3.2 Limiting factors of present-day BA changes

Recent BA changes are influenced by a range of factors. Although these can interact, nevertheless factorial simulations help to attribute the dominant limiting

factors to the BA changes (Zhu et al., 2016). At global scale, over the period 1987-2016, the factorial simulations suggest that present-day fire on 40% of global burnt land grid cells is dominantly limited by the distance to human communities, here is represented as an average distance from the nearest city (DIS; km), followed by climate factors: precipitation (P; mm) (35%), temperature (T; °C) (12%), and wind speed (W; m s^{-1}) (2%) with 11% attribution to other socioeconomic factors (e.g., population density (POP) and ratio of rural to total population (RUR)). Overall, climate (as the sum of T, P, and W) and human activity (as the sum of DIS, POP, and RUR) are almost equally dominant limiting factors to present-day fire over 49% and 51% of the global burnt land grid cells, respectively. A map of dominant limiting factors is presented in Figure 2.5. The effects of DIS, representing human fire suppression, in causing BA reductions contribute the (geographically) largest BA change, especially in the areas with frequent fires such as the Amazon, Central Africa, Alaska, Southeast Asia, and northeast China. Climate factors, in particular T and P, are the dominant limiting factors for the Northern Hemisphere high latitude areas and for the areas of regions where urbanization is historically finished decades ago, like in European countries or the Eastern coast of the USA.

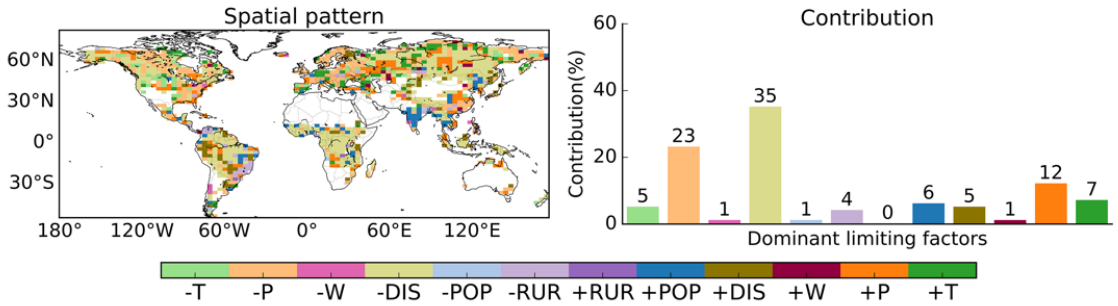

Figure 2.5 Attribution of dominant limiting factors of spatial patterns of present-day BA change over the period 1987-2016. Bar plots (right) indicate the fraction of global burnt land grid cells (%) attributed to different dominant fire-limiting factors; A prefix '+' means a recent change in a limiting factor has a positive impact on BA trend whereas '−' means a recent change in a limiting factor has a negative impact on BA trend

2.3.3 Future BA trend projection

We project future global BA trends represented as the four ensemble-means across 34 GCM LPJ-SEVER simulations under four experimental scenarios S1-S4 (see Table 2.1) over the period 2014-2100. Figure 2.6a shows a slight decreasing simulated BA trend under the high mitigation (e.g., low emissions, middle population growth and slow urbanization) S1 scenario (-0.03 Mha yr^{-1}). However, we find a significant increasing BA trend for the more 'business-as-usual' scenario (e.g., high emissions, rapid population growth and rapid urbanization) in S4 scenario (0.88 Mha yr^{-1}, $P < 0.01$). A significant decreasing BA trend is simulated under a typical mitigation S2 scenario with middle level emissions, but slow population growth (-1.69 Mha yr^{-1}, $P < 0.01$), while the projected trend under the intermediate mitigation S3 scenario (close in emissions to S2 scenario, but with middle population growth) is significantly decreasing but the intensity is weaker than S2 scenario (-0.58 Mha yr^{-1}, $P < 0.01$). To understand the climate & human limiting factors of future BA change, we conduct a set of factorial analysis using the S3 scenario for three GCMs covering a range of future global precipitation change for the period 1860 to 2100. From Figure 2.6b we see

that anthropogenic fire suppression, described by proximity to city settlements (DIS) is a major factor limiting potential growth of global BA driven mainly by demographic change (e.g., exponential population growth, see Figure 2.7), i.e., almost three times larger areas would burn by the end of 21st century under an intermediate mitigation scenario if the world would continue to use the fire suppression and management at the level of 1950s (i.e., without consideration of reduction in DIS and associated time to extinguish fire). To clarify priority in sequence of the human impacts on BA dynamics, a sensitivity analysis under RCP6.0 CO_2 emission scenario (see Table 2.1) covering the range of possibilities in population growth/urbanization rates is performed and shown in Figure 2.6c. Beyond our finding on the dominance of population density as a driver on global BA dynamics (Figure 2.7), we can see from the sensitivity analysis that when population growth is rapid then global BA is increasing with slowing of urbanization.

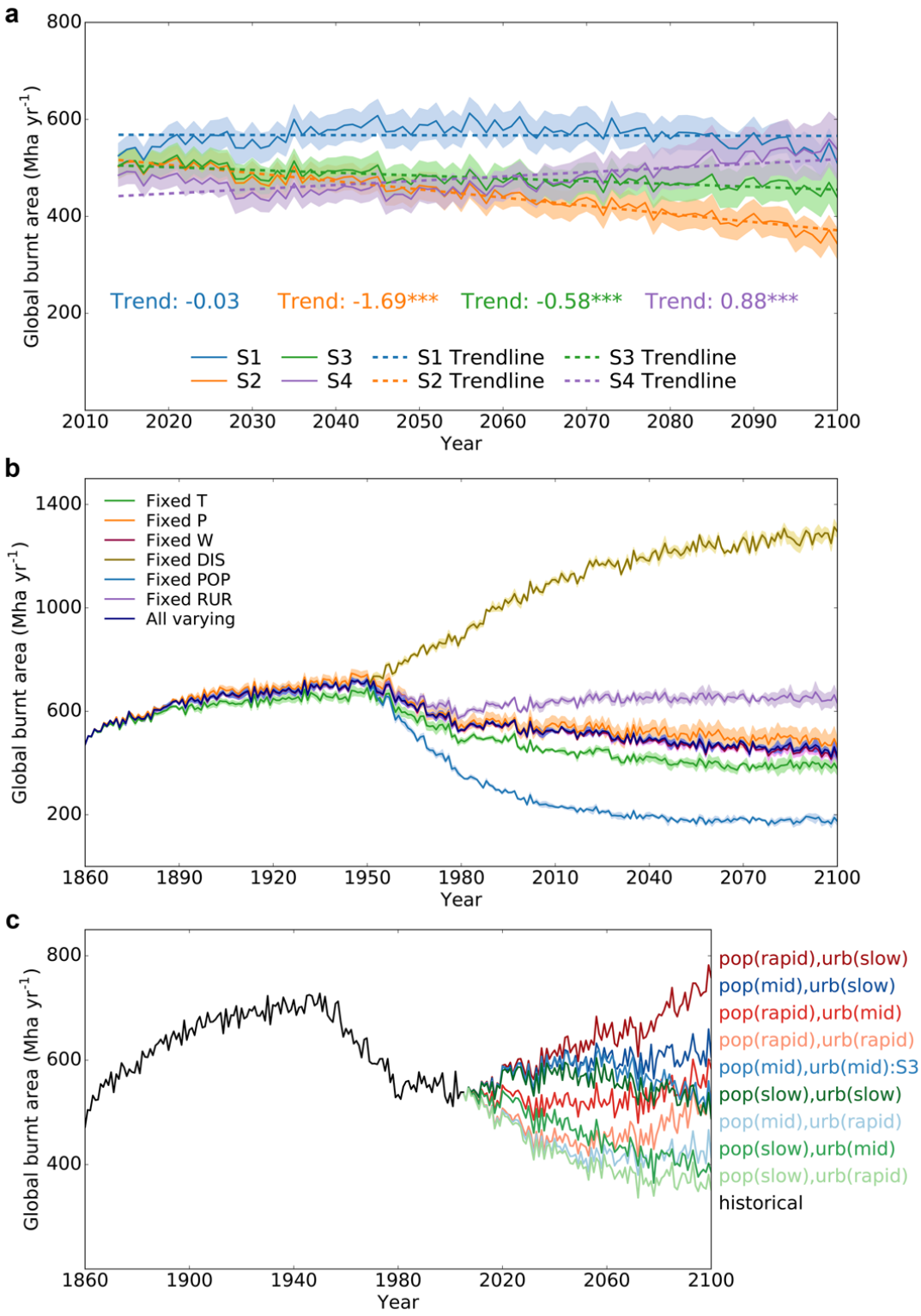

Figure 2.6 Projected global BA trends. Shown are future BA trends over the period 2014-2100 using four experimental scenarios (see Table 2.1) (a), factorial analysis on global BA in S3 scenario over the period 1860-2100 (b) and sensitivity analysis under RCP6.0 CO_2 emission scenario by exploring all combinations of population growth and urbanization rates from SSPs (c). 'mid' represents 'middle' in Table 2.1 and 'S3' represents the S3 scenario in Table 2.1

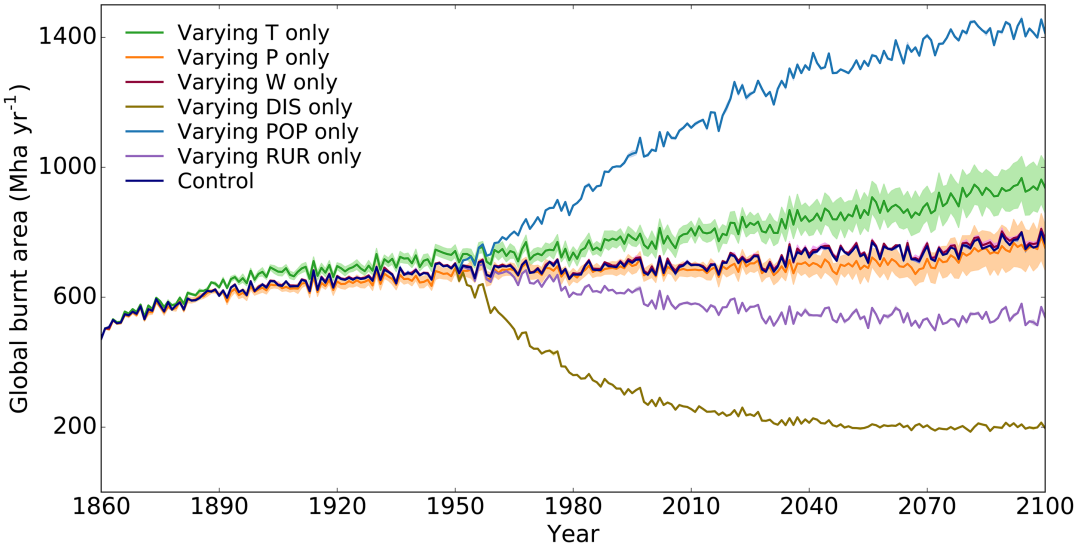

Figure 2.7 Sensitivity analysis on global BA in S3 scenario over the period 1860-2100. Shown are by varying one driver either climatic (T, P, and W) or socioeconomic (POP, RUR, and DIS) at a time

The spatial patterns of LPJ-SEVER GCM-ensemble mean BA trends in four scenarios S1 to S4 (see Table 2.1) over the period 2071-2100 are shown in Figure 2.8. Results show large differences among scenarios. For scenario S1, globally, there is a significant decreasing trend (-1.78 Mha yr^{-1}; $P < 0.01$; inset of Figure 2.8a); large areas with significant decreasing trends are seen in the Amazon, Central Africa, Siberia and South Asia. For S2, a significant decreasing trend (-2.39 Mha yr^{-1}; $P < 0.01$; inset of Figure 2.8b) is projected at global scale and larger BAs distribute in North America (excluding Alaska) and western Europe compared to S1 (Figure 2.8b versus 2.8a). For S3, similar patterns to S1 and S2 prevail, since the spatial pattern of BA trends does not change a lot. However, now the Amazon begins to produce larger BA and smaller decreasing trend is simulated across Siberia (Figure 2.8c), giving the global BA trend of -0.59 Mha yr^{-1} ($P < 0.05$; inset of Figure 2.8c). For S4, globally, there is a significant increasing trend (2.18 Mha yr^{-1}, $P < 0.01$; inset of Figure 2.8d) over the last 30 years of this century. Here large significant increasing BA trends are simulated across the Amazon (larger than 1000 ha yr^{-1} in each grid cell) and simulated large

BA in northwest Eurasia and Southeast Asia (Figure 2.8d).

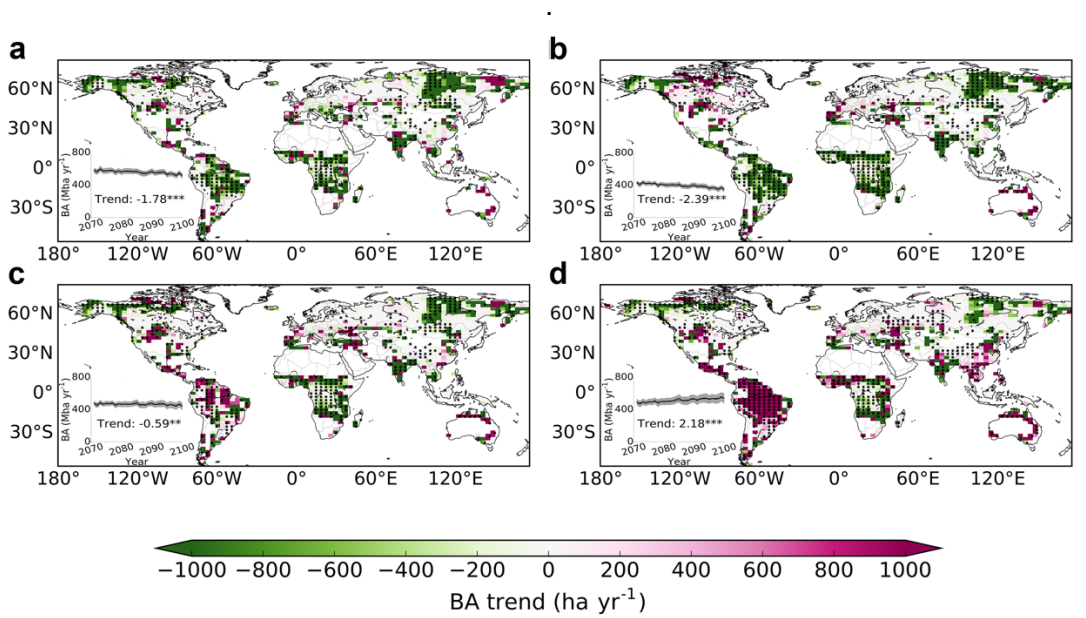

Figure 2.8 Spatial patterns of future BA trends. Shown are BA trends over the period 2071-2100 for the four scenarios listed in Table 2.1. Panels are (a) S1, (b) S2, (c) S3, and (d) S4. Line plots (inset) indicate global BA trend for the same period

2.3.4 Drivers of future BA trend

We estimate contributions to BA changes by three climatic (T, P, and W) and three socioeconomic factors (POP, RUR, and DIS) for 2071-2100 by fixing all but one investigated factor, and find that the dominant drivers of regional BA trends in future are changes in population density and climate change, with magnitude contributions varying with emission scenario. This is illustrated in Figure 2.9 and 2.10. For scenario S2 (second lowest emissions, slow population growth and middle urbanization) regional BA changes follow the decrease of population in South America, tropical Africa, Southeast Asia, and Russia with increase in BA following some population increase in Europe and North America. The changes in geographic BA trend distribution are explained mainly by the SSP5 demographic scenario (Kc and Lutz, 2017) and influence of climate factors (mainly temperature) is seen only in high latitudes and mountains (Figure 2.9b

and 2.10b). For scenario S3 (second highest emissions, middle population growth and middle urbanization) one can see that climatic drivers (sum of T, P, and W) increased significantly their influence upon global BA trend (globally, 29% of global burnt land grid cells is dominantly driven by climate for S2 scenario, against 47% for S3 scenario, see bar plots in Figure 2.9b and c). The influence of climate factors are now seen not only in Russia, Scandinavia and North America due to temperature changes (where population almost does not change according to SSP2 demographic scenario (Kc and Lutz, 2017)), but also in the northern part of Amazon and in Central Africa due to changes in precipitation. Eastern Africa and Europe shows decrease in BA trend following decrease in population from SSP2 for these regions (Figure 2.9c). The driving role of urbanization is seen when looking to BA trends for scenario S1 (lowest emissions, middle population growth and slow urbanization) for northwestern area of Russia, here climate factors do not influence BA (due to lowest from all scenarios warming), but distance from the cities decreases, leading to a decrease in BA (Figure 2.9a and 2.10a). The most extreme scenario S4 (highest emissions, rapid population growth and rapid urbanization) shows that BA follows population growth in the major part of Central Africa and Southeast Asia or decline in Europe. Meanwhile, climate factors, which now determine 52% of global BA trend, are increasing BA either due to warming (high latitude, e.g., Russia and Canada), or to drying (tropics and subtropics) (Figure 2.9d and 2.10d). In addition, there exists possible compensatory effects going from the local scale to the globe (Jung et al., 2017), i.e., although globally, population density dominantly drives future BA changes (Figure 2.9 and 2.7), climate change will compensate locally, e.g., temperature drives high latitude BA trend and precipitation starts to impact more in tropical areas (Figure 2.10c and d).

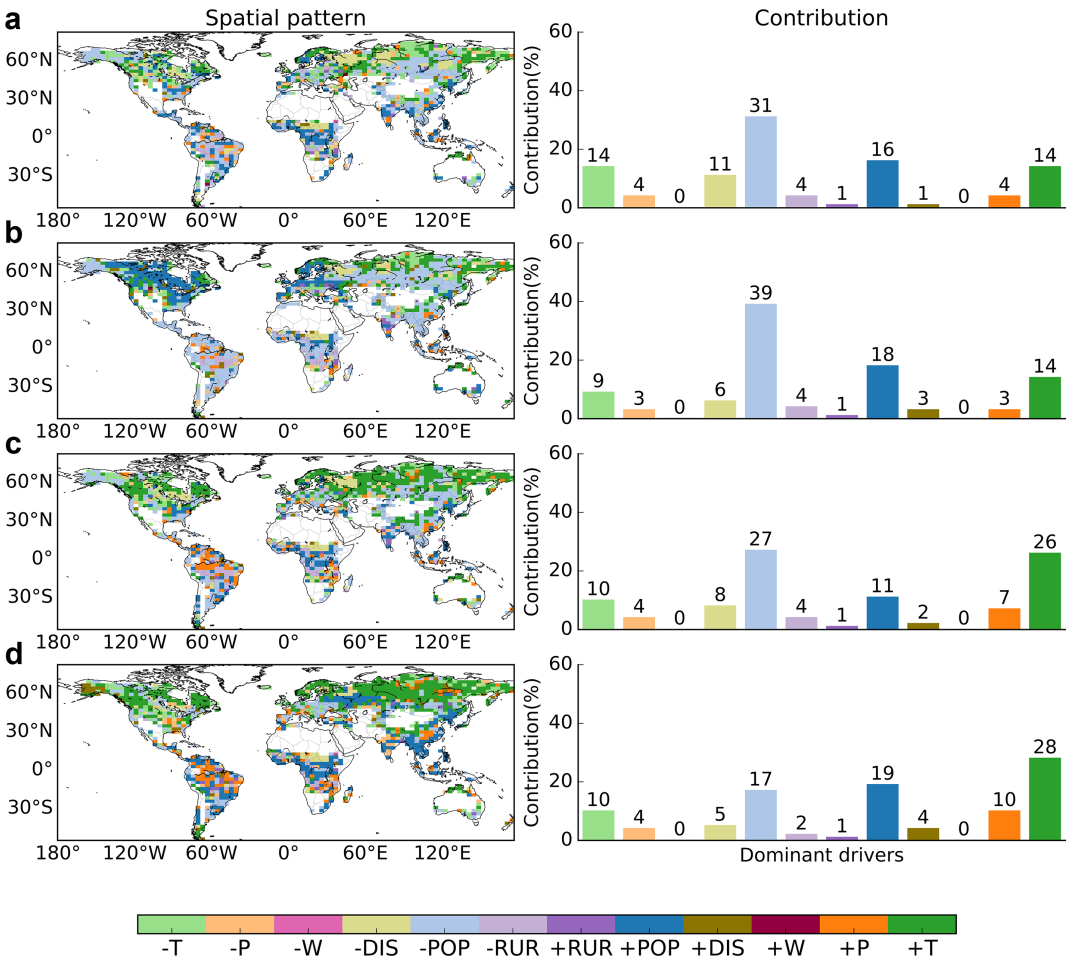

Figure 2.9 Attribution of dominant drivers of spatial patterns of future BA change over the period 2071-2100. Shown are for the four scenarios listed in Table 2.1. Panels are (a) S1, (b) S2, (c) S3, and (d) S4. Bar plots (right) indicate the fraction of burnt land grid cells (%) where changes in BA are attributed to different dominant drivers. A prefix '+' means a recent change in a driver has a positive impact on BA trend whereas '−' means a recent change in a driver has a negative impact on BA trend

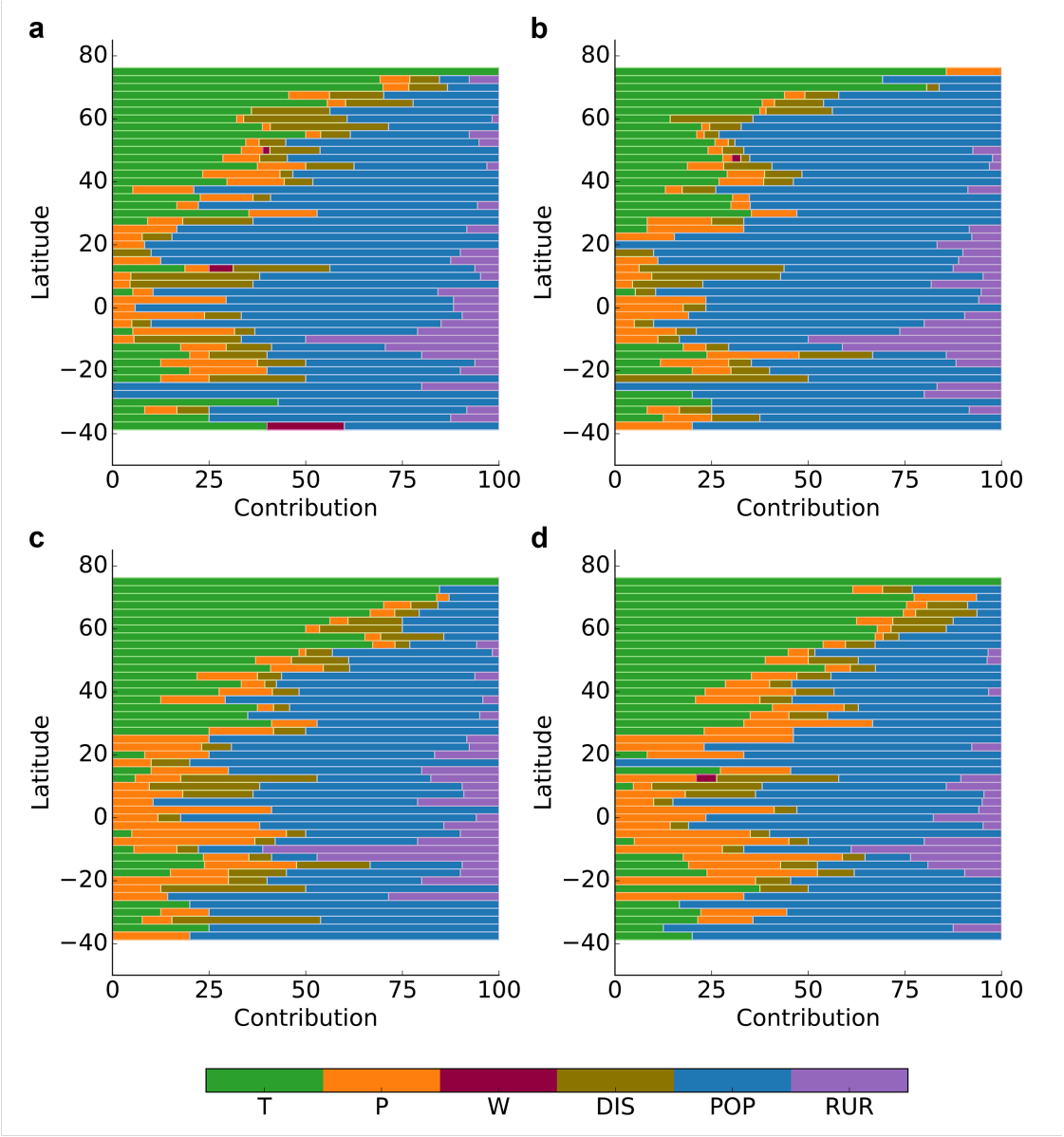

Figure 2.10 Fraction of burnt land grid cells (%) for latitudinal bands attributed to different dominant drivers of future BA change over the period 2071-2100. Shown are for the four scenarios listed in Table 2.1. Panels are (a) S1, (b) S2, (c) S3, and (d) S4. Here, we combine both positive and negative effects for each driver

2.4 Discussion

2.4.1 BA trends in present day and future

Our simulations reproduced the GFED4s-based observed decreasing BA trend over the recent historical period (Andela et al., 2017). The reasons might come from the design of the structure and process in the fire models, specific to

the description of the human activity in the model (Andela et al., 2017, Hantson et al., 2016), for example, fire termination, dependent on the distance from city, and human induced ignitions, dependent on population density and ratio of rural population, which are included in SEVER-FIRE (Venevsky et al., 2019) The spatial patterns of simulated BA trends are generally consistent with existing studies showing that large decreasing trends occurred in tropical savannas of South America and Africa (Andela et al., 2017, Kloster and Lasslop, 2017). However, the model underestimates BA in North America, where lightning has been the dominant driver of big fires recently (Veraverbeke et al., 2017). Despite SEVER-FIRE reproducing qualitatively lightning fires in this region (Venevsky et al., 2019), their number and duration and, thus, areas burnt might be underestimated. Lightning fires in boreal regions of Northern Hemisphere are influenced both by climatically determined fuel moisture and thermodynamic state of the atmosphere deserve a separate study.

For the future, our study indicates global decreasing BA trends in all but the highest atmospheric greenhouse gas emissions scenarios (S1-S3 scenario in Figure 2.6a). With highest emissions and rapid population growth and urbanization (S2 and S4 scenarios in Figure 2.6a), global BA trend will increase. These qualitative changes are determined by changes of population growth in tropical and subtropical areas and warming and drying over high latitude and mountainous areas. The largest spatial difference in BA trends among scenarios occurs during the period 2071-2100 across the Amazon and northern Eurasia (e.g., Siberia) (Figure 2.8a-d. Rapid population growth and precipitation changes is projected to lead the Amazon to change into a fire-prone ecosystem. It also causes more vegetation to be burnt in northern Eurasia areas due to climate change (Figure 2.9d), leading to a significant increasing BA trend globally, which

is consistent with Knorr et al. (2016), to some degree. Increases in BA is strongly limited by fire suppression, described by proximity to human settlements (e.g., DIS) for the present-day (Figure 2.5 limiting BA in 40% of global burnt land grid cells) and in future (see Figure 2.11, limiting factor over 47-54 % of global burnt land grid cells across the four scenarios) as it is seen from the factorial analysis. This, confirms findings of Knorr et al. (2016) on the role of urbanization on fire regimes. However, unlike their study we found that particularly strong increases in global area burnt are expected under the 'business-as-usual' scenario. That is, where emissions are highest and population growth and urbanization are the most rapid of our four experimental scenarios (S1-S4 in Table 2.1). Our sensitivity analysis covering the range of possibilities in population growth/urbanization rate to investigate the human impacts on BA dynamics suggests that rapid population growth will produce larger BA with slowing of urbanization. Urbanization offsets potential increases in global BA mainly driven by socioeconomic factors (e.g., population growth (Figure 2.7)), but appearance of new frontiers of fire suppression, related to new cities, wildfire-human settlement interface is insufficient to fully offset other factors, and therefore, one cannot rely on a decrease in areas burnt in the future simply due to the redistribution of population in cities, unless fire suppression becomes more effective with application of new technologies (e.g., improved operational satellite monitoring of fires and application of drones for termination for improved warning systems). It is also seen from our study of global BA dynamics that rapidly developing BRICS countries (including Brazil, Russia, India, China, and South Africa) might be major contributors to future global fire regimes both for climatic and anthropogenic reasons (Figure 2.8 and 2.9). Thus, fire suppression in these countries may strongly influence global BA dynamics and contribute via this mechanism to

global climate change mitigation and policy development (i.e., strategies for fire management and Reducing Emissions from Deforestation and Degradation (REDD+)) (Aragao et al., 2018, Aragão and Shimabukuro, 2010, Barlow et al., 2012). However, caution should be exercised in interpretation our results due to the single fire model used. Multiple modelling and model Intercomparison are necessary to convince our results.

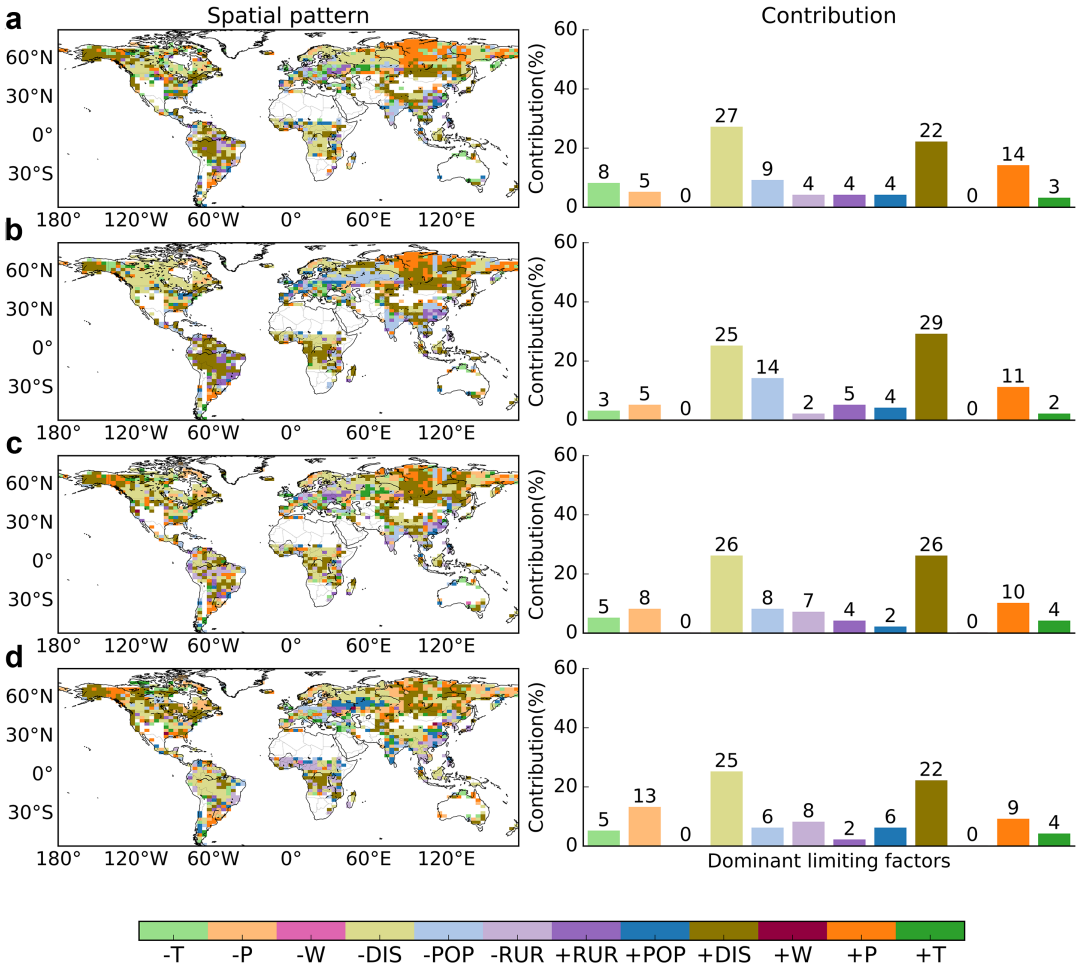

Figure 2.11 Attribution of dominant limiting factors of spatial patterns of future BA change over the period 2071-2100. Shown are for the four scenarios listed in Table 2.1. Panels are (a) S1, (b) S2, (c) S3, and (d) S4. Bar plots (right) indicate the fraction of global burnt land grid cells (%) attributed to different dominant limiting factors to BA changes at global scale

2.4.2 Drivers and limiting factors of BA trends

We demonstrated that BAs are driven to a large extent by humans at the global (Andela et al., 2017, Knorr et al., 2016) and regional scales (Syphard et

al., 2017) (Turetsky et al., 2011), now and in the future. However, human activities are represented in multiple ways and are spatially different (Archibald et al., 2009, Bistinas et al., 2014), e.g., population growth, agricultural production, fire management, and land use and land cover change except for urbanization and landscape accessibility, which have been discussed in this study. At the global scale, population density shows a strong negative relationship with recent BA change largely owing to the human-caused landscape fragmentation and fuel reduction (Bistinas et al., 2014). While at the local scale, based on the correlation analysis, the human-relevant variables (population density, cropland areas, and livestock) negatively influence BA changes in savannas and grasslands and a stronger positive relationship between population density and BA in Eurasia than North America (Andela et al., 2017), which is consistent with our findings (Figure 2.5a and b). Besides, Andela and van der Werf (2014) also suggest that recent BA trends in Africa are driven by cropland expansion over the period 2001-2012, which is not described in this study. A greater research emphasis is needed on the human pyrogenic behaviour related to land use and cultural traditions (Pereira et al., 2015). However, based on our study, climate change also dominates the future BA trends in some local areas, e.g., temperature drives high latitudinal BA changes and precipitation-dependent BA trends in the Amazon. However, the sign of climate driven impacts on BA varies by local area, leading to compensatory effects going from the local scale to the globe (Jung et al., 2017).

Other factors like lightning (Veraverbeke et al., 2017), and atmosphere, vegetation and fire regime interactions (e.g., vegetation with different susceptibility to fires impacts the local fire regime (Thonicke et al., 2001) and fire also helps to shape biome composition in flammable ecosystems (Wu et al., 2017)) and feedbacks (e.g., aerosol feedback) (Randerson et al., 2006) also

contribute to the fire dynamics. Understanding the mechanisms behind long-term BA trends is a first, yet critical, step towards better understanding the influence of human and climate and other multiple factors on fire regime, and towards improving future projections and predictions of wildfires dynamic, in order to learn how to coexist with them (Moritz et al., 2014).

2.4.3 Novelty

Although many studies have focused on future trends in global BA from wildfires, large uncertainties exist regarding this trend and its dominant drivers (Kloster and Lasslop, 2017, Knorr et al., 2016, Krawchuk et al., 2009, Moritz et al., 2012, Scholze et al., 2006). Most studies suggest an increasing trend in BA, especially during the last three decades of 21st century mainly due to climate change (Moritz et al., 2012, Scholze et al., 2006). Pechony and Shindell (2010) reported that projections of increasing fire activity are not globally uniform and have strong spatial differences. In contrast, based on a semi-empirical simple fire model (SIMFIRE), incorporated into a global dynamic vegetation model, Knorr et al. (2016) projected that the global BA will decrease under a moderate emissions scenario, and this trend is determined mainly by demographic drivers rather than climate change. SIMFIRE, however, does not differentiate between the range of possible ignition sources and in particular does not account for expected future changes in the rural-urban population distribution. Our SEVER-FIRE model extends this by including an improved description of pyrogenic human behaviours resulting from socioeconomic and demographic conditions in different geographical domains (Venevsky et al., 2019). Our study demonstrates the importance of the spatial urban-rural population distribution, which strongly influences fire termination due to human suppression in SEVER-FIRE, and thus limits the global potential BA. We also consider the complex interactions among

vegetation, human, and wildfires using a range of possible futures (i.e., multiple scenarios of changing climate and altered human demographic dynamics) using the fully coupled online framework, IMOGEN-LPJ-SEVER. This framework includes the dynamic response of ecosystems to changing fires and feedbacks between atmosphere and terrestrial ecosystems. Based on this, the topic of climate-carbon feedbacks derived from changing fires and carbon and water cycles driven by changing fires deserve further study (Harrison et al., 2018). Our analysis will help to develop wildfire management strategies in conditions of different possible future socioeconomic development paths of the world, to assess future ecological changes, and to help inform adaptation and mitigation options to global climate change.

2.5 Chapter summary

Although many studies attempt to project future BA extent, the magnitude and even the sign of the trend remain controversial, along with the dominant drivers of changes in wildfire activities. Such changes are influenced by both climatic changes and changes in social demographics (such as urbanization). A better understanding of the effects of both climate and direct human controls, as well as their mutual interactions, is required to improve projections of future BA changes.

We have revised the Lund–Potsdam–Jena (LPJ) dynamic global vegetation model to include a new process-based fire module, SEVER-FIRE which aims to take an additional closer step to a first-principle global mechanistic fire mode, capable of calculating chances in fire extent as both climate and societal demographics evolve. LPJ is placed within a coupled climate-carbon system that emulates 34 global climate models from the CMIP5 database. We show that the simulated global BA has decreased in recent decades, the global BA has actually

decreased. This result is in keeping with Andela et al. (2017) who reported a recent decreasing in global BA from remote sensing data. This consistently builds confidence in our simulation framework. Under future climate change and a range of possible societal changes, we estimate that this decreasing trend will reverse and the BA will increase. This is particularly for Amazon, northwest Eurasia, and Southeast Asia.

Our analysis is an advance on that of Knorr et al. (2016) who predicted that future fire risk will be driven mainly by human activities. Their semi-empirical fire model, SIMFIRE, does not differentiate between the range of possible ignition sources, and in particular, does not account for expected future changes in the rural-urban population distribution. Our SEVER-FIRE model extends Knorr et al. (2016) by including an improved description of pyrogenic human behaviours, resulting from socioeconomic and demographic conditions and separating potential sources of fire ignition. Furthermore, SEVER-FIRE includes a fire termination module, which allows us to directly model fire suppression by humans. We estimate that global BA would be over three times larger without expected enhanced human fire suppression and management.

Chapter 3 Fire-induced climate-carbon feedbacks

3.1 Introduction

Fire is an important disturbance in terrestrial ecosystem. Better understanding of future fire changes will be essential to the global carbon cycle and resulting feedback to climate. However, as an important component in modulating future climate change, the global-scale contribution of biomass burning to the climate-carbon feedback is poorly understood. Here, we update the Lund-Potsdam-Jena dynamic global vegetation model (LPJ-DGVM) (Sitch et al., 2003) by coupling a process-based SEVER-FIRE (Socio-Economic and natural Vegetation ExpeRimental global fire model) (Venevsky et al., 2019). The coupled system is then forced by Integrated Model Of Global Effects of climatic aNomalies (IMOGEN), which emulates 34 General Circulation Models (GCMs) from the Coupled Model Intercomparison Project Phase 5 (CMIP5), composing a fully coupled model framework (IMOGEN-LPJ-SEVER). Our study investigates the fire dynamics and possible drivers, carbon-cycle effects of fire on the global carbon cycle, and the climate-carbon feedbacks derived from changing fires and their uncertainties over the period of 1860-2100. This is performed in a fully coupled model that incorporates complex sub-models of vegetation dynamics and terrestrial and oceanic feedbacks to atmosphere under multiple pathways of emissions-dependent global warming and human demography. Our analysis will help to develop wildfire management strategies suitable for different possible future socioeconomic development pathways, to assess the future global carbon cycle, and to help inform adaptation and mitigation options to global climate change.

3.2 Methods

3.2.1 Fully coupled model framework

Our process-based SEVER-FIRE (Venevsky et al., 2019) is used to simulate fire dynamics and the role of fire in the earth system, which is coupled to the LPJ-DGVM (Sitch et al., 2003). Human and lightning ignited fires are separately designed in SEVER-FIRE and the fire carbon emissions calculations within the model follow up Venevsky et al. (2002). We innovatively introduce the pyrogenic behaviour of humans (e.g., timing of their activities and their willingness and necessity to ignite or suppress fire), which is related to socioeconomic and demographic conditions in a geographical domain of the model application, aiming for better representation of wildfire processes (Venevsky et al., 2019). LPJ-SEVER conceives the complete terrestrial biogeochemical process with fire disturbance and provides the land feedback to atmosphere via Net Ecosystem Production (NEP).

LPJ-SEVER is then forced by a common base climatology plus patterns of changing meteorological conditions fitted against the 34 CMIP5 GCMs to minimalize the uncertainties within GCMs (Huntingford et al., 2017). We employ pattern-scaling to calculate change, where regional and seasonal changes are assumed linear in global warming over land (Huntingford et al., 2010, Huntingford et al., 2013). An energy balance model calculates global warming amounts by changes in atmospheric greenhouse gases (GHGs), also fitted to the CMIP5 ensemble. This IMOGEN is operated ‘online’ with a closed carbon cycle and thus forced with anthropogenic CO_2 emissions. Annual CO_2 concentrations are updated at the end of each simulation year by annual CO_2 emissions and changes in global land and ocean carbon fluxes from LPJ-SEVER and a simple global oceanic model, respectively (Sitch et al., 2008). The extra radiative forcing

change from non-CO_2 greenhouse gases and aerosols is prescribed to the energy balance model (Huntingford et al., 2013). IMOGEN-LPJ-SEVER composed the fully coupled model framework aiming for assessing the interaction and feedback between atmosphere and land derived from changing fires.

3.2.2 Datasets and experimental design

In this study, we discuss two types of IMOGEN-LPJ-SEVER fully coupled model simulations (or fire control experiments) starting from the year 1860 after 1000 years model spin up. In a 'Standard' experiment with fire disturbance effects, the prescribed fossil fuel CO_2 emissions and external demographic and socioeconomic input (i.e., POP, RUR, and DIS) for fire model follow historical levels for the period 1860-2005 (Venevsky et al., 2019), 4 RCP emission scenarios from CMIP5 and three Shared Socioeconomic Pathways (SSP) for the period 2006-2100. This criteria of selection for SSP has been extensively discussed in Knorr et al. (2016). To isolate the carbon-cycle effects of large-scale fire on the terrestrial carbon cycles and climate-carbon feedbacks, a 'Without fire' experiment is identical to the Standard experiment except that fire disturbance is not to allowed by switching SEVER-FIRE off starting from the year 1860. In both the Standard and the Without fire cases, we perform coupled simulations for 4 RCP scenarios × 34 GCMs times (see Table 3.1).

Table 3.1 Experimental design in this study. 4 Standard Experiments (bold) were selected in different RCP scenarios for 34 GCMs runs. 9 SSP combinations (Case in the table) in each RCP scenario were used to explore the demographic uncertainties based on CESM1-BGC. Parallel experiments 'Without fire' were conducted when we switch fire module off

			Urbanization	
Case	**CO_2 emission**	**POP**	**RUR**	**DIS**
pop_slow_urb_slow	RCP2.6	SSP5(slow†)	SSP3(slow)	SSP3(slow)

Continued Table 3.1 Experimental design in this study. 4 Standard Experiments (bold) were selected in different RCP scenarios for 34 GCMs runs. 9 SSP combinations (Case in the table) in each RCP scenario were used to explore the demographic uncertainties based on CESM1-BGC. Parallel experiments 'Without fire' were conducted when we switch fire module off

pop_slow_urb_mid	RCP2.6	SSP5(slow)	SSP2(middle)	SSP2(middle)
pop_slow_urb_rap	RCP2.6	SSP5(slow)	SSP5(rapid)	SSP5(rapid)
pop_mid_urb_slow	RCP2.6	**SSP2(middle)**	**SSP3(slow)**	**SSP3(slow)**
pop_mid_urb_mid	RCP2.6	SSP2(middle)	SSP2(middle)	SSP2(middle)
pop_mid_urb_rap	RCP2.6	SSP2(middle)	SSP5(rapid)	SSP5(rapid)
pop_rap_urb_slow	RCP2.6	SSP3(rapid)	SSP3(slow)	SSP3(slow)
pop_rap_urb_mid	RCP2.6	SSP3(rapid)	SSP2(middle)	SSP2(middle)
pop_rap_urb_rap	RCP2.6	SSP3(rapid)	SSP5(rapid)	SSP5(rapid)
pop_slow_urb_slow	RCP4.5	SSP5(slow)	SSP3(slow)	SSP3(slow)
pop_slow_urb_mid	RCP4.5	**SSP5(slow)**	**SSP2(middle)**	**SSP2(middle)**
pop_slow_urb_rap	RCP4.5	SSP5(slow)	SSP5(rapid)	SSP5(rapid)
pop_mid_urb_slow	RCP4.5	SSP2(middle)	SSP3(slow)	SSP3(slow)
pop_mid_urb_mid	RCP4.5	SSP2(middle)	SSP2(middle)	SSP2(middle)
pop_mid_urb_rap	RCP4.5	SSP2(middle)	SSP5(rapid)	SSP5(rapid)
pop_rap_urb_slow	RCP4.5	SSP3(rapid)	SSP3(slow)	SSP3(slow)
pop_rap_urb_mid	RCP4.5	SSP3(rapid)	SSP2(middle)	SSP2(middle)
pop_rap_urb_rap	RCP4.5	SSP3(rapid)	SSP5(rapid)	SSP5(rapid)
pop_slow_urb_slow	RCP6.0	SSP5(slow)	SSP3(slow)	SSP3(slow)
pop_slow_urb_mid	RCP6.0	SSP5(slow)	SSP2(middle)	SSP2(middle)
pop_slow_urb_rap	RCP6.0	SSP5(slow)	SSP5(rapid)	SSP5(rapid)
pop_mid_urb_slow	RCP6.0	SSP2(middle)	SSP3(slow)	SSP3(slow)
pop_mid_urb_mid	RCP6.0	**SSP2(middle)**	**SSP2(middle)**	**SSP2(middle)**
pop_mid_urb_rap	RCP6.0	SSP2(middle)	SSP5(rapid)	SSP5(rapid)
pop_rap_urb_slow	RCP6.0	SSP3(rapid)	SSP3(slow)	SSP3(slow)
pop_rap_urb_mid	RCP6.0	SSP3(rapid)	SSP2(middle)	SSP2(middle)
pop_rap_urb_rap	RCP6.0	SSP3(rapid)	SSP5(rapid)	SSP5(rapid)
pop_slow_urb_slow	RCP8.5	SSP5(slow)	SSP3(slow)	SSP3(slow)
pop_slow_urb_mid	RCP8.5	SSP5(slow)	SSP2(middle)	SSP2(middle)
pop_slow_urb_rap	RCP8.5	SSP5(slow)	SSP5(rapid)	SSP5(rapid)
pop_mid_urb_slow	RCP8.5	SSP2(middle)	SSP3(slow)	SSP3(slow)
pop_mid_urb_mid	RCP8.5	SSP2(middle)	SSP2(middle)	SSP2(middle)
pop_mid_urb_rap	RCP8.5	SSP2(middle)	SSP5(rapid)	SSP5(rapid)
pop_rap_urb_slow	RCP8.5	SSP3(rapid)	SSP3(slow)	SSP3(slow)
pop_rap_urb_mid	RCP8.5	SSP3(rapid)	SSP2(middle)	SSP2(middle)
pop_rap_urb_rap	RCP8.5	**SSP3(rapid)**	**SSP5(rapid)**	**SSP5(rapid)**

† Similar to Table 2.1, ‘Slow’, ‘middle’, and ‘rapid’ in ‘POP’ mean the general levels of population growth rate while in ‘RUR’ and ‘DIS’, they mean urbanization rate.

Meanwhile, to minimalize the uncertainties within demographic controls, we use a GCM with roughly middle global land temperature changes in the year 2100 relative to pre-industrial, CESM1-BGC (see Figure 3.1) to perform additional 4 RCP scenarios × 9 SSP combinations (i.e., the all possibilities for population growth and urbanization rates, see Table 3.1) simulations in both the Standard and the Without fire experiments.

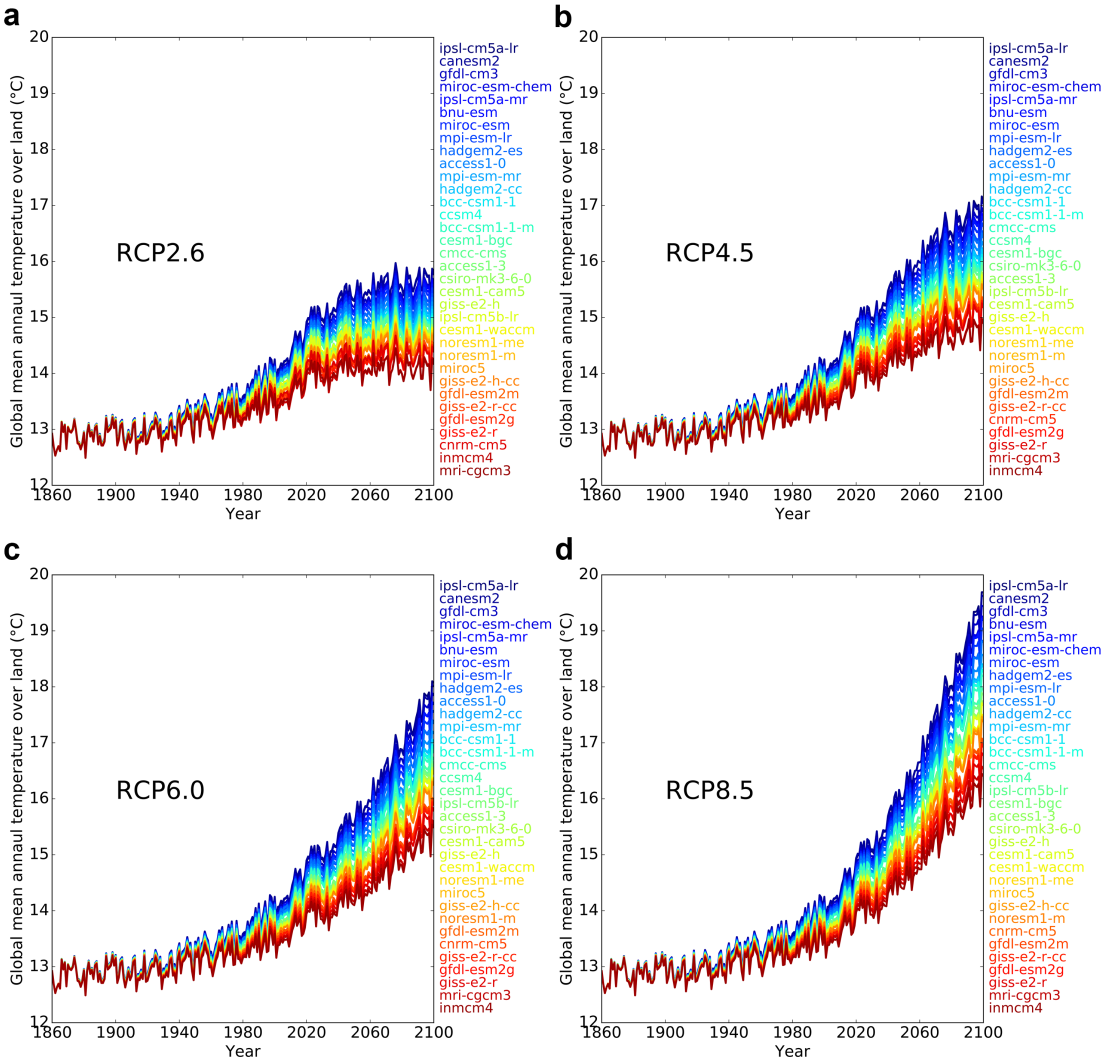

Figure 3.1 Global mean temperature over land changes. Panels are in (a) RCP2.6, (b) RCP4.5, (c) RCP6.0, and (d) RCP8.5 scenarios. Names of 34 GCMs are shown

SEVER-FIRE has been extensively validated in the previous study (Venevsky et al., 2019). Here, we compare the annual mean fire carbon emissions from the satellite-based Global Fire Emissions Database version 4

product that includes small fires (GFED4s) (van der Werf et al., 2017) with those simulated by SEVER-FIRE, and as driven by (1) ‘offline’ observed Climate Research Unit (CRU)/National Centers Environmental Prediction (NCEP) climatology (Harris et al., 2013, Kalnay et al., 1996) and (2) climate forcing based on 34 GCMs over the period 1997-2013, respectively. Figure 3.2 suggests a convincing simulation for our model, especially for the good agreement on the pattern of fire carbon emissions in Austria, Southeast Asia, South America, large parts of North America, and northern Eurasia between satellite data, offline simulations forced with observed climate, and the GCM-ensemble projections. However, we underestimate the fire emitted carbon in large areas of savanna in middle part of Africa, this can be attributed to underestimate the long-term effects of fire regime changes on soil carbon and nitrogen limitations (no nitrogen cycle process is included in our coupled model (Sitch et al., 2003)) on plant growth in large savanna regions (Pellegrini et al., 2018).

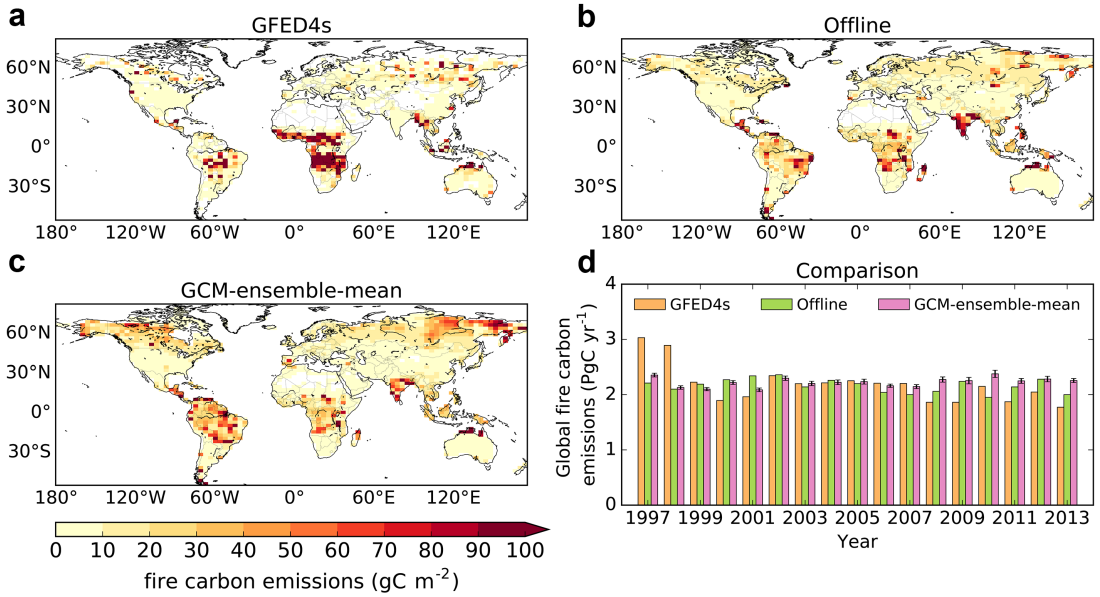

Figure 3.2 Present-day fire carbon emissions. Spatial mean annual fire carbon emissions over the period 1997-2013 observed from (a) GFED4s, simulated by (b) SEVER-FIRE (offline), and (c) SEVER-FIRE (mean across the 34 GCMs emulated). (d) Global fire carbon emissions over the period 1997-2013. Offline: the global fire carbon emissions driven by CRU/NCEP observed climatology. GCM-ensemble mean: the mean of global fire carbon emissions simulated by SEVER-FIRE across the 34 GCMs emulated. Error bars represent the standard deviation of 34 GCM ensemble members

3.2.3 Analysis

The carbon-cycle effects of fires on terrestrial carbon cycles and carbon-climate feedbacks are described as the difference in the Standard experiment relative to the Without fire case. However, this effect exists an initial but small signal in climate from 1860 to 1950 owing to the unavailable demographic and socioeconomic input for fire model before the year 1950. Global temperature change is the main evaluation to explore the carbon feedback to climate derived from changing fires. Following up Huntingford et al. (2010), global (spatial-) mean annual average temperature change $\Delta T_{Global,yr}$ (K) is computed as:

$$\Delta T_{Global,yr} = f \times \Delta T_{Ocean,yr} + (1 - f) \times \Delta T_{Land,yr}, \quad \text{Eq. (3.1)}$$

where yr is simulation year, f is the GCM-specific parameter of global fraction of Earth covered by ocean, $\Delta T_{Land,yr}$ (K) and $\Delta T_{Ocean,yr}$ (K) are the

warming anomalies from pre-industrial (year 1860) over the land and oceans, respectively. They are calculated as:

$$\Delta T_{Land,yr} = T_{Land,yr} - T_{Land,1860}, \quad \text{Eq. (3.2)}$$

$$\Delta T_{Ocean,yr} = \frac{\Delta T_{Land,yr}}{\mu}, \quad \text{Eq. (3.3)}$$

where $T_{Land,yr}$ (K) is the global (spatial-)mean annual average temperature over land, μ is a GCM-specific land-sea temperature contrast parameter, linearly relating warming over land $\Delta T_{Land,yr}$(K) to warming over ocean $\Delta T_{Ocean,yr}$ (K).

The feedback from land to atmosphere $Feed_{Land\_to\_atm}$ (PgC yr^{-1}) is computed as:

$$Feed_{Land\_to\_atm} = -NEP = RH + C_{Fire} - NPP, \quad \text{Eq. (3.4)}$$

where NEP (PgC yr^{-1}) is net ecosystem production, C_{Fire} (PgC yr^{-1}) is fire carbon emissions. A positive value of $Feed_{Land\_to\_atm}$ indicates a net carbon source for land while a minus value suggests a net carbon sink for land.

3.3 Results

3.3.1 Carbon-cycle effects of fire on global carbon cycle

With global warming, atmospheric CO_2 concentration will increase to 982 ± 36 ppm at the end of 21st century in the 'business as usual' (i.e., RCP8.5) scenario while large variations in projected future atmospheric CO_2 concentration within emission scenarios in the Standard experiment (see Methods and Figure 3.3a) (unless otherwise specified, reported numbers are the ensemble mean across 34 GCMs simulated in IMOGEN-LPJ-SEVER ± 1 standard deviation). The CO_2 concentration difference suggest that the carbon-cycle effects of fires in RCP8.5 contribute the most (22 ± 3 ppm) to the CO_2 concentration changes, globally compared to the additional three RCP scenarios (Figure 3.4a). In the

Standard experiment, our results indicate a net increasing carbon sink in the present-day terrestrial ecosystem (Piao et al., 2018), e.g., in the 1990s, simulated land–atmosphere fluxes of -2.0 $\pm$ 0.9 PgC yr^{-1} (Figure 3.3b) are close to the IPCC mean value of -2.6 and range of -4.3 to -1.0 PgC yr^{-1} (Sitch et al., 2008). However, the magnitude of future land uptake varies markedly among scenarios even positive land-atmosphere fluxes in lower emission scenarios suggest a net carbon source for land (Figure 3.3b). Fire shows a weakening negative role on the land carbon sequestration since pre-industrial but the effects will be stronger in the higher emission scenarios during the second half of 21st century (Figure 3.4b). Fire increase net primary production (NPP) since large variations (ranges of 0.8 $\pm$ 0.2 to 1.4 $\pm$ 0.1 PgC yr^{-1} in 2100) exist in the different scenarios. This may be because fire enriches nutrients through re-deposition (Pellegrini et al., 2018). Furthermore, anthropogenic CO_2 emissions may limit the re-deposition process, resulting less NPP difference in higher CO_2 emission scenarios (Figure 3.4c). Fire decreases heterotrophic respiration (RH) ranging from 0.9 $\pm$ 0.1 to 2.1 $\pm$ 0.3 PgC yr^{-1} in 2100 among future scenarios because of litter/biomass combustion, leading to reduced input to soil C pools (Figure 3.4d). Similarly, at most 21.2 $\pm$ 3.8 and 47.0 $\pm$ 2.8 PgC yr^{-1} losses of vegetation and soil carbon are predicted resulting from fire disturbance in 2100, respectively (Figure 3.4e, f).

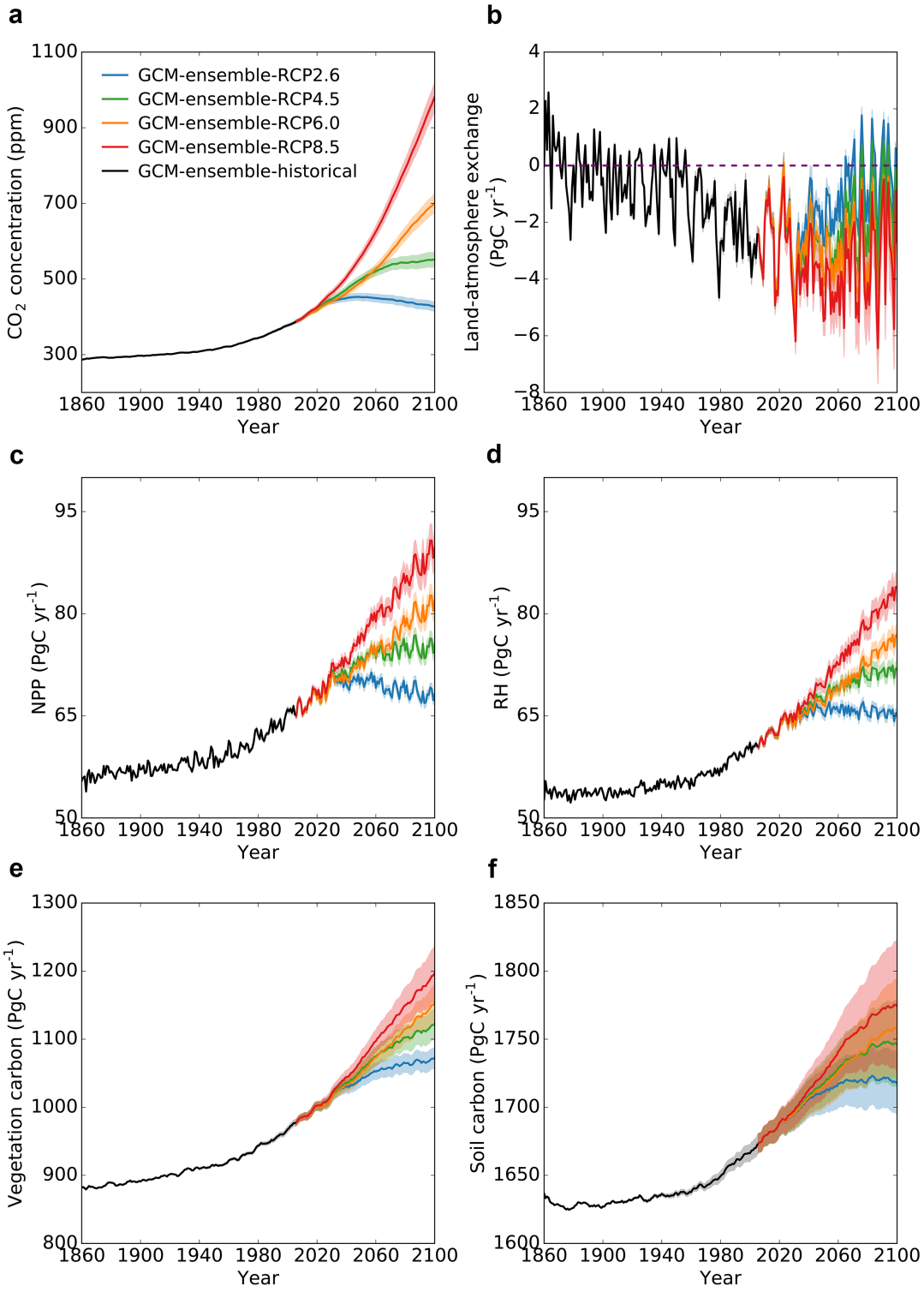

Figure 3.3 Global terrestrial carbon cycle. Simulated annual (a) CO_2 concentration, (b) land-atmosphere exchange, (c) NPP, (d) RH, (e) vegetation carbon, and (f) soil carbon for the Standard experiments in 4 RCP scenarios over the period 1860-2100. GCM-ensemble are the mean values simulated by the fully coupled model across the 34 GCMs emulated. The shaded areas represent the standard deviation of 34 GCM ensemble members

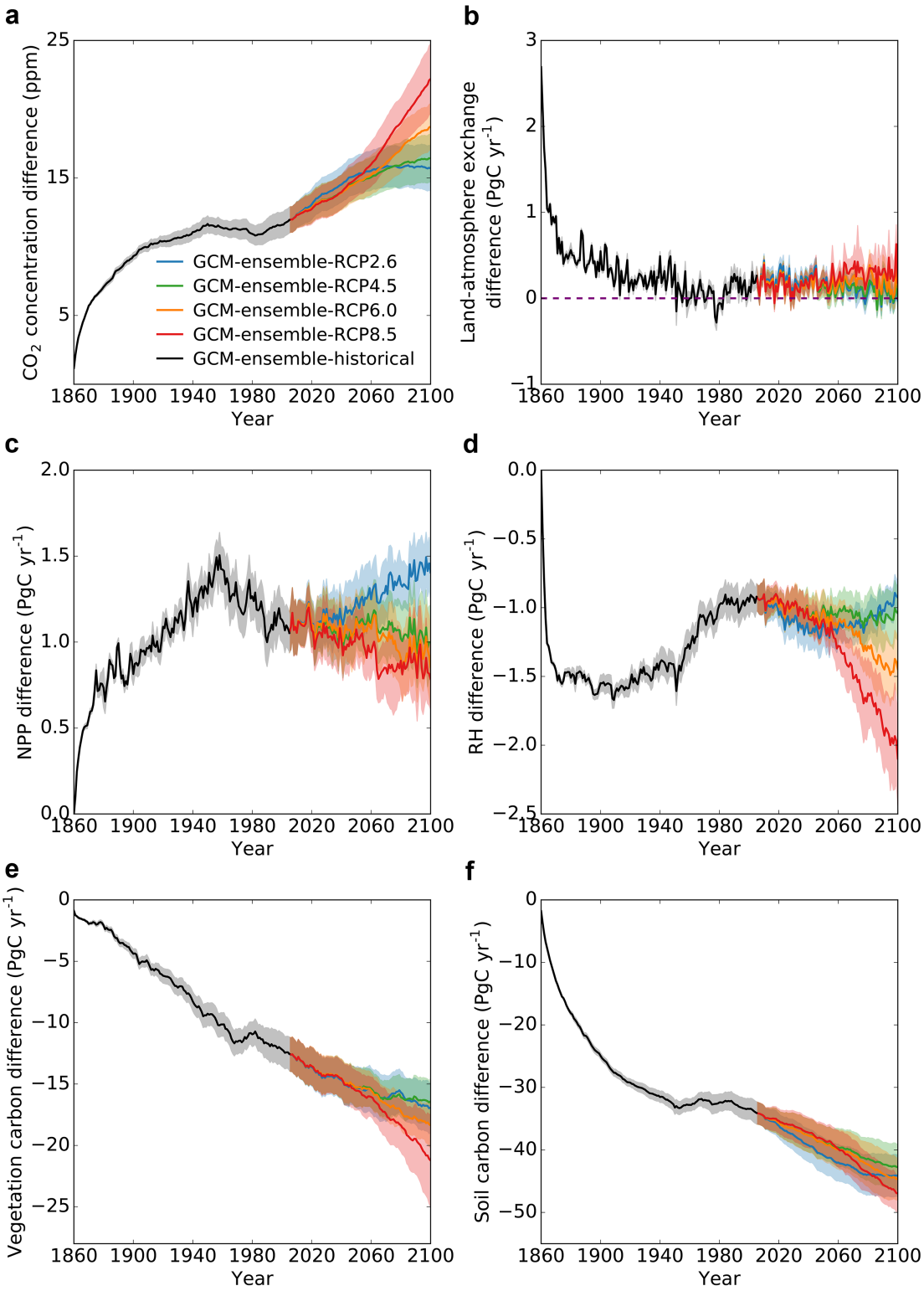

Figure 3.4 Carbon-cycle effects of fire on global carbon cycle. Simulated annual (a) CO_2 concentration, (b) land–atmosphere exchange, (c) NPP, (d) RH, (e) vegetation carbon, and (f) soil carbon difference between the Standard experiments and the 'Without fire' experiments in 4 RCP scenarios over the period 1860-2100. GCM-ensemble are the mean values simulated by the fully coupled model across the 34 GCMs emulated. The shaded areas represent the standard deviation of 34 GCM ensemble members. The purple horizontal line: land-atmosphere flux is equal to zero

Figure 3.5 shows that the historical total carbon storage increases with global warming and higher atmospheric CO_2 concentration in both the Standard and the Without fire experiments, suggesting an increasing carbon sink for land. The land carbon storage sensitivity to global temperature changes in the Standard case is lower than that in the Without fire case, indicating a negative fire carbon-cycle effect on carbon storage. Land continues to be a net carbon sink and fire carbon-cycle effect will be stronger with global warming and CO_2 concentration increasing in the higher emission scenarios, i.e., RCP4.5, RCP6.0, and RCP8.5. However, when CO_2 concentration or temperature changes achieve their peaks (164 ppm or 1.74 °C in the Standard case), i.e. productivity no longer increases allowing RH to 'catch-up', and in fact the land starts to revert to a net carbon source (see Figure 3.5, 3.4b, and Figure 3.3b) in the mitigation scenario, i.e., RCP2.6. In addition, our result in the Standard case suggests that both RCP2.6 and RCP4.5 scenarios could constitute a safe upper limit to global warming 2.0 °C target and only RCP2.6 scenario will achieve 1.5 °C at the end of 21st century when carbon-cycle effect of fire is considered (Figure 3.5b).

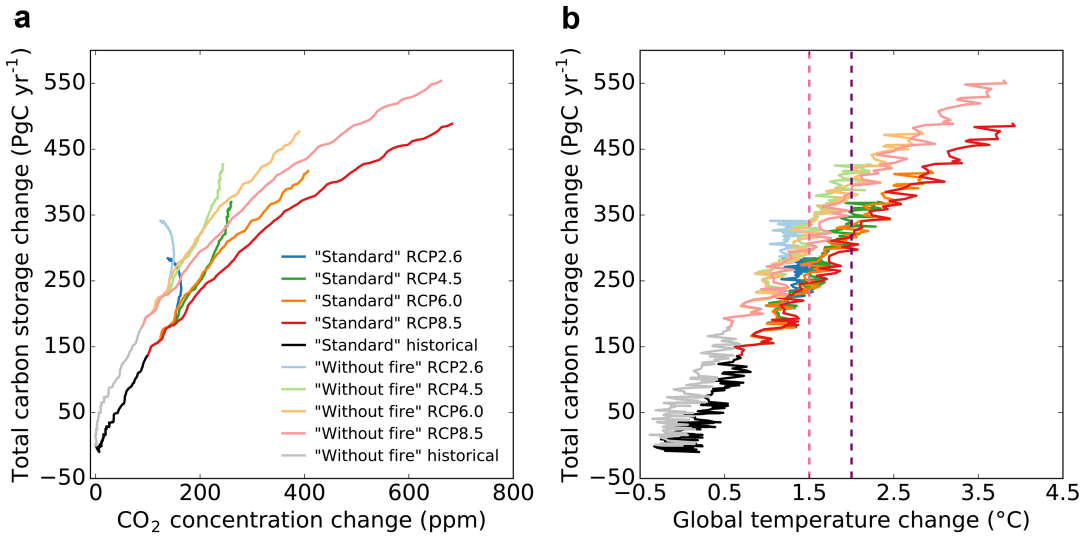

Figure 3.5 Simulated land carbon storage sensitivity to atmospheric CO_2 concentration and global temperature. Simulated change in land carbon storage sensitivity to change in (a) atmospheric CO_2 concentration and (b) global mean temperature relative to pre-industrial (1860) for the Standard experiments and the 'Without fire' experiments in 4 RCP scenarios based on CESM1-BGC. Pink and purple vertical lines represent global temperature increasing 1.5 and 2.0 °C lines, respectively. The range between two experiments represents the fire carbon-cycle effects on total carbon storage

3.3.2 Climate-carbon feedbacks derived from changing fires

Fire changes significantly with global warming and human demography (Kloster and Lasslop, 2017, Knorr et al., 2016). Figure 3.6 shows that the global fire carbon emissions decrease since the 1950s, which agrees well with Arora and Melton (2018). However, a wide range of emitted carbon from fires are simulated in the future with different CO_2 fossil fuel emissions forcing (Figure 3.6a). Even within the same RCP scenario, uncertainties in global fire carbon emissions come from both GCMs-dependent climate (Figure 3.6a) and demographic controls (Figure 3.6b). In the Standard cases, fire emits more carbon in RCP2.6 than RCP4.5 scenario, this results from our experimental design of the specific combination between emission and demographic scenarios (see Table 3.1) based on van Vuuren et al. (2011), in which population growth is faster in RCP 2.6 than RCP4.5 scenario in the future projection. This suggests

that population growth might be the principal driver on global fire carbon emissions. In addition, SSP-ensemble results show that fire emissions follow up the order of fossil fuel emissions scenarios in the future (Figure 3.6b), together with Figure 3.6a, indicating an important role of human activities in global fire dynamics.

Relative to fire carbon emissions, the carbon-cycle effects of fire on the projected atmospheric CO_2 concentration and global temperature changes are robust in the divergent RCP scenarios, especially for the last 20 years of 21st century (Figure 3.6c-f). Atmospheric CO_2 concentration difference relative to the Without fire cases for GCM-ensemble and SSP-ensemble simulations over the period 2081-2100 indicate a positive carbon-cycle effects of fire on global atmospheric CO_2 concentration. For the GCM uncertainties, fire increases mean atmospheric CO_2 concentration by 16, 16, 18, and 21 ppm in the RCP2.6, RCP4.5, RCP6.0, and RCP8.5 scenarios over the period 2081-2100, respectively (Figure 3.6c). Similarly, 15, 17, 19, and 22 ppm higher fire-induced CO_2 concentration in the Standard than the Without fire case in the corresponding scenarios are performed by SSPs-ensemble simulations (Figure 3.6d). However, both GCMs and SSPs uncertainties simulations present reverse trends between atmospheric CO_2 concentration difference and global mean temperature difference induced by fire disturbance, i.e. higher CO_2 concentrations difference leads to lower temperature changes, since our results suggest a positive climate-carbon feedback derived from changing fires (Figure 3.6c-f). For example, in the 'mitigation scenario' over the period of 2081-2100, fire increases global mean temperature by 0.18 ± 0.04 (or 0.17 ± 0.01) °C (GCMs (or SSPs) uncertainties) while in the 'business as usual' scenario, carbon-cycle effects of fire contribute to 0.13 ± 0.03 (or 0.14 ± 0.01) °C (here, reported numbers in the brackets are the

ensemble mean across 9 SSP combinations simulated in IMOGEN-LPJ-SEVER ± 1 standard deviation, see Table 3.1). This indicates that fire is extremely important to restrict global warming to below the agreed 1.5 °C targets, i.e., fire takes up around 10% of the distance to the 2.0 °C warming threshold for Paris Agreement.

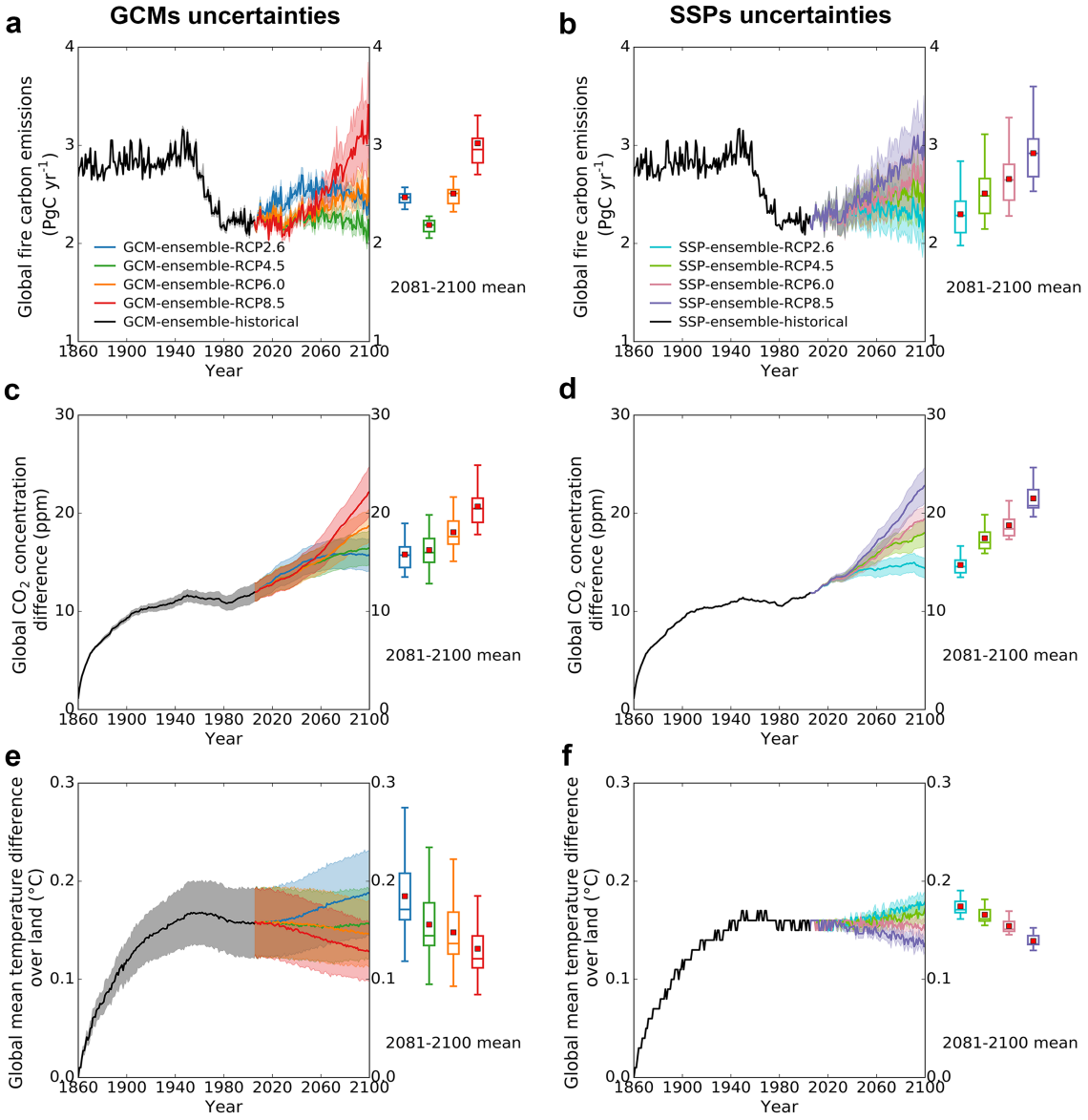

Figure 3.6 Climate-carbon feedback derived from changing fires. Global fire carbon emissions (a, b), global CO_2 concentration difference (c, d), and global mean temperature difference over land (e, f) between the Standard experiments and the 'Without fire' experiments in 4 RCP scenarios over the period 1860-2100. (a), (c), and (e) show the mean values simulated by the fully coupled model across the 34 GCMs emulated; (b), (d), and (f) represent the mean values simulated by the fully coupled model across the 9 SSP combinations emulated using CESM1-BGC. The shaded areas represent the standard deviation of 34 GCM or 9 SSPs combinations ensemble members. Box plots shows the mean values over the period 2081-2100 and red squares within the boxes represent mean values of ensemble members

The spatial pattern of temperature differences over land suggests that the strongest warming effects from fire is associated with the boreal forest fires in the Northern Hemisphere high latitudes over the period 2081-2100. However, the tropical fires in South America, Africa, Southeast Asia, and Austria contribute less to global warming (Figure 3.7a). With the higher emission scenarios, carbon-cycle effects from boreal forest fires weaken since they are still the main contribution of fire-induced global warming and less warming is simulated in the other parts of the world (Figure 3.7c, e, g). The mean grid-cell magnitude of temperature difference over land components for latitudinal bands reveals an obvious decreasing trend of fire-induced warming effects from high latitudes in Northern Hemisphere to high latitudes in Southern Hemisphere. This is because in general, warming over high latitude land regions is predicted by ESMs to be much high than the global mean (Huntingford and Mercado, 2016), expected in part due to polar amplification accounted by the snow-ice-albedo effect (Holland and Bitz, 2003) (Figure 3.7b, d, f, h).

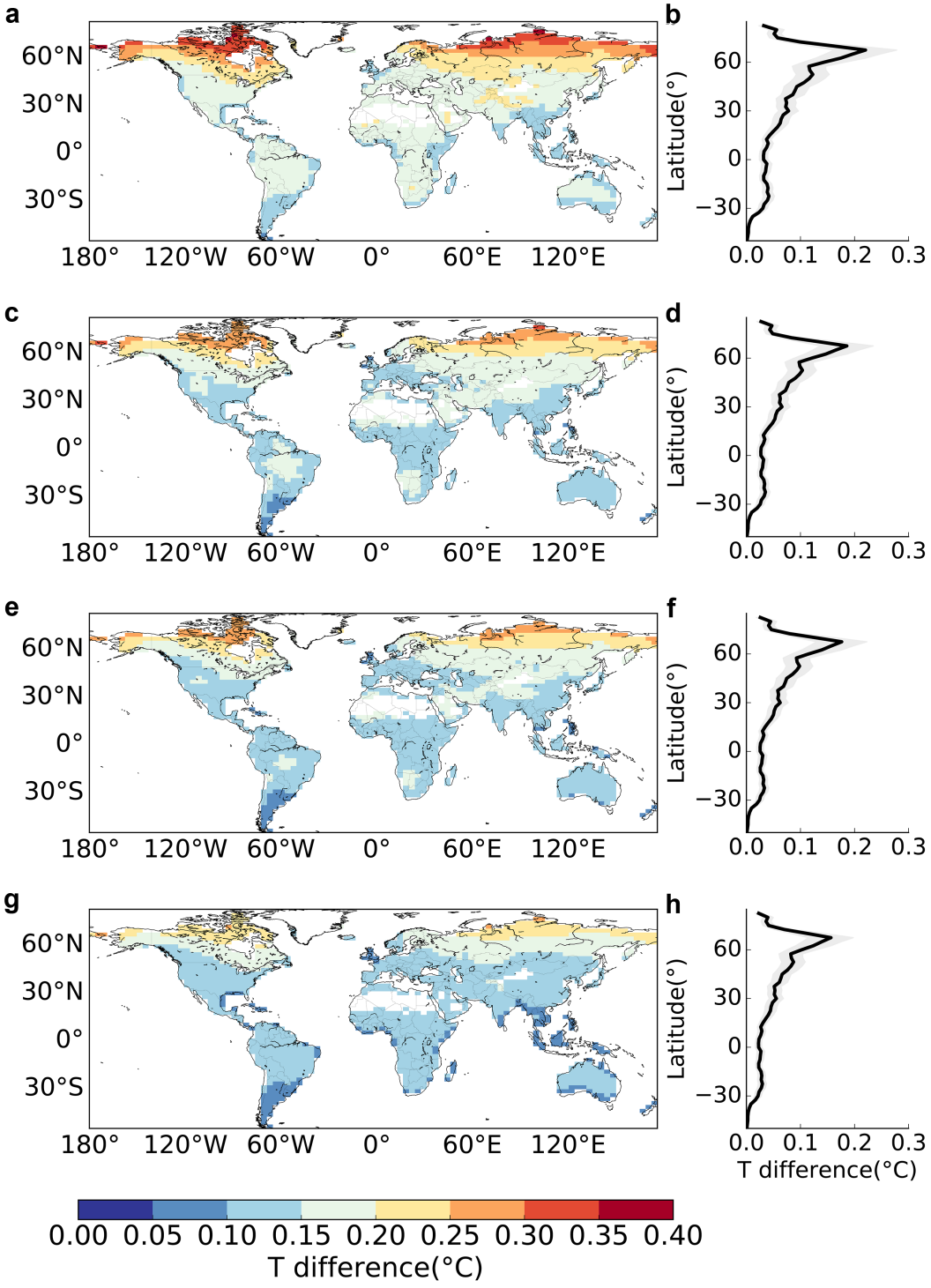

Figure 3.7 Carbon-cycle effect of fire on future global land temperature. Simulated spatial mean temperature (T) differences over burnt land between the Standard experiments and the 'Without fire' experiments in (a) RCP2.6, (c) RCP4.5, (e) RCP6.0, and (g) RCP8.5 scenarios over the period 2081-2100. Burnt land are retrievals of where there are areas burnt based on fire emissions in corresponding scenarios. (b), (d), (f), and (h) show mean grid-cell magnitude of temperature difference over land components for latitudinal bands in the same period. The shaded areas represent the standard deviation of 34 GCM ensemble members

3.3.3 Demographic drivers of fire in low CO_2 emission scenario

As mentioned fire's importance on achieving 1.5 °C global warming target, to explore the demographic controls on fires and resulting fire carbon-cycles effects on climate, we conduct simulations in RCP2.6 scenario based on every possibility of the combination between population growth and urbanization rate (Figure 3.8 and Table 3.1). Figure 3.8 reveals that the global fire carbon emission is dominantly driven by population density as it will produce more potential fire ignitions. Scenarios with more rapid population growth and slower urbanization produce higher fire carbon emissions and the range of all possibilities is from 1.8 to 2.7 PgC yr^{-1} in 2100. However, the demographic uncertainty of global land mean temperature difference is small relative to fire carbon emissions, ranging from 0.20 °C in the scenario of rapid population growth and slow urbanization rate to 0.17 °C with slow population changes and middle urbanization rate (Figure 3.8b) at the end of 21st century. Similarly, population density drives the carbon-cycle effects of fire on climate. Our results suggest that the actions controlling population increases and moderately urbanization might help to mitigate global warming below the agreed 1.5 °C targets.

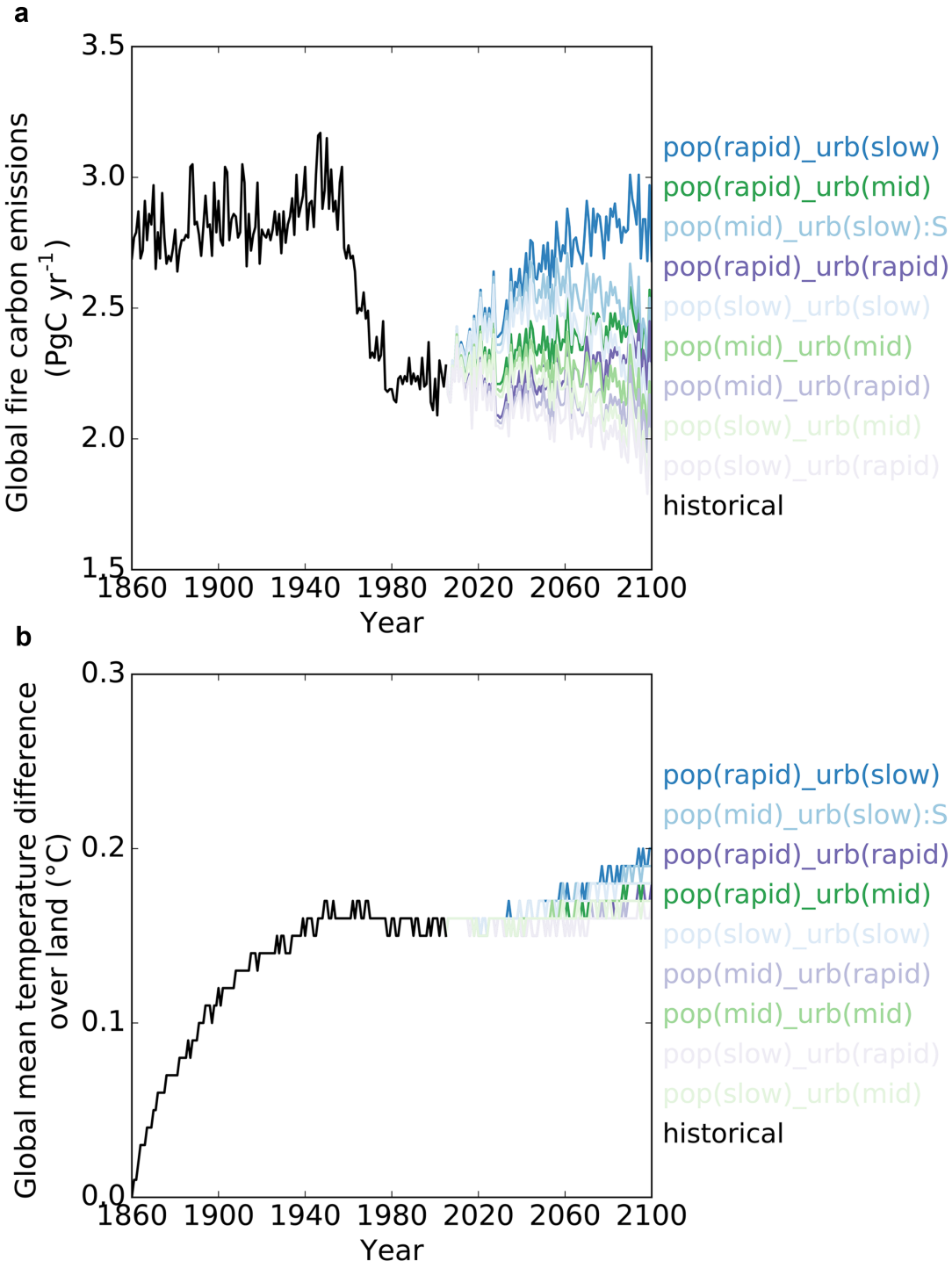

Figure 3.8 Demographic Uncertainties of global fire carbon emissions and temperature difference over land. Global fire emissions (a) and global mean temperature difference over land (b) between the Standard experiments and the ‘Without fire’ experiments among 9 SSP combinations in RCP2.6 scenario. ‘pop’, population density; ‘urb’, urbanization; ‘historical', historical period; ‘Slow’, ‘mid’, and ‘rapid’ reveal the general levels of population growth rate or urbanization rate over the future period

3.4 Discussion

3.4.1 Terrestrial carbon cycle and the impact from fires

Understanding how the fire regime, specific to fire emitted carbon will change induced by climate change is essential to the future of territorial carbon sink (Pellegrini et al., 2018). Our results suggest that after a strong reduction since the 1950s (Arora and Melton, 2018), the global fire carbon emissions will change dramatically dependent on the anthropogenic CO_2 emissions (2.0 ± 0.1 to 3.1 ± 0.4 PgC yr^{-1} in 2100 in Figure 3.6a) and demographic controls, especially for population growth (2.1 ± 0.3 to 2.9 ± 0.3 PgC yr^{-1} in 2100 in Figure 3.6b) and this is consistent with the projected future global fire carbon emissions from multiple Earth system models (Kloster and Lasslop, 2017). Although we indicate that fire generally restricts land carbon sequestration in the historical period with the associated reduced fire carbon emission, fire shows a signal of accelerating terrestrial carbon sink during the 1960s to 1990s, associated with reduced fire carbon emissions (Figure 3.4b). This may result from fire suppression and landscape fragmentation rather than potential cropland expansion (Arora and Melton, 2018). However, whether beneficial or restrictive from fire on global terrestrial carbon sink in the future is dependent on the future human society development, i.e., fossil fuel CO_2 emissions and resulting fire carbon emissions (Figure 3.4b). Except for fire emitted carbon, the net effects of fire on land carbon uptake also depend on NPP and HR. Fires accelerate the natural cycle of primary production (Bowman et al., 2009) and stimulate plant productivity (Knapp and Seastedt, 1986) mainly by promoting the establishment of more-productive plant species and the leaching of ash downwards into soils to enrich the soil nutrients (Pellegrini et al., 2018, Wan et al., 2001) (Figure 3.4c). While increased burning

may consume soil organic matter, because repeated burning reduces organic inputs to soils and leads to declines in soil carbon (Figure 3.4f) and nutrients and then decease NPP (Pellegrini et al., 2018, Reich et al., 2001). Since fire accelerate RH by increasing microbial decomposition, our results showed decreased global RH by fires is possibly attributed to the dead plant material/litter burnt by fires. However, caution should be exercised in interpretation because our estimates of fire-driven carbon losses, which primarily focus on losses from vegetation biomass pools, may underestimate the effects of long term changing fires in savanna grasslands (Pellegrini et al., 2018), e.g., our results show lower fire carbon emissions in African savannas than satellite observations (Figure 3.3a-c).

3.4.2 Fire feedback to climate

Fire-disturbance-induced terrestrial ecosystem change has been found to be an important uncertainty for climate prediction (Liu et al., 2019). The overall feedback between fires and climate is complicated because not only changes of the CO_2 budget are involved, but also variations in biophysical changes, e.g., albedo (Randerson et al., 2006), heat and moisture fluxes (Heinze et al., 2018), and changes in aerosol forcing (Andela et al., 2017, Bowman et al., 2009). Our model suggests an approximate global-mean warming of ~0.16 °C from carbon-cycle effects over the period 2005-2014 (Figure 3.6e, f). If we further assume that the transient temperature increasing of 0.15 °C from biophysical effects of forest fires (Liu et al., 2019), the warming net effect of carbon-cycle and biophysical from global fires is around 0.31 °C, and this effect will be stronger with climate change and human demography, indicating that fire management (Figure 3.7 and Liu et al. (2019)) is decisive to climate change mitigation, especially importance to restrict global warming to below the agreed 1.5 °C targets.

We may overestimate the positive role of fire on climate owing to not considering biophysical impact from fires, e.g. aerosols, surface albedo variations in our model (Sitch et al., 2003, Venevsky et al., 2019). The resulting changes of negative radiative forcing from increasing albedo after fires should be used to update the averaged radiative forcing together with fire emitted greenhouse gases in the fully coupled model, suggesting the necessity to include energy budget in the future development of global fire model. However, associated with the biophysical effects of fire on climate exist a larger uncertainty (Arneth et al., 2010) even contradiction. For example, Randerson et al. (2006) suggested strong negative radiative forcing of albedo changes after boreal fires would suppress climate warming, while Liu et al. (2019) found that the biophysical effect of fire on land surface temperature is much stronger in higher latitude boreal regions, resulting in a strong positive climate-fire feedback. Furthermore, the influence of albedo changes on climate might be very limited. For instance, although changes in boreal forest albedo can have a considerable cooling effect on Northern Hemisphere climate, these changes are offset by accompanying changes in carbon sequestration (Betts, 2000), so the net effect of land cover change on climate may be close to neutral at a global scale when both surface energy balance and CO_2 fluxes are considered (Randerson et al., 2006). However, caution should be exercised in explaining the results due to the uncertainties existed in our study. For example, the fully coupled framework is only based on one vegetation-fire model. Although SEVER-FIRE enables us to better estimate the fire dynamics, it is still on the way to the fully mechanism global fire model. In addition, the uncertainties also come from the forcing datasets (both climate and socioeconomic forcing) and the results. Multiple fire models Intercomparison studies are needed to confirm and estimate our results.

3.4.3 Novelty

Despite growing interest in the influence of climate change, demographic drivers, and plant species on fire dynamics (Andela et al., 2017, Bowman et al., 2009, Knorr et al., 2016, Rogers et al., 2015), the global-scale contribution of biomass burning to the climate-carbon feedback has been poorly quantified (Harrison et al., 2018). Inclusion of pyrogenic behaviour of humans may allow SEVER-FIRE to produce a more realistic estimation of future fire risks and feedbacks. We use a fully coupled model to comprehensively quantify the biogeochemical effects of fire on global temperature changes under multiple CO_2 emission and SSP scenarios and analyse the uncertainties that stem from both GCMs discrepancies and human behaviours. The results presented here highlight the need to employ climate-carbon models to comprehensively evaluate the carbon cycle effects of fire on climate, especially as fire regimes change under global warming, and suggest an important role for fire on climate mitigation to achieve the Paris Agreement.

3.5 Chapter summary

Here we present results from global-scale fire control experiments performed with a fully coupled global fire-vegetation-climate-carbon model system that emulates 34 climate models from the CMIP5 database. We find that fire increased annual global-mean temperature by ~0.16 °C yr^{-1} owing to carbon-cycle effects over the period 2005-2014. Future global fire carbon emissions will change dramatically depending on anthropogenic CO_2 emissions and the level of human influences (2.0 to 3.1 PgC yr^{-1}). We estimate that fires will contribute approximately 15–22 ppm yr^{-1} to increasing atmospheric CO_2 concentrations and about 0.13 to 0.18 °C yr^{-1} to global-mean warming. Fire impacts are especially

strongest at high latitudes. However, we also find the unexpected result that fire-induced increases in CO_2 concentrations show a robustly reverse trend to fire-induced global warming among the analysed anthropogenic emissions and demographic development pathways.

Chapter 4 Impact of fire on regional vegetation distribution

4.1 Introduction

Climate is as an important determinant of biogeography. Although climate is directly important for vegetation composition in boreal forests, these ecosystems are strongly sensitive to indirect effects of climate via fire disturbances. However, the balance between fire disturbances and climate in driving variations of biome composition is poorly understood. In this study we quantitatively analyse the individual contributions of these two factors for the boreal forests of Heilongjiang province, China, and their responses to climate change under four global warming scenarios (+1.5, 2.0, 3.0, and 4.0 °C). This study employs the statistical methods Redundancy Analysis (RDA) and variation partitioning combined with simulation results from a Dynamic Global Vegetation Model, SEVER-DGVM, remote sensing global land cover data (GLC2000) and the Global Fire Emissions Database (GFED3). The results show that the present-day vegetation distribution is mainly determined directly by climate (35%) rather than by fire (1%-10.9%). However, with a future global warming of 1.5 °C, the local vegetation composition may be determined more by fires than by climate (36.3% > 29.3%). Above a 1.5 °C warming, temperature becomes more important than fires in regulating the vegetation distribution, although other factors like precipitation also contribute. The spatial pattern of vegetation composition over the region, as evaluated by a Moran's Eigenvector Map (MEM), has a significant impact on local vegetation coverage; i.e. composition at any individual location is highly related to that in its neighbourhood. This factor represents the largest contribution to the vegetation

distribution in all scenarios, but this has no obvious impact on the balance between climate and fires in driving biome composition. Our results are highly relevant for forest and wildfire management.

4.2 Methods

4.2.1 Study area

The study area is located in Heilongjiang province between 42°30′–51°20′N and 121°40′–128°30′E in northeast China, covering an area of around 4.54×10^5 km^2. The summers are usually hot and humid while the winters are cold and dry. The mean annual temperature is between –4 and +5°C from north to south and the annual precipitation ranges from 400 to 700 mm from west to east (Zhang et al., 2015). The main vegetation types include Evergreen Needleleaf Forest (ENF), Deciduous Needleleaf Forest (DNF), Deciduous Broadleaf Forest (DBF) and cultivated and managed areas/grass land (see Figure 4.1 and Table 4.1) based on the remote sensed GLC2000 (Bartholomé and Belward, 2005). Existing research shows that historically, the most common fire type was frequent, low intensity surface fires mixed with infrequent stand-replacing fires in this area and Burnt Area (BA) was usually large with fire return interval ranged from 30 to 120 years and the average number of fires was 317 per year during 1980 – 1987 (Dahl, 1979, Liu et al., 2012). However, after a catastrophic fire which was occurred in 1987 in this area, burning a total area of 1.3Mha, forest harvesting and fire suppression have changed the fire regime of this area. Currently, fire regime is characterized by infrequent but more intense fires and larger BA, with a fire return interval of more than 500 years (Chang et al., 2008, Liu et al., 2012). The total number of grid cells in Heilongjiang province is 216 at a spatial resolution of 0.5° × 0.5°.

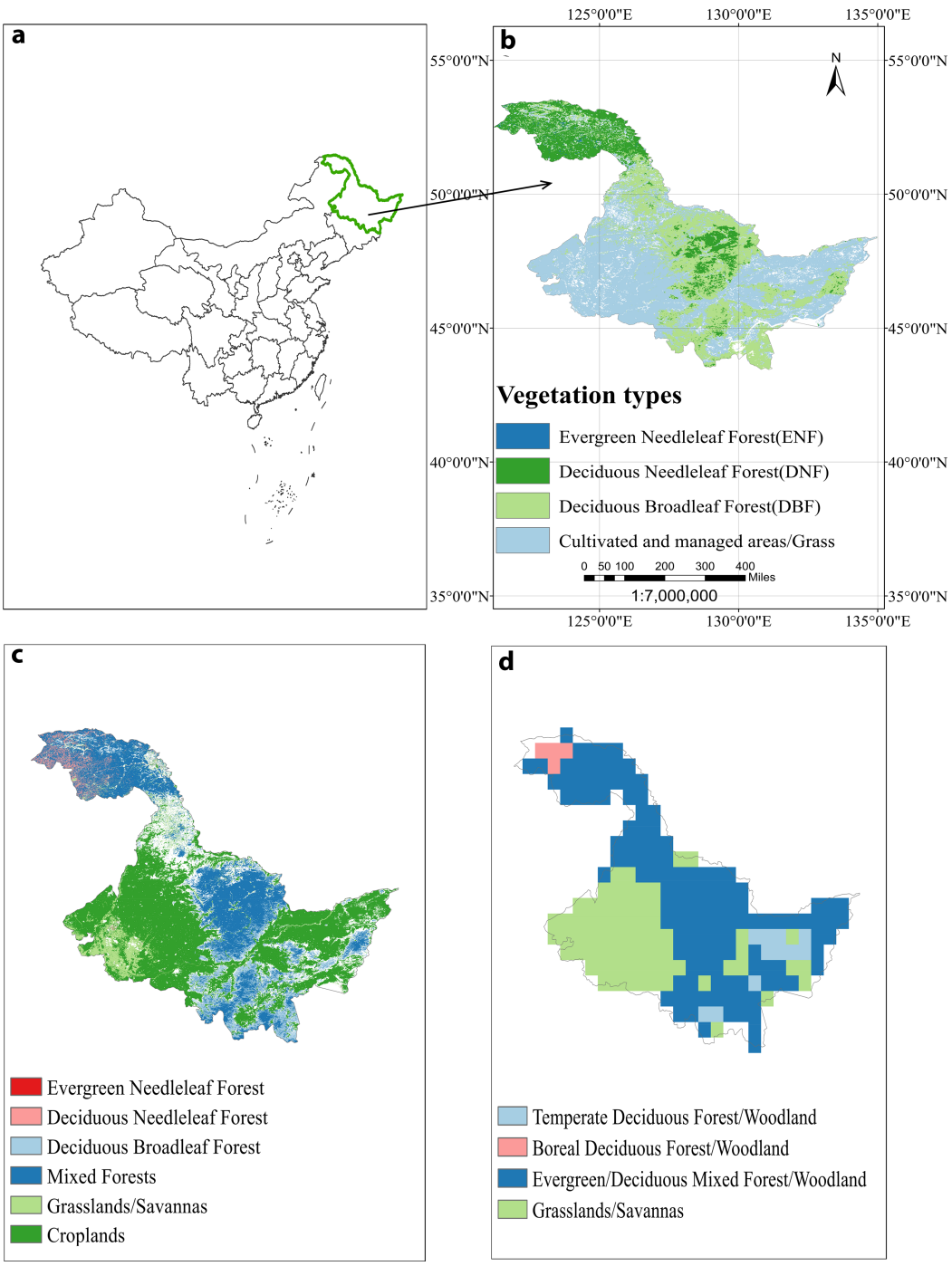

Figure 4.1 Location and dominant vegetation types in Heilongjiang province. The source of datasets is from (b) GLC2000, (c) 0.5 km MODIS-based Global land cover climatology, and (d) Global potential vegetation dataset

Table 4.1 Plant Function Types (PFTs) in SEVER-DGVM and corresponding DGVM phenology and the GLC2000 legend (according to FAO Land Cover Classification System (LCCS)) in Heilongjiang province, China

PFTs in SEVER-DGVM	Phenology Class	GLC Global Class (GLC ID)
Tropical broad-leaved evergreen (TrBE)	Evergreen Broadleaf Forest (EBF)	†
Tropical broad-leaved raingreen (TrBR)	Deciduous Broadleaf Forest (DBF)	†
Temperate needle-leaved evergreen (TeNE)	Evergreen Needleleaf Forest (ENF)	Tree Cover, needle-leaved, evergreen (4)
Temperate broad-leaved evergreen (TeBE)	Evergreen Broadleaf Forest (EBF)	†
Temperate broad-leaved summergreen (TeBS)	Deciduous Broadleaf Forest (DBF)	Tree Cover, broadleaved, deciduous, closed (2)
Boreal needle-leaved evergreen (BoNE)	Evergreen Needleleaf Forest (ENF)	Tree Cover, needle-leaved, evergreen (4)
Boreal needle-leaved summergreen (BoNS)	Deciduous Needleleaf Forest (DNF)	Tree Cover, needle-leaved, deciduous (5)
Boreal broad-leaved summergreen (BoBS)	Deciduous Broadleaf Forest (DBF)	Tree Cover, broadleaved, deciduous, closed (2)
C3 grasses (C3)	Grass	Herbaceous Cover, closed-open (13)
C4 grasses (C4)	Grass	Herbaceous Cover, closed-open (13)

† means that there are not one-to-one corresponding GLC2000 Global Class in GLC2000 legend, meanwhile, there are no such PFTs in Heilongjiang province, China based on simulation and GLC2000 map.

4.2.2 Datasets and tools

Present-day PFT coverages and BA simulation. SEVER-DGVM, as an intermediate-complexity DGVM, is developed from the LPJ-DGVM (Sitch et al., 2003) with much improvement for high-latitudes (Venevsky and Maksyutov, 2007), e.g., including a daily time step description for dynamics of soil temperature, potential evapotranspiration and fire disturbance, is used to simulate PFT coverages. Meanwhile, BA is simulated by Glob-FIRM (Thonicke et al., 2001), which is incorporated into SEVER-DGVM. Here some simplifying hypotheses are made. First, fire occurrence is only dependent upon fuel load and litter moisture (i.e. the amount of dry material available), which combines both the influence of climate and vegetation. Ignition is assumed to take place sooner or later, without

specific consideration. Secondly, fire effects are mainly driven by the length of the fire season and the PFT-dependent fire resistances. Thirdly, we assumed that the smallest BA in each grid cell is 250ha and fire intensity is not considered in this study.

All input datasets are provided at a 0.5° × 0.5° spatial resolution. We use NCEP/NCAR Reanalysis data (http://www.esrl.noaa.gov/psd/) as the input climatology in SEVER-DGVM, including daily temperature, precipitation, and shortwave radiation during the period 1957 - 2002, which are down-scaled to a 0.5° grid from Kalnay et al. (1996). The soil physical and thermodynamic characteristics are determined by simplified FAO soil dataset (FAO 1991). We use historical observed CO_2 concentration from 1957-2002 (Meinshausen et al., 2011). The global DGVM applications often misrepresent vegetation dynamics on a regional scale (Seiler et al., 2014). Therefore a PFT parameterizations, suitable for Eurasian boreal forests, is used here, based on Khvostikov et al. (2015). A transient simulation with SEVER-DGVM started from 'bare ground' (no plant biomass present) and 'spun up' 1012 years until approximate equilibrium was reached with respect to carbon pools and vegetation cover. We use climate data during 1957-2002 repeated 22 times and a prescribed constant atmospheric CO_2 concentration of the year 1957 is used. The present-day simulation by SEVER-DGVM is run in the transient phase 1957-2002 with historical changes in atmospheric CO_2 and climate.

Future PFT coverages and BA projection induced by climate change. Four different global warming targets (1.5, 2.0, 3.0, and 4.0 °C, relative to pre-industrial climate) are used to simulate the response of future PFT coverages and BA to climate change. We select 22 General Circulation Models (GCMs) from Coupled Model Intercomparison Project Phase 5 (CMIP5) (see Table 4.2), which have

been bias corrected, to project the future climate in this study though the number of GCMs actually used depending on different global warming targets (see Table 4.3). The year, when a GCM-specific global warming target is reached, from the multi-model ensemble (MME) is recorded (see Table 4.3 and Table 4.2). Daily precipitation and temperature used in SEVER-DGVM for each global warming target are the integrated climate data from the GCMs when the specific global warming target is reached. Here, we ignore the future climatic inter-annual variation and use a simple method to recycle the daily precipitation and temperature of the target year in each warming scenario for the future simulations (starting from 2002) (see Table 4.3). we assume daily shortwave radiation used in SEVER-DGVM will not change and keep the same values with the year 2002. CO_2 concentration data in different global warming targets during running years are from the RCP8.5 emission scenario (Riahi et al., 2007). Soil data and parameters needed in SEVER-DGVM stay the same as present day.

Table 4.2 Year when a specific global warming target reached in 22 GCMs

Models	**1.5°C**	**2°C**	**3°C**	**4°C**
Multi-model mean (MME)	2026	2040	2063	2085
ACCESS1-0	2034	2054	999999†	999999
ACCESS1-3	2041	2056	999999	999999
bcc-csm1-1	2022	2037	2061	2085
BNU-ESM	2013	2024	2047	2066
CanESM2	2016	2028	2051	2070
CCSM4	2017	2032	2059	2079
CMCC-CM	2030	2040	2060	2078
CNRM-CM5	2031	2045	2068	2088
CSIRO-Mk3-6-0	2036	2045	2066	2083
FGOALS-s2	2011	2012	2036	2054
GFDL-CM3	2025	2038	2056	2072
GFDL-ESM2G	2040	2056	2082	999999

Continued Table 4.2 Year when a specific global warming target reached in 22 GCMs

GFDL-ESM2M	2039	2054	2083	999999
HadGEM2-CC	2040	2059	999999	999999
HadGEM2-ES	2025	2037	2056	2073
IPSL-CM5A-MR	2017	2033	2051	2068
MIROC5	2037	2051	2073	999999
MIROC-ESM-CHEM	2019	2030	2049	2068
MIROC-ESM	2021	2031	2053	2071
MPI-ESM-LR	2028	2049	999999	999999
MRI-CGCM3	2042	2054	2078	999999
NorESM1-M	2035	2050	2074	999999

† 999999 means it cannot achieve a specific global warming target in current GCM.

Table 4.3 Future SEVER-DGVM simulation in different global warming targets

Global warming target	**Number of GCMs used**	**The year when warming target was reached**	**Running years**
Temperature + 1.5°C	22	2026	24
Temperature + 2.0°C	22	2040	38
Temperature + 3.0°C	18	2063	61
Temperature + 4.0°C	13	2085	83

4.2.3 Validation of present-day PFT coverages and BA

The accuracy of simulated PFT coverages against current remote sensing products is an important component to reduce the uncertainty of terrestrial biogeochemistry to climate change (Poulter et al., 2011). Three independent datasets are used validate the present-day PFT coverages in Heilongjiang province. Firstly, we select an observed potential vegetation dataset by Ramankutty and Foley (1999), which is based on satellite data at 0.5° × 0.5° spatial resolution and includes 15 categories of vegetation. Four main categories are extracted for Heilongjiang province (see Figure 4.1d). Secondly, in order to obtain the latest land cover which also considers human disturbance on forests in study area, we use a 0.5 km MODIS-based Global Land Cover Climatology

(Broxton et al., 2014), which is based on 10 years (2001-2010) of Collection 5.1 MCD12Q1 land cover type data as comparison with potential vegetation datasets (see Figure 4.1c). We find that the large grasslands and savannas areas are actually replaced by cropland. However, our study is mainly focused on forest ecosystems. Furthermore, cropland and grassland are usually assessed as the greatest uncertainty in PFT classification (Poulter et al., 2011). Therefore, we extract the forest areas based on the grasslands/Savannas category in Figure 4.1d. Finally, we use GLC2000, which is based on SPOT 4 satellite and provides the year 2000 global land cover, to validate the simulated present-day PFTs distribution. Although GLC2000 contains 17 different global categories of vegetation, only four main categories are used for validation in Heilongjiang province (see Figure 4.1b). Using the PFT mapping methods in DGVMs by Poulter et al. (2011), GLC2000 datasets are first reclassified into phenology-based categories consistent with the PFTs used in SEVER-DGVM (see Table 4.1). And then three main forests (DNF, DBF and ENF) are translated to a spatial resolution of 0.5° by summing the area of each PFT class within corresponding 0.5° grid cell and dividing by the grid cell area (Poulter et al., 2011).

In recognition of fires as a large scale and important agent of change in earth system has led to the development of long term, spatially and temporally-explicit global burned area data sets based on satellite (Boschetti et al., 2015, Giglio et al., 2009, Giglio et al., 2013, Justice et al., 2002, Randerson et al., 2012, Roy et al., 2008). The third version of Global Fire Emissions Database (GFED3) (Giglio et al., 2010) is used to validate the BA simulated by SEVER-DGVM in this study. GFED3 provides global monthly BA estimates in 0.5° spatial resolution from July 1996 to mid-2009. We use Glob-FIRM to compare the similarity of the annual BA between GFED3 and SEVER-DGVM during 1996-2002 and evaluate it by a

student-t test.

4.2.4 Quantifying individual contributions

Contributions of climate and fire to explaining present-day vegetation distribution are detected by two independent experiments. One is based on the observed remote sensing dataset, and the other is dependent upon the simulations. The latter is also applied in the future global warming scenario simulations (see Table 4.4).

Table 4.4 Data used to produce RDA in different experiment designs

Scenarios	PFTC	BA	MAT	MAP	MAR	Periods
Present-day 1	GLC2000†	GFED3‡	NCEP	NCEP	NCEP	1957-2002
Present-day 2	SEVER-DGVM	Glob-FIRM‡	NCEP	NCEP	NCEP	1957-2002
Temperature + 1.5°C	SEVER-DGVM	Glob-FIRM	NCEP	NCEP	NCEP	2002-2026
Temperature + 2.0°C	SEVER-DGVM	Glob-FIRM	NCEP	NCEP	NCEP	2002-2040
Temperature + 3.0°C	SEVER-DGVM	Glob-FIRM	NCEP	NCEP	NCEP	2002-2063
Temperature + 4.0°C	SEVER-DGVM	Glob-FIRM	NCEP	NCEP	NCEP	2002-2085

† means that the year of PFTC in 'present-day1' scenario is the projected year of land cover in GLC2000 product.
‡ means that the periods for GFED3 and Glob-FIRM are 1996-2002, which are the overlapping years between GFED3 and present-day simulation. All the data are provided at a 0.5° × 0.5°spatial resolution. The number of samples is 216.

We select Plant Function Types Coverages (PFTC) of the last year of the simulation period as the response variable and mean annual burnt area (BA, ha), simulated by Glob-FIRM, as the explanatory variable, representing the impact of fires. Mean annual temperature (MAT, °C), mean annual shortwave radiation (MAR, W m^{-2}) and mean annual precipitation (MAP, mm/yr) are used to be the

climatically explanatory variables. Mean annual BA in Glob-FIRM is determined by PFT specific soil moisture and flammability threshold and, thus, depends on MAT and MAP in a non-linear way.

RDA, whose aim is to explore a series of linear combinations of the explanatory variables that can best explain the variation in the response variables (Borcard et al., 2011a), and variation partitioning are used to quantify the individual contributions of climate and fires to the vegetation distribution in the boreal forest ecosystem of China in different scenarios. The data used to produce RDA are shown in Table 4.4. Second, we use the R packages 'vegan' version 2.3-2 (Oksanen et al., 2015) to build RDA sequence: rda (formula = PFTC ~ BA + MAT + MAP + MAR). Next, we produce forward selection and collinearity test to determine critical factors. Collinearity test on explanatory variables is based on Variance Inflation Factors (VIF), and it is considered that there is little/no collinearity when VIF < 4. Finally, we test the RDA results using 'Permutable test' with 999 runs. R packages 'vegan' version 2.3-2 is also applied in variation partitioning, which is shown as Venn diagrams by R packages 'VennDiagram' version 1.6.17 (Chen and Boutros, 2011). Here, we only focus on the impacts of climate and fires on the vegetation distribution, the contributions of other controls (e.g., soil and human activities) are described as residuals.

Spatial structures play a crucial role in the analysis of ecological data. If external forcing (e.g., climatic, physical and chemical) are spatially structured, biomes that are actually controlled by these factors, will be spatially structured at many scales (Borcard et al., 2011b). This can be confirmed by autocorrelation of quantitative biome characteristics in space, which is referred as spatial pattern in this study (Borcard et al., 2011b). In order to analyse individual contributions of vegetation spatial pattern, climate and fire in regulating vegetation distribution,

we use variation partitioning and Moran's Eigenvector Map (MEM) spatial analysis method (Dray et al., 2006), which is based on sets of variables describing spatial structures in the way of deriving from the coordinates of the samples or from the neighbourhood relationships among samples and could model structures at multiple scales and allow the modelling of any type of spatial structures (Borcard and Legendre, 2002), by R package 'vegan' version 2.3-2 (Oksanen et al., 2015). However, a linear trend in vegetation distribution should be considered as a source of variation if the test for response data is significant (Borcard et al., 2011b). The whole explanatory variables are standardized firstly. All calculations are based on RStudio version 0.99.489 software environment (RStudio, 2015).

4.3 Results

4.3.1 Present-day PFTC and BA distribution

We simulated PFTC in forest areas of Heilongjiang province in 2002 and compared with the main forest types from GLC2000 (see Figure 4.2a). We found that simulated PFT coverages were relatively consistent with GLC2000 for categories DBF and DNF, especially in the northwest parts of the Heilongjiang province. However, a large difference exists for ENF and we only captured the ENF distribution in the northwest, this might be the results of the misclassification in GLC2000 between ENF and mixed forests in other parts of study areas. Based on remote sensing products (see Figure 4.1c and d), we find that large areas of mixed forests exist in Heilongjiang province, which has been proved by the vegetation atlas of China (Tan et al., 2007). Also, mixed forests were twice as large in extent as DNF in this area (Xiao et al., 2002).

The results of the validation in the mean annual BA between GFED3 against simulation are shown in Figure 4.2b. We suggest that the simulated total BA reproduced GFED3. The student-t test demonstrated that there was not a significant difference between SEVER-DGVM and GFED3 at the 90% confidence level (t = 0.63512, n = 7, d.f. = 12, p-value = 0.5373).

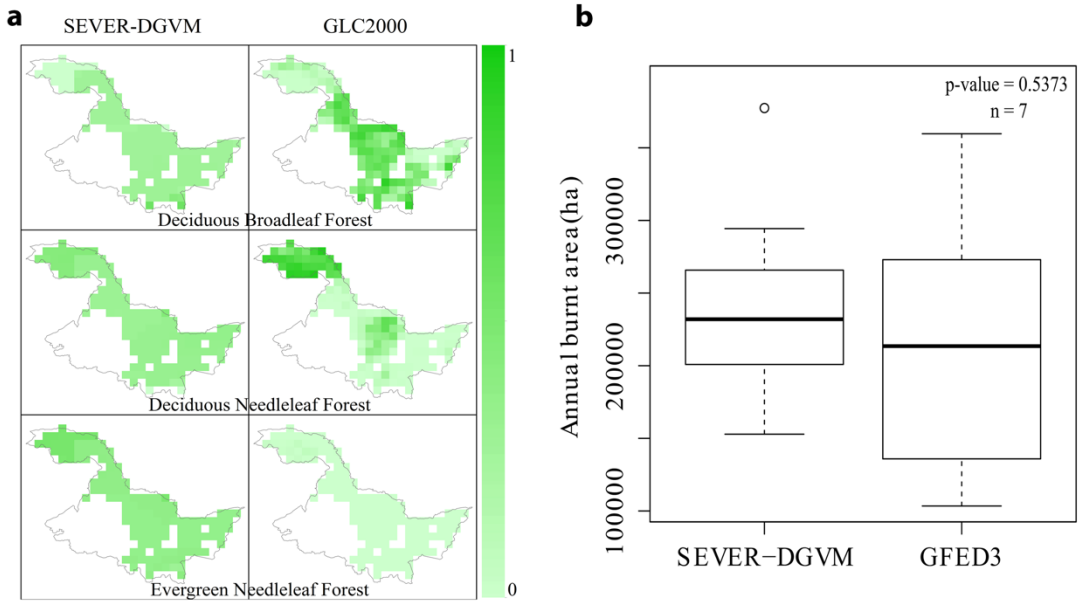

Figure 4.2 Present-day PFTC (a) and mean annual BA (b) during 1996-2002 in forest areas of Heilongjiang province

4.3.2 Present-day contributions of climate and fire in regulating PFTC

First, we use the 'present-day 1' experiment to quantify present-day individual contributions of climate and fire in regulating PFTC. The correlation analysis between climate and fire factors revealed that MAR and MAT had a strong relationship (Adjusted R^2 = 0.91). Considering the ecological meanings, we excluded MAR from the explanatory variables. Thus MAP, MAT and BA consist on the explanatory variables in this study.

Results from a Principal Component Analysis (PCA) showed that the first two components (PCA1 and PCA2) could together explain 77.8% of the total variation. The RDA for PFTC and explanatory variables demonstrated that RDA1 and RDA2 were able to explain 35.5% of the total variation. Then forward selection

revealed that MAP, MAT and BA were the significant factors in determining PFTC (P = 0.015), meanwhile, none had obvious collinearity among explanatory variables (VIF < 4). Next the 'Permutable test' of the RDA results was significant (F = 40.436, d.f. = 3, P < 0.001) and all the canonical axes were significant as well. The adjusted bimultivariate redundancy statistic (R^2) was 0.3550. The RDA results are shown in Figure 4.3a. Similarly, experiment results from 'present-day 2' are shown in Figure 4.3b. The RDA results are described as 'triplot', including three different entities: sites, response variables (without arrowheads, red) and explanatory variables (with arrowheads, blue). The 'triplot' were interpreted as 'Scaling 2 - correlation biplot', in which the angles between variables (explanatory and/or response variables) reflect their correlations. We found that DNF distribution was negatively related to temperature while temperature would contribute to the growth of DBF as well. Meanwhile, fire would decrease the distribution of flammable DNF according to both present-day experiments. However, the influence of precipitation on biome composition was uncertain in these two scenarios.

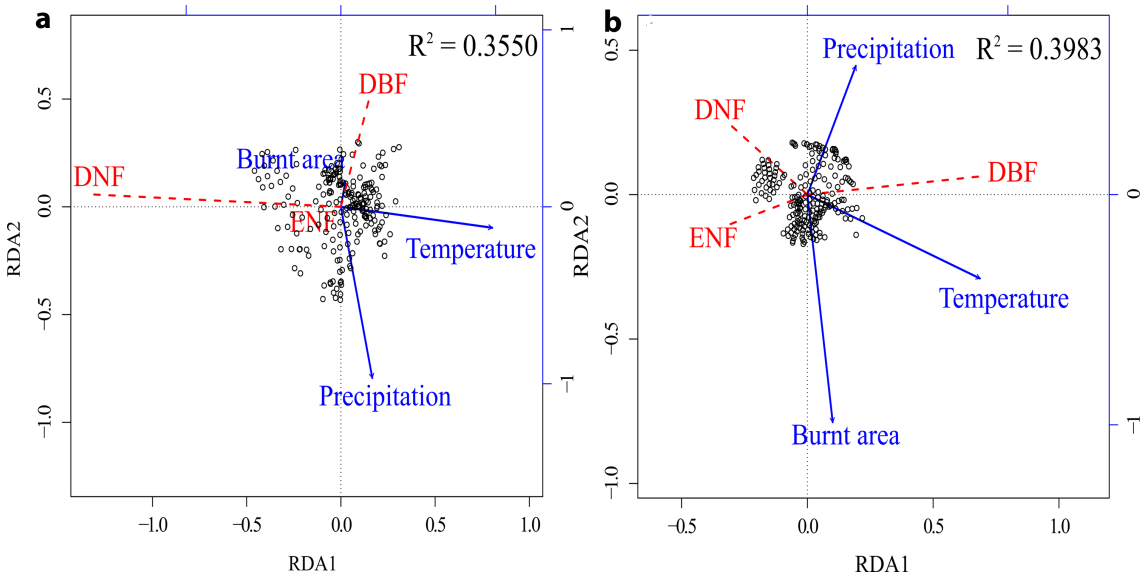

Figure 4.3 Correlation triplot based on a Redundancy Analysis (RDA) depicting the relationship between the selected climate and fire variables and the variation of coverages among different PFTs in (a) present-day 1and (b) present-day 2

Variation partitioning illustrated that fire and climate factors could explain 35.5% of the total variation in PFTC from 'present-day 1'. Furthermore, fires alone could only explain around 1% while climatic individual contributions were around 35.8% of the total variation (see Figure 4.4a). Here we ignored the minus values and it could be considered as zero, for the joint contributions of explanatory factors, which indicated that the explanatory variables did worse than random normal variables (Borcard et al., 2011a). Moreover, temperature was much more important than precipitation in regulating the PFTC (30.6% > 4.5%). All the results were significant (P < 0.001) based on permutation tests.

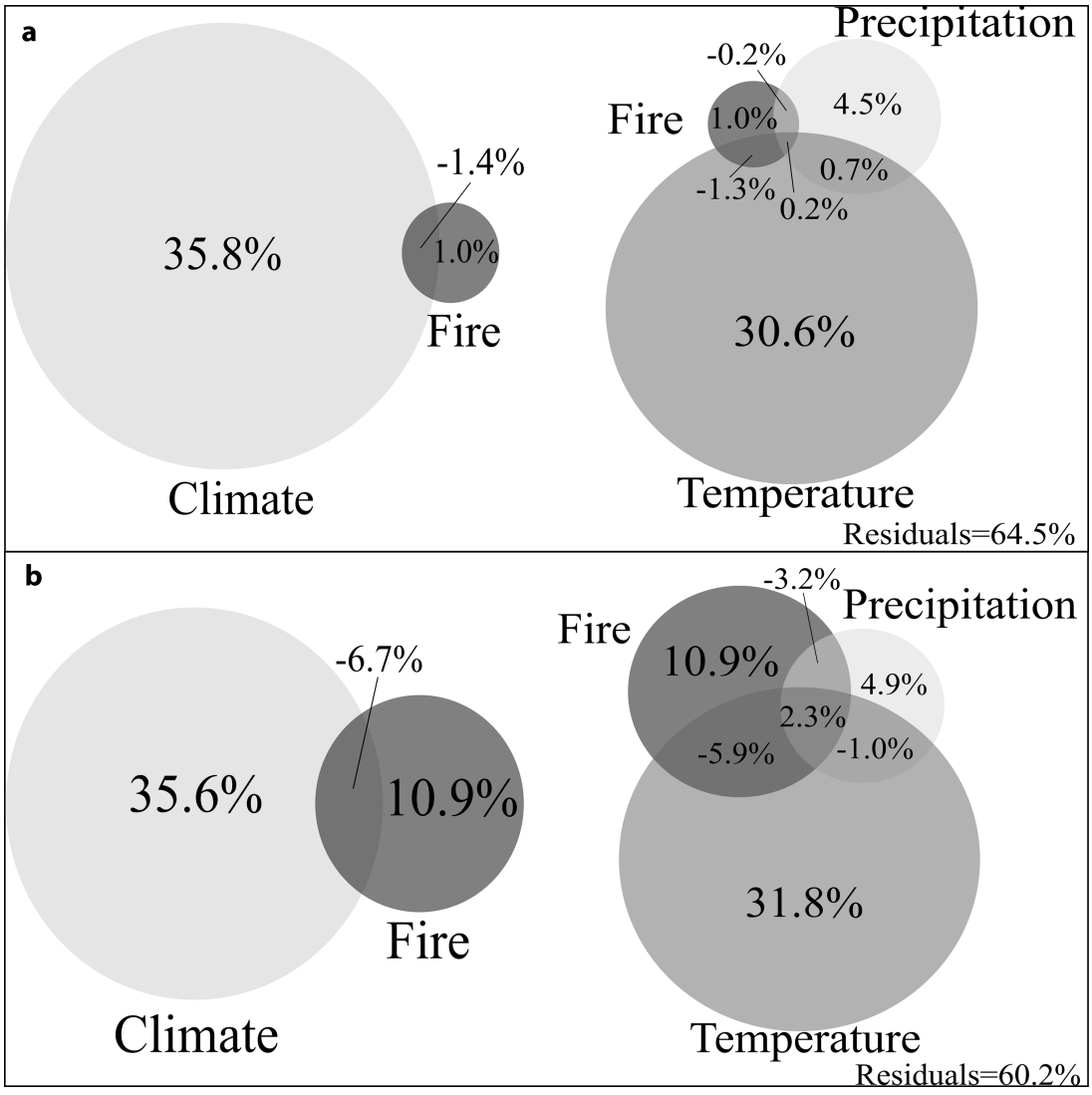

Figure 4.4 Individual contributions of fires and climate in regulating PFTC in 'present-day 1' (a) and 'present-day 2' (b). Left: climate consists of comprehensive effects of temperature and precipitation; right: individual effects of temperature and precipitation

Next, based on the experiment 'present-day 2', we found that 39.8% of the total variation could be explained by climate and fires in determining vegetation distribution (see Figure 4.4b). Different from 'present-day 1', fire could describe 10.9% of the total variation based on modelling. However, individual contributions of climate factors did not change much. Therefore, based on two independent present-day experiments, the results illustrate that the distribution of boreal forests in China is more determined by climate rather than fires, meanwhile, the response of vegetation is more sensitive to temperature than precipitation at the present day. Even though, the contribution of fire in regulating PFTC is strongly dependent on the data source and accuracy of BA changing from 1% to 10.9% in our study. In contrast, climate contributes around 30%, largely driven by temperature, to the distribution of vegetation in boreal forests of China.

4.3.3 Spatial pattern in regulating PFTC

Spatial pattern over the region is important in the analysis of individual contributions of fires and climate factors in regulating local vegetation distribution, i.e. one can interpret this as the importance of the vegetation in the surrounding area for the composition at a specific location. Essentially it gives an indication of the level of spatial homogeneity in vegetation across the region, and its importance for determining local vegetation cover. Based on the 'present-day 1' scenario, there is a strong linear trend in the spatial distribution of vegetation ($F = 57.121$, d.f. = 2, $P < 0.001$). After detrending the data (Borcard et al., 2011b), the MEM spatial analysis showed that spatial pattern could explain 82.0% of the distribution of vegetation. Spatial scale and regression analysis help to analyse whether the spatial pattern of vegetation distribution is related to environmental factors (climate and fire disturbance in this study) at different scales. The different scales here are defined as the significant MEM variables map according to the

scales of the patterns they represent. And the results illustrated that the vegetation distribution was significant at the broad scale ($F = 19.066$, d.f. = 11, $P < 0.001$) and produced two significant canonical axes to explain the spatial pattern. The first canonical axis was significant to MAP ($R^2 = 0.3033$, $P < 0.001$) while the second canonical axis was significant to BA, MAT and MAP ($R^2 = 0.2229$, $P < 0.001$). However, there were no obvious spatial differences at medium and fine scales ($P > 0.05$). The reason might be that at finer spatial scale, vegetation often displayed properties of inertia, contingency and hysteresis, most frequently because of climatic variability across multiple time scales and the episodic nature of disturbance and establishment (Jackson, 2013).

A similar analysis was produced for the 'present-day 2' scenario. Variation partitioning results are shown in Table 4.5. Spatial pattern has a strong impact on the quantitative analysis of the individual contributions of fire and climate factors to PFTC. Fires, climate and spatial information could explain around 90% of the total variation. Compared to the small influence of fire disturbance (0 - 4.2%), climate could explain around 30% of the total variation. However, as an important source of variation, the linear trend in vegetation spatial distribution itself cannot be ignored. Therefore, we should consider spatial information, including spatial pattern and trend in vegetation distribution when we quantify the contributions of explanatory variables even if there is no significant influence on the driving balance between climate and fires. Here, the fact that contributions of fires, climate, spatial pattern and trend might add up to more than 100% is the reason to consider the overlap among individual factors.

Table 4.5 Individual contributions† of fires, climate and spatial pattern on PFTC in present day and warming scenarios

Scenarios	Fire	Climate	Spatial	Trend	Residuals
Present-day 1	0	34.5%	88.4%	34.3%	11.2%
Present-day 2	4.2%	28.9%	83.6%	42.0%	13.6%
Temperature + 1.5°C	36.3%	29.3%	89.7%	32.7%	7.4%
Temperature + 2.0°C	7.2%	42.1%	90.1%	45.1%	8.5%
Temperature + 3.0°C	3.4%	62.3%	90.4%	59.5%	8.6%
Temperature + 4.0°C	5.6%	59.4%	93.7%	55.9%	5.3%

† Individual contributions had included the joint contributions (Fire: fire contributions; Climate: climate contributions; Spatial: spatial pattern contributions; Trend: the linear trend of PFTC contributions; Residuals: the contributions that could not be explained).

4.3.4 Future PFTC and BA projection

Climate change, especially global warming is projected to strongly impact the future vegetation distribution, possibly leading to important biome-level changes (Gauthier et al., 2015). PFTC projections for four different global warming targets (1.5, 2.0, 3.0 and 4.0 °C) are shown in Figure 4.5. We find that the dominant forests in Heilongjiang province are ENF in the present day, which is consistent with actual vegetation distribution, such as *Pinus koraiensis, Pinus sylvestris var. mongolica, Picea koraiensis* and *Abies nephrolepis*. Besides DBF occupies large areas as well, such as *Jugjans mandshurica and Quercus mongolica Ledeb*. In response to climate change, the biome composition would change in different scenarios. When temperature increased, DNF would decrease from south to north until 'temperature + 4.0 °C', almost no DNF existed in this area. ENF would increase at lower temperature increases, however, above 2.0 °C, large areas of ENF would be replaced by temperate forests. Meanwhile, as temperature increased, DBF would start to shift from the south to the north until the time when temperature increased by 3.0 °C, DBF would be the most dominant PFT in this region. There also some minor areas of grass distributed in the transition areas between boreal forests and temperate vegetation. This is in

line with the evidence that there would be a gradual northward migration of temperate deciduous tree species into the boreal region (Gauthier et al., 2015). There also some minor areas of grass distributed in the transition areas between boreal forests and temperate vegetation.

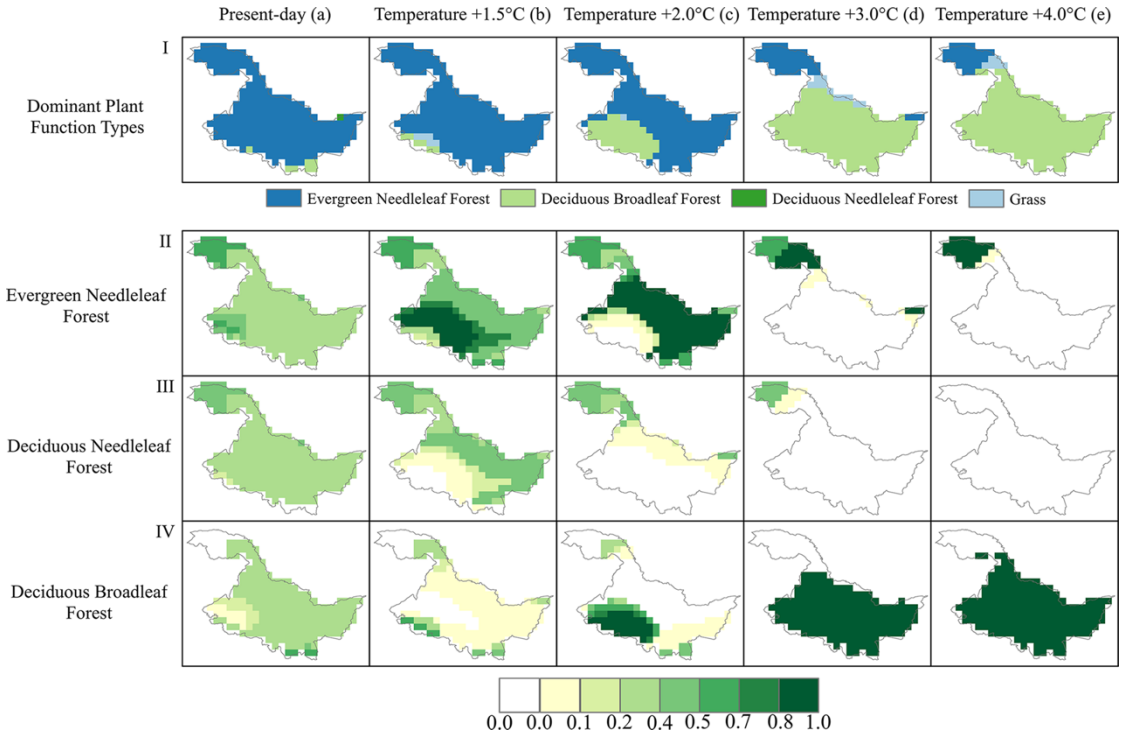

Figure 4.5 PFTs distribution simulated by SEVER-DGVM in Heilongjiang province, China. (a) present-day; (b) temperature increase by 1.5 °C; (c) temperature increase by 2.0 °C; (d) temperature increase by 3.0 °C; (e) temperature increase by 4.0 °C; I: dominant PFTs; Tree cover in each grid cell: II, III, IV

Climate change would impact the fire regime as well, in particular, BA. We used Glob-FIRM to simulate the spatial distribution of mean annual BA in Heilongjiang province. As shown in Figure 4.6, compared to the present-day BA, climate change would decrease BA. When temperature increased by 1.5 °C, the areas most disturbed by wildfires are centred in the areas with large flammable boreal forests, like DNF and ENF (see Figure 4.5). However, when temperature increased by more than 2.0 °C, BA decreases rapidly and hotspots of wildfires move from south to north, which is consist with the shift from boreal forests to temperate forests. That is, the wildfires induced by global warming is strongly

dependent on the PFTs and flammability of the vegetation. In addition, although global warming will decrease precipitation compared to the present day, there is a slight increase in precipitation when temperature increases from + 1.5 °C to + 4.0 °C (see Figure 4.7), which might lead to the decrease of BA in different scenarios.

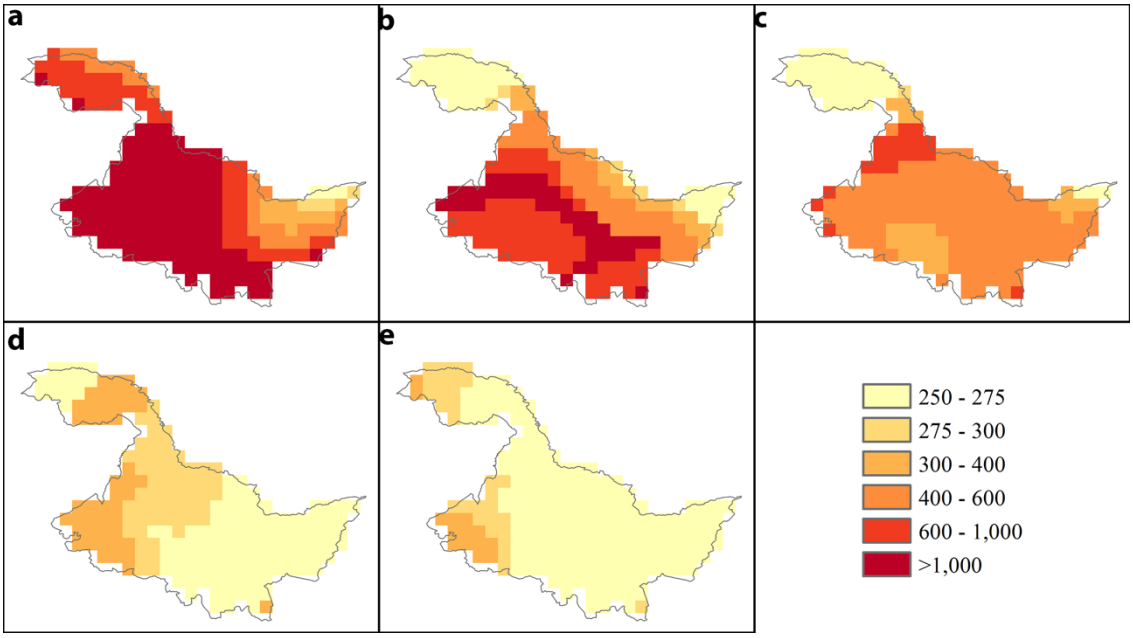

Figure 4.6 Mean annual BA (ha) spatial distribution simulated by Glob-FIRM in Heilongjiang province, China (a) present day; (b) temperature increase by 1.5 °C; (c) temperature increase by 2.0 °C; (d) temperature increase by 3.0 °C; (e) temperature increase by 4.0 °C

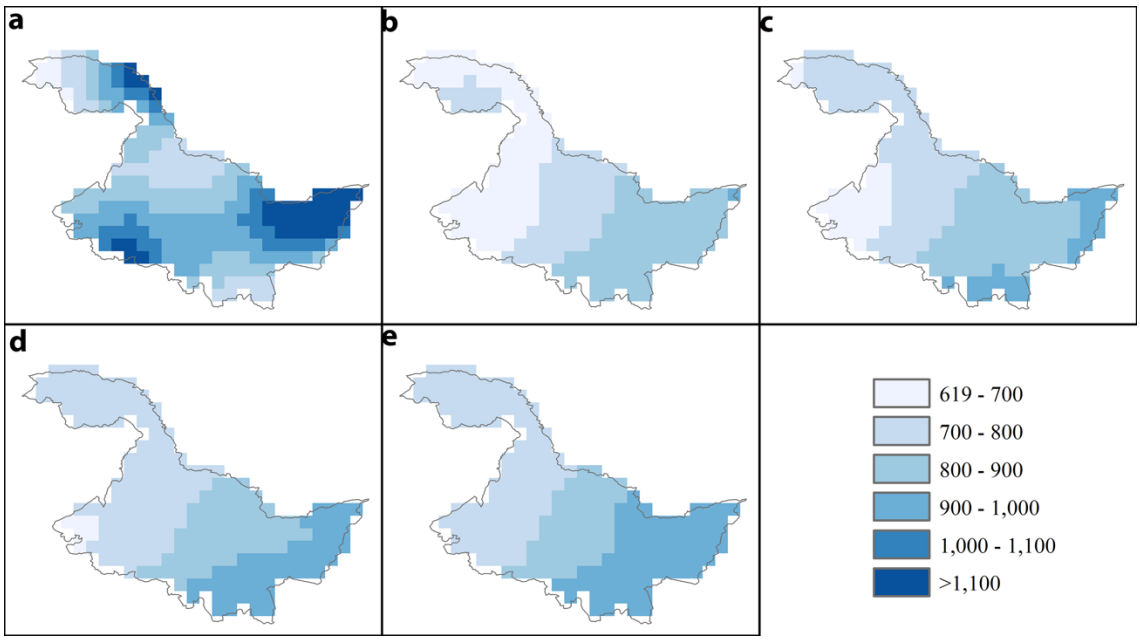

Figure 4.7 Annual mean precipitation (mm/yr) spatial distribution in Heilongjiang province, China. (a) present day; (b) temperature increase by 1.5 °C; (c) temperature increase by 2.0 °C; (d) temperature increase by 3.0 °C; (e) temperature increase by 4.0 °C

4.3.5 Future contributions of climate and fire in regulating PFTC

Similar to the present-day scenarios, we excluded MAR from the explanatory variables in the future analysis. RDA results from the four global warming experiments are shown in Figure 4.8. DNF, as one type of main flammable forest, was strongly and negatively related to BA and temperature in all scenarios. With temperature increasing, precipitation would firstly contribute to the growth of DNF, but when temperature increased by 2.0 °C, precipitation would limit the distribution of DNF. The growth of DBF is strong dependent on temperature and more DBF will exist in a warmer world, which is consistent with Figure 4.5. In addition, when the temperature increased by high than 2.0 °C, temperature and precipitation would be the dominant limitation factors in regulating ENF. RDA results are significant by permutation test ($p < 0.001$).

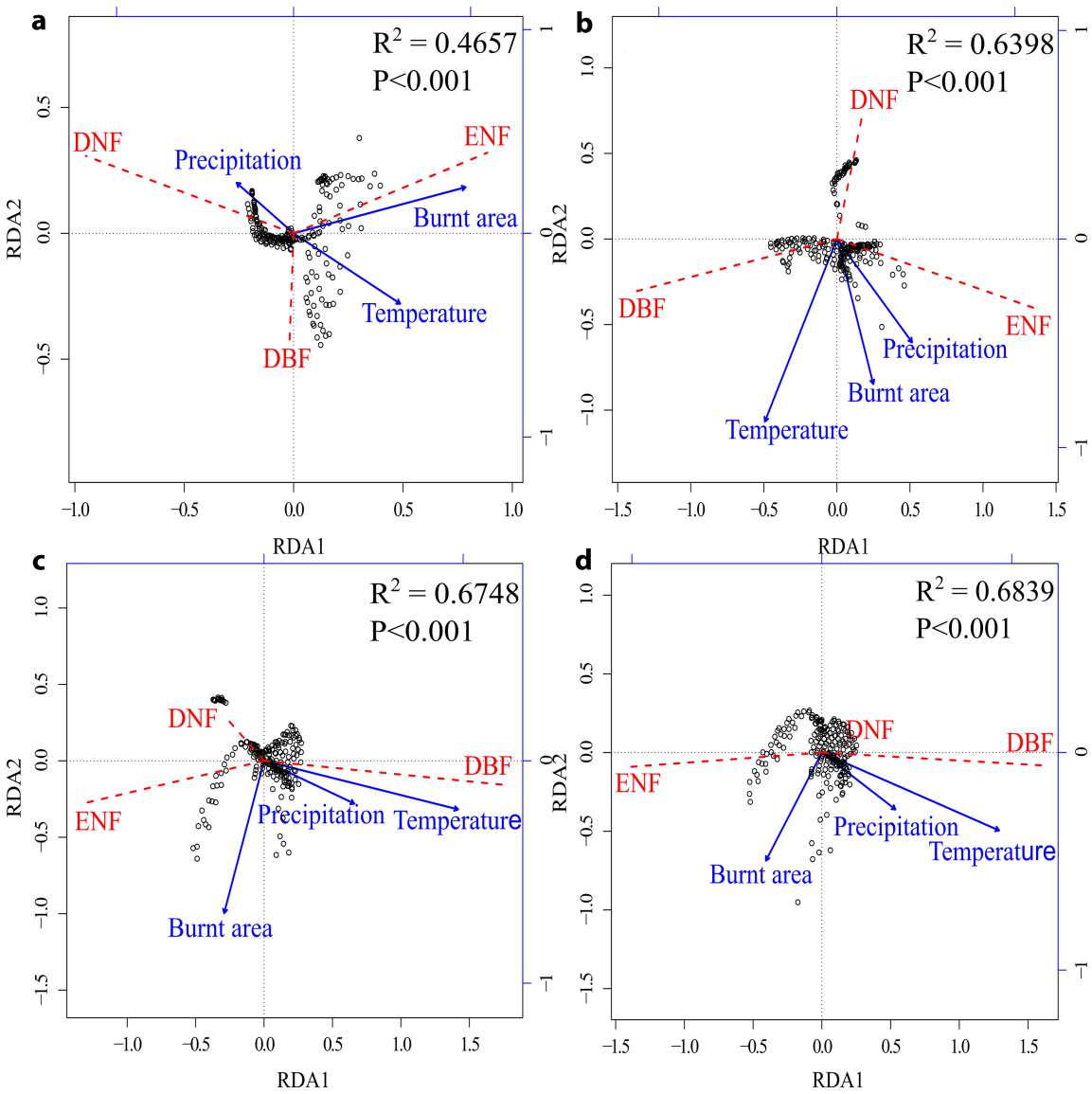

Figure 4.8 Correlation triplot based on a Redundancy analysis (RDA) depicting the relationship between the selected climate and fire variables and the variation of coverages among different PFTs. (a) temperature increase by 1.5 °C; (b) temperature increase by 2.0 °C; (c) temperature increase by 3.0 °C; (d) temperature increase by 4.0 °C

Variation partitioning can be applied to analyse the individual contributions of climate factors and fires in regulating PFTC in different warming scenarios quantitatively (see Figure 4.9). Compared to fire influence, generally climate factors are more important in regulating PFTC, whose individual contributions are larger than fires' except the scenario of 'temperature + 1.5 °C' (Fire 36.3% > Climate 29.3%). When temperature increased by 1.5 °C, the vegetation

distribution of Heilongjiang province would be mainly determined by fires rather than climate. When temperature increased by higher than 1.5 °C, the individual contributions of climate would be much larger than the contributions of fires. What is more, we found temperature to be more important than precipitation in regulating PFTC. All the results from permutation tests were significant ($p < 0.001$).

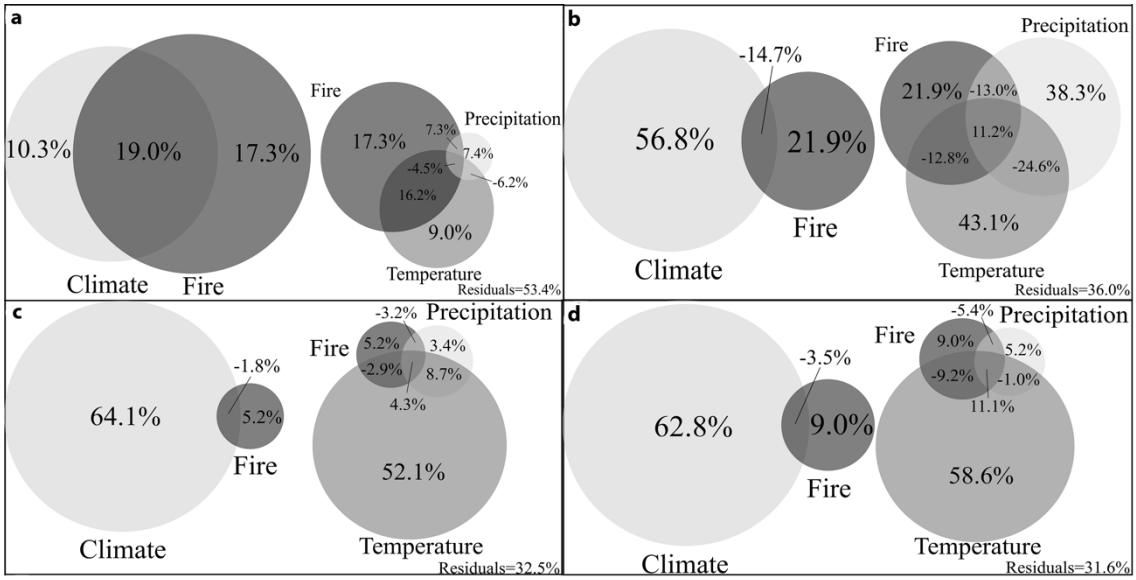

Figure 4.9 Individual contributions of fires and climate in regulating PFTC (Climate consisting from comprehensive effects of Temperature and Precipitation. (a) temperature increase by 1.5 °C; (b) temperature increase by 2.0 °C; (c) temperature increase by 3.0 °C; (d) temperature increase by 4.0 °C

4.3.6 Spatial pattern in regulating future PFTC

We cannot ignore the impact of the spatial pattern when analysing the individual contributions of climate and fire disturbance factors to the PFTC under a changing climate. The results of MEM spatial analysis are also shown in Table 4.5. Results show how spatial pattern represents the largest contribution to regulating PFTC for the whole four scenarios, that is, the vegetation distribution is strongly dependent on the spatial difference. Except the scenario of 'temperature + 1.5 °C', the other three scenarios showed that climate factors were more important than fires on PTFC. When temperature increased by 1.5 °C,

the vegetation distribution was strongly dependent on wildfires (Fire 36.29% > Climate 29.31%), which is consistent with the results in Figure 4.9. All the permutation test results were significant ($P < 0.001$).

4.4 Discussion

4.4.1 Climatic, weather, and fire impacts on forest ecosystem

Climate change is likely to exert a strong influence on plant physiology and vegetation coverage (Betts et al., 2000). Temperature affects biome composition mainly through the impacts on plant physiological processes, especially photosynthesis (Collatz et al., 1991) and respiration (Tjoelker et al., 2001). Besides, temperature, combined with Growing Degree Days (GDD), have a significant influence on plant phenology and growing season length (Chen and Pan, 2002, Tao et al., 2006). Precipitation controls vegetation distribution by changing water supply, evapotranspiration and runoff, leading to the water balance change of the ecosystem (Stephenson, 1990). It is reported that, generally, savanna would be replaced by the forest when annual precipitation exceed around 1500 mm/yr (Lewis, 2006). Moreover, Hirota et al. (2011) implied that actually the global tropical forests and savannas are controlled by annual precipitation. In addition, the boundaries of boreal forests are modified by precipitation as influenced by oceans and mountains (Volney and Fleming, 2000). Drought stress, which is strongly related to precipitation and temperature, will also impact biome composition (Allen and Breshears, 1998). Different from the long-term impact from climate, generally the impact of weather happens in a short period of time. E.g., Climate determines the dominant vegetation in the regions, but plants can still be damaged or killed by extreme weather. The impact of weather is always related to extreme weather evens, e.g., drought, flood and

storm, which would strongly impact the vegetation composition (Parmesan et al., 2000). In addition, weather-related stress can also make plants more susceptible to disease and insect problems. However, vegetation will also modify weather by changing surface albedo, transpiration and evaporation of water vapor, aerodynamic effects, and emission of hydrocarbons whose oxidation can form aerosol particles (Brown et al., 2005). Extreme, large scale weather events are likely to trigger ecosystem-level disturbance, e.g., wildfires, which may affect the species composition and diversity (Parmesan et al., 2000).

Fire is an important and necessary natural disturbance in forest ecosystems, especially for flammable communities (e.g., boreal forests, grasslands, savannas, and Mediterranean shrub lands). All of these fire-prone ecosystems occupy around 40% of the world's land surface (Bond et al., 2005). Fires help to shape global biome distribution and maintain the structure and function of fire-prone communities. Meanwhile, climate plays a decisive impact on vegetation growth and distribution, which is also an important factor for vegetation classification around the world (Corbett and Berger, 2004, Cramer et al., 2001, Nemani et al., 2003, Parmesan and Yohe, 2003, Raich and Schlesinger, 1992). Bond et al. (2005) suggested that some flammable ecosystems were actually determined by fires. However, few studies focus on the analysis of the actual contributions of fire to ecosystems later.

Our quantitative analysis further supplements Bond's ideas on a regional scale. Regardless of spatial pattern, similar to climate impact, fires also play a substantial role on biome composition. Contributions of climate to the vegetation distribution are larger than contributions of fires for the present-day boreal forests (around 35% vs. 1% - 10.9%, see Figure 4.4). The reasons might be that the climate influence is a long-term and permanent process, which has been widely

considered as the dominant factor for vegetation growth and distribution by the ecologists. Thus, the local vegetation has adapted to the local climate environment and vegetation coverages and will remain stable under normal growth unless encountering sudden disturbance, like wildfires. Fire not only changes directly the forests distribution but also will affect subsequent (postfire) nutrient availability, soil moisture, soil temperature, rates of mineralization, and light availability, and all of these potential influences will lead to competition among vegetation (Mills et al., 2006). What is more, vegetation coverages will not change much once vegetation is established and occupies the area in a certain climatic environment. But fires will kill plants and decrease PFTC quickly, especially in the flammable ecosystems and heat-stimulated germination is globally widespread in numerous fire-prone ecosystems (Bond and Keeley, 2005), making fire the necessary condition for growth and distribution of vegetation in these ecosystems. This might be another reason why fires will have a decisive impact on vegetation components. However, fire occurrence is also dependent on the regional climate conditions to some degree, e.g., temperature and precipitation (Liu et al., 2012) and this might be an important reason to explain the larger contribution of climate than fires. Although Mills et al. (2006) suggests that there might be a danger when we use fire to account for the existence of the vegetation state because fire is not an ultimate cause, fire has been treated as separate effects to explore quantitatively contributions of controls to carbon balance and biome composition (Bond-Lamberty et al., 2007, Murphy and Bowman, 2012, Soja et al., 2007). In addition, the contribution of fire is uncertain in the two independent present-day experiments (1% vs. 10.9%). This might be the reason for the accuracy of the projections of BA and ENF and the latter is quite different between DGVM simulation and GLC2000 land cover dataset (see

Figure 4.2a). Although the evaluation of the annual BA is acceptable in Figure 4.2b, there are differences in spatial distribution in BA.

4.4.2 Other controls in regulating vegetation distribution

Many controls, including soil, topography, insect outbreak, permafrost and human activity, also play important roles in vegetation distribution and dynamics in the boreal region, in addition to climate and fire disturbance (Murphy and Bowman, 2012, Scheffer et al., 2012). We find large residuals (around 60%) exist in this study, which represent the other controls that are beyond the scope of our study. Bond (2008) used the terms 'bottom-up' and 'top-down' to classify the controls into resource-based (e.g., water, nutrient) and disturbance-based (e.g., fire, insects). As mentioned earlier, water availability is related to climate. Nutrient availability is strongly dependent on soils and it provides a large nutrient pool (such as soil organic matter) to facilitate the growth and productivity of the forests, which in turn impact rates of succession (Bond, 2008, Murphy and Bowman, 2012). However, in this study, the soil may not be the dominant control, Chen et al. (2015) also proved that the vegetation-atmosphere carbon fluxes (GPP, RE, NEP) in the Northern Hemisphere were not significantly related to soil factors ($R = -0.11$ to 0.14, $P > 0.05$). In addition, large areas of permafrost exist in Heilongjiang province, which is an important control on vegetation and soil carbon dynamics as well by influencing hydrology and soil thermal conditions in boreal forests (Jiang et al., 2016), meanwhile permafrost is quite sensitive to climate change (Ran et al., 2012). Recent trends of continuous and island permafrost degradation in Northeast China are pushing boreal ecosystems into a disequilibrium state. This may influence the relative role of climate factors and fires in determining vegetation distribution. Recent thaw of permafrost in Northeast China can be relatively fast. So, winter baseflow at two watersheds in

permafrost area of Northeast China had a distinct annual increasing trend 1 - 2% and lagged mean annual temperature increase by only two years (Duan et al., 2017). However, the area where these processes are happening is relatively small and does not change our 'present-day' results significantly. Similar to fire, insect outbreaks alter the accumulation and distribution of vegetation and strongly disrupt and redirect succession in forest ecosystem (McCullough et al., 1998). Moreover, human activities in forest areas impact not only vegetation composition and forest structure (e.g., deforestation and forest management), but also ecological processes, nutrient availability, and biodiversity (Josefsson et al., 2009). However, the controls as noted earlier are actually interacting with each other in a complicated manner in boreal forests (Murphy and Bowman, 2012, Soja et al., 2007), for example, the influence of topography affects vegetation state by impacting water, nutrient availability, and fire activity.

4.4.3 PFTs vs. Species

In this study, the vegetation distribution is described as the fraction of different PFTs from the simulation of SEVER-DGVM or the classification of GLC2000 remote sensed product. Although using PFTs, which are widely used in DGVMs and Earth system models, as vegetation classification can help us to easily broaden the study area and provide larger scale vegetation composition, the limitation of PFTs are also obvious. Modelers define PFTs to account, in a very general way, for the variation of structure and function among plants (Sitch et al., 2003). Especially, fixed values of leaf-level traits such as carboxylation capacity and nitrogen content per unit leaf area to PFTs does not adequately describe the plasticity of such traits and the variation within PFTs (Prentice and Cowling, 2013). Therefore, the new trend in local and global scale simulations of vegetation dynamics is to replace the 'static' representation of functional diversity

with trait continua, that is incorporating functional trait variation into DGVMs (Fyllas et al., 2017). Meanwhile, species level analysis has been widely used in the studies of vegetation compositions and their impact factors (Bond-Lamberty et al., 2007, Mitchell et al., 2017, Soja et al., 2007). Rogers et al. (2015) used remote-sensing imagery, climate reanalysis data and field inventories to evaluate the differences in boreal fire dynamics between North America and Eurasia and their main drivers based on the species level and found the difference of fire regime between two regions then suggested that species-level traits should be considered in the evaluation of fire impacts and response to climate change. However, the difference of fire regime is inferred from the large different species between two regions. Although the analysis based on species level provide the insights into a smaller spatial scale and closer to the fire itself, many other impact factors relevant to species level, such as the impact of soil organic matter, peatland fires, permafrost, the runoff in the forest and the interactions between different species, should be also considered.

4.4.4 Climate change impacts on PFTC

Climate change impacts the boreal forest health and plant physiology (Piao et al., 2008). Conceivably, boreal forests are more sensitive to climate change than other biome communities (Bradshaw and Warkentin, 2015, Magnani et al., 2007, Pan et al., 2011, Steffen et al., 2015). Under a globally averaged prediction of a warming of 4.0 °C, boreal regions would experience temperature increased from 4 to 11 °C, which will lead to boreal functional groups being replaced by other more temperate PFTs, such as woodland/shrubland biomes (Gauthier et al., 2015, Scheffer et al., 2012). In our study, we further analysed the future PFT distribution in four different global warming scenarios (see Figure 4.5). Our results suggest that boreal forests in Heilongjiang province of China will face a severe

challenge to be replaced by other biomes due to climate change. The fastest increasing biomes will be thermophilic PFT, like DBF, which quickly reacts to temperature.

Climate change will also impact the PFTC by altering global fire regime (Jolly et al., 2015). However, there is great uncertainty on fire regimes in boreal forests of Northeast China (Liu et al., 2012). Fire frequency, BA, and severity are projected to increase considerably induced by warming (Gauthier et al., 2015, Heon et al., 2014). However, based on a statistic model between fire activity and different environmental controls, Krawchuk et al. (2009) predicted that fire would decrease in this region. In our simulation, BA will be the greatest when temperature increased by 1.5 °C, because vegetation combustion is dependent not only on temperature but on fuel characters as well. Compared to temperate forests, boreal biomes, like DNF, are more flammable and can provide more fuels to potential fires (see Figure 4.5). Meanwhile, the precipitation is lowest in this scenario (see Figure 4.7). The relative importance of fire and climate change acts in a non-linear way from between + 1.5ºC and + 4ºC with a general decrease in fire influence with a small increase thereafter (see Table 4.5). This can be explained by the appearance of a small patch of ENF forest substituting grasslands in the most northern mountainous part of Heilongjiang province (see Figure 4.5). Furthermore, human disturbance and simulation uncertainty should be considered as well (Knorr et al., 2014, Syphard et al., 2007).

This is the first time, research has focused on whether the future boreal forests in China will be determined by fires or climate and their individual contributions to vegetation distribution. Our study suggests that the present-day boreal forest ecosystem of China is mainly determined by climate rather than fires disturbance. However, climate change may change the driving balance between

climate and fires. When temperature increases by 1.5 °C relative to pre-industrial climate, the boreal forest will be mainly determined by fires. It is likely due to a peak in coverage by flammable PFTs (DNF), which accelerate fire spread. What is more, climate change will impact the temperature sensitivity of SOC decomposition (Karhu et al., 2010) and further influence the fire regime by changing fuel loads. However, when the temperature increases by higher than 1.5 °C, climate will be the dominant factor in regulating PFTC, according to our study. We also find that the individual contribution of temperature is generally greater than precipitation. The reason might be that boreal forests are more sensitive to global warming than other ecosystems (Gauthier et al., 2015) and because of their physiological and ecological characters. The influence of precipitation on vegetation is based on changing water balance of ecosystems, involving in multi-processes, including evapotranspiration, which is also strongly dependent upon temperature. Other uncertainties relate to model uncertainty (Jiang et al., 2012, Verheijen et al., 2015), climate data uncertainty (e.g., underling climate models have considerable disagreements in precipitation values, which may significantly impact the results) and RDA methods' uncertainty are not the focus of this study.

4.5 Chapter summary

The vegetation distribution in the present-day boreal forest of Heilongjiang province, China is mainly determined by climate rather than fire disturbances. Climate can explain around 35% of the vegetation distribution while fire contributes 1% - 10.9%. Climate change, especially global warming, can have a strong impact on PFT coverage and fire regimes, such as the BA. In addition, boreal forests will contract in the future in response to rising temperatures while deciduous broadleaf forests will expand rapidly until they become the dominant

vegetation in Heilongjiang province. Climate change will change the driving balance between climate and fires in regulating the local biome distribution. Temperature increase of 1.5 °C would result in the local biomes distribution being determined primarily by fires rather than climate (36.3% > 29.3%). In other scenarios, temperature will be more important than fires, although other climatic factors like precipitation also contribute. The spatial pattern has a significant impact on the biome composition (representing the largest part of the total variation) but does not change the balance between fires and climate with respect to determining the vegetation distribution. Our results are highly relevant for local forest and wildfire management.

Chapter 5 Summary and opportunities for further development

5.1 Summary

Wildfire an important natural disturbance in many terrestrial ecosystems and has a strong impact on vegetation distribution and structure, global carbon cycle, and climate system. Especially when the wildfire dynamics has been significantly influenced by global warming and frequent human activities.

In this thesis, I use a newly developed global fire model, SEVER-FIRE mainly including pyrogenic behaviour of humans to better represent fire dynamics and then couple SEVER-FIRE into a dynamic global vegetation model LPJ and forced by multiple GCMs (aiming for decreasing climate forcing uncertainties). Using the fully coupled model, I reproduced the historical global burnt area trend and comprehensively predict the future global burnt area for a range of pathways of global warming and human demography. Meanwhile, I distinguish the drivers and limiting factors of burnt area trends. In parallel, I investigate the climate-carbon feedbacks derived from changing fires and quantify the carbon-cycle effects of fire on global land temperature changes. Finally, I investigate the impact of fire on the regional vegetation distribution and analyse the driving balance of fire and climate on the biome composition in a boreal forest ecosystem of China based on the statistical methods combined with simulations and remote sensing technology.

This thesis will help the development of wildfire management strategies in conditions of different possible future socioeconomic development pathways, to assess future ecological changes and help to inform adaptation and mitigation

options to global climate change.

5.2 Limitation and opportunities for further development

The main limitations are the uncertainties associated with the simulations, including vegetation and fire model (i.e., LPJ-SEVER) mechanisms uncertainties, input data uncertainties, and results uncertainties. Although our model successfully reproduces the recent decreasing trend in global burnt area, the spatial patterns of burnt area trends are not totally well captured, especially in boreal regions and Australia. Although we are making an effort to step a closer towards a first-principle global mechanistic fire model, some mechanisms are still not well described, and some processes remain too simplistic. For example, we assume that fire can last no longer than two days. Fortunately, this may be improved in the near future by introducing information from the latest global fire duration datasets (Andela et al., 2018).

The second limitation comes from the GCM emulator (i.e., IMOGEN), which uses the ‘pattern scale’ concept that approximate linear relationships can be derived between local and seasonal meteorological variations and the amount of global average warming over land, this will limit us to more reasonably simulate inter-annual variations of fire dynamics. Furthermore, the coupled model driven by IMOGEN uses a very coarse spatial resolution that cannot fully describe the ecological process important to fires. However, IMOGEN substantially reduces requirements for computing power and the complexity of the task, and allow us to emulate multiple GCMs to decrease the uncertainties from climate forcing (Zelazowski et al., 2018).

Finally, our analysis of the role of fire on regional vegetation distribution and the relative balance of drivers between fire and climate in this distribution only conducted for a single boreal forest ecosystem in China. The results may be

different for different types of ecosystems. Even within the same forest type (e.g., boreal forest), the species, ecological processes and fire regimes can be quite different (Gauthier et al., 2015, Rogers et al., 2015). Therefore, further studies should focus on distinguishing spatiotemporal differences in the driving balance between fire and climate in regulating local vegetation distribution in different regions and ecosystems (e.g., tropical forest, temperate forest, and savannas).

Investigation of the net effects of fire on climate systems deserves a separate future study. Net effects of fire include both biogeochemical (e.g., the carbon-cycle effects in this study) and biophysical effects (e.g., fire-emitted aerosols and resulting changes in radiative forcing; Randerson et al., 2006). Fire-induced albedo changes (Randerson et al., 2006), and evapotranspiration derived from fires (Liu et al., 2019) may also have strong impacts on the global climate system. Furthermore, the analysis of climate-carbon feedbacks derived from changing fire activities at regional scales will also help to supplement our existing understanding of complex interactions and feedbacks among fire, vegetation, carbon, and climate.

Bibliography

Allen CD, Breshears DD (1998) Drought-induced shift of a forest-woodland ecotone: rapid landscape response to climate variation. Proceedings of the National Academy of Sciences of the United States of America, 95, 14839-14842.

Andela N, Morton DC, Giglio L et al. (2017) A human-driven decline in global burned area. Science, 356, 1356-1362.

Andela N, Morton DC, Giglio L et al. (2018) The Global Fire Atlas of individual fire size, duration, speed, and direction. Earth System Science Data Discussions, 2018, 1-28.

Andela N, Van Der Werf GR (2014) Recent trends in African fires driven by cropland expansion and El Nino to La Nina transition. Nature Climate Change, 4, 791-795.

Angel S, Parent J, Civco DL et al. (2011) The dimensions of global urban expansion: Estimates and projections for all countries, 2000-2050. Progress in Planning, 75, 53-107.

Aragao L, Anderson LO, Fonseca MG et al. (2018) 21st Century drought-related fires counteract the decline of Amazon deforestation carbon emissions. Nature Communications, 9, 536.

Aragão LEOC, Malhi Y, Barbier N et al. (2008) Interactions between rainfall, deforestation and fires during recent years in the Brazilian Amazonia. Philosophical Transactions of the Royal Society B: Biological Sciences, 363, 1779-1785.

Aragão LEOC, Shimabukuro YE (2010) The Incidence of Fire in Amazonian Forests with Implications for REDD. Science, 328, 1275-

1278.

Archibald S, Roy DP, Van Wilgen BW et al. (2009) What limits fire? An examination of drivers of burnt area in Southern Africa. Global Change Biology, 15, 613-630.

Arneth A, Harrison SP, Zaehle S et al. (2010) Terrestrial biogeochemical feedbacks in the climate system. Nature Geoscience, 3, 525-532.

Arora VK, Boer GJ (2005) Fire as an interactive component of dynamic vegetation models. Journal of Geophysical Research-Biogeosciences, 110, G02008.

Arora VK, Melton JR (2018) Reduction in global area burned and wildfire emissions since 1930s enhances carbon uptake by land. Nature Communications, 9, 1326.

Bachelet D, Ferschweiler K, Sheehan TJ et al. (2015) Projected carbon stocks in the conterminous USA with land use and variable fire regimes. Global Change Biology, 21, 4548-4560.

Bala G, Caldeira K, Wickett M et al. (2007) Combined climate and carbon-cycle effects of large-scale deforestation. Proceedings of the National Academy of Sciences of the United States of America, 104, 6550-6555.

Barlow J, Parry L, Gardner TA et al. (2012) The critical importance of considering fire in REDD+ programs. Biological Conservation, 154, 1-8.

Bartholomé E, Belward AS (2005) GLC2000: a new approach to global land cover mapping from Earth observation data. International Journal of Remote Sensing, 26, 1959-1977.

Betts RA (2000) Offset of the potential carbon sink from boreal forestation

by decreases in surface albedo. Nature, 408, 187-190.

Betts RA, Cox PM, Woodward FI (2000) Simulated responses of potential vegetation to doubled-CO2 climate change and feedbacks on near-surface temperature. Global Ecology and Biogeography, 9, 171-180.

Bistinas I, Harrison SP, Prentice IC et al. (2014) Causal relationships versus emergent patterns in the global controls of fire frequency. Biogeosciences, 11, 5087-5101.

Bond WJ (2008) What Limits Trees in C_4 Grasslands and Savannas? Annual Review of Ecology, Evolution, and Systematics, 39, 641-659.

Bond WJ, Keeley JE (2005) Fire as a global 'herbivore': the ecology and evolution of flammable ecosystems. Trends in Ecology & Evolution, 20, 387-394.

Bond WJ, Woodward FI, Midgley GF (2005) The global distribution of ecosystems in a world without fire. New Phytologist, 165, 525-537.

Bond-Lamberty B, Peckham SD, Ahl DE et al. (2007) Fire as the dominant driver of central Canadian boreal forest carbon balance. Nature, 450, 89-92.

Borcard D, Gillet F, Legendre P (2011a) Canonical Ordination. In: Numerical Ecology with R. (eds Borcard D, Gillet F, Legendre P) pp Page. New York, NY, Springer New York.

Borcard D, Gillet F, Legendre P (2011b) Spatial Analysis of Ecological Data. In: Numerical Ecology with R. (eds Borcard D, Gillet F, Legendre P) pp Page. New York, NY, Springer New York.

Borcard D, Legendre P (2002) All-scale spatial analysis of ecological data by means of principal coordinates of neighbour matrices. Ecological Modelling, 153, 51-68.

Boschetti L, Roy DP, Justice CO et al. (2015) MODIS-Landsat fusion for large area 30 m burned area mapping. Remote Sensing of Environment, 161, 27-42.

Bowd EJ, Banks SC, Strong CL et al. (2019) Long-term impacts of wildfire and logging on forest soils. Nature Geoscience, 12, 113-118.

Bowman DM, Balch JK, Artaxo P et al. (2009) Fire in the Earth system. Science, 324, 481-484.

Bradshaw CJA, Warkentin IG (2015) Global estimates of boreal forest carbon stocks and flux. Global and Planetary Change, 128, 24-30.

Brown AE, Zhang L, Mcmahon TA et al. (2005) A review of paired catchment studies for determining changes in water yield resulting from alterations in vegetation. Journal of Hydrology, 310, 28-61.

Broxton PD, Zeng XB, Sulla-Menashe D et al. (2014) A Global Land Cover Climatology Using MODIS Data. Journal of Applied Meteorology and Climatology, 53, 1593-1605.

Chang Y, He HS, Hu YM et al. (2008) Historic and current fire regimes in the Great Xing'an Mountains, northeastern China: Implications for long-term forest management. Forest Ecology and Management, 254, 445-453.

Chen H, Boutros PC (2011) VennDiagram: a package for the generation of highly-customizable Venn and Euler diagrams in R. BMC Bioinformatics, 12, 35.

Chen XQ, Pan WF (2002) Relationships among phenological growing season, time-integrated normalized difference vegetation index and climate forcing in the temperate region of eastern China. International Journal of Climatology, 22, 1781-1792.

Chen Z, Yu G, Ge J et al. (2015) Roles of climate, vegetation and soil in regulating the spatial variations in ecosystem carbon dioxide fluxes in the Northern Hemisphere. PloS One, 10, e0125265.

Collatz GJ, Ball JT, Grivet C et al. (1991) Physiological and Environmental-Regulation of Stomatal Conductance, Photosynthesis and Transpiration - a Model That Includes a Laminar Boundary-Layer. Agricultural and Forest Meteorology, 54, 107-136.

Corbett KD, Berger JM (2004) Structure, molecular mechanisms, and evolutionary relationships in DNA topoisomerases. Annual Review of Biophysics and Biomolecular Structure, 33, 95-118.

Cramer W, Bondeau A, Woodward FI et al. (2001) Global response of terrestrial ecosystem structure and function to CO2 and climate change: results from six dynamic global vegetation models. Global Change Biology, 7, 357-373.

Dahl MV (1979) Chemotaxis: death march of the phagocyte. Archives of Dermatology, 115, 1407-1408.

Dray S, Legendre P, Peres-Neto PR (2006) Spatial modelling: a comprehensive framework for principal coordinate analysis of neighbour matrices (PCNM). Ecological Modelling, 196, 483-493.

Duan LL, Man XL, Kurylyk BL et al. (2017) Increasing Winter Baseflow in Response to Permafrost Thaw and Precipitation Regime Shifts in Northeastern China. Water, 9, 25.

Fyllas NM, Bentley LP, Shenkin A et al. (2017) Solar radiation and functional traits explain the decline of forest primary productivity along a tropical elevation gradient. Ecology Letters, 20, 730-740.

Gauthier S, Bernier P, Kuuluvainen T et al. (2015) Boreal forest health and

global change. Science, 349, 819-822.

Giglio L, Loboda T, Roy DP et al. (2009) An active-fire based burned area mapping algorithm for the MODIS sensor. Remote Sensing of Environment, 113, 408-420.

Giglio L, Randerson JT, Van Der Werf GR et al. (2010) Assessing variability and long-term trends in burned area by merging multiple satellite fire products. Biogeosciences, 7, 1171-1186.

Giglio L, Randerson JT, Van Der Werf GR et al. (2013) Analysis of daily, monthly, and annual burned area using the fourth-generation global fire emissions database (GFED4). Journal of Geophysical Research-Biogeosciences, 118, 317-328.

Hantson S, Arneth A, Harrison SP et al. (2016) The status and challenge of global fire modelling. Biogeosciences, 13, 3359-3375.

Harris I, Jones PD, Osborn TJ et al. (2013) Updated high-resolution grids of monthly climatic observations – the CRU TS3.10 Dataset. International Journal of Climatology, 34, 623-642.

Harrison SP, Bartlein PJ, Brovkin V et al. (2018) The biomass burning contribution to climate–carbon-cycle feedback. Earth System Dynamics, 9, 663-677.

Heinze C, Eyring V, Friedlingstein P et al. (2018) Climate feedbacks in the Earth system and prospects for their evaluation. Earth System Dynamics Discussions, 2018, 1-94.

Heon J, Arseneault D, Parisien MA (2014) Resistance of the boreal forest to high burn rates. Proceedings of the National Academy of Sciences of the United States of America, 111, 13888-13893.

Hirota M, Holmgren M, Van Nes EH et al. (2011) Global resilience of

tropical forest and savanna to critical transitions. Science, 334, 232-235.

Holdridge LR (1947) Determination of World Plant Formations From Simple Climatic Data. Science, 105, 367-368.

Holland MM, Bitz CM (2003) Polar amplification of climate change in coupled models. Climate dynamics, 21, 221-232.

Huntingford C, Atkin OK, Martinez-De La Torre A et al. (2017) Implications of improved representations of plant respiration in a changing climate. Nature Communications, 8, 1602.

Huntingford C, Booth BBB, Sitch S et al. (2010) IMOGEN: an intermediate complexity model to evaluate terrestrial impacts of a changing climate. Geoscientific Model Development, 3, 679-687.

Huntingford C, Cox PM (2000) An analogue model to derive additional climate change scenarios from existing GCM simulations. Climate dynamics, 16, 575-586.

Huntingford C, Mercado LM (2016) High chance that current atmospheric greenhouse concentrations commit to warmings greater than 1.5 °C over land. Scientific Reports, 6, 30294.

Huntingford C, Zelazowski P, Galbraith D et al. (2013) Simulated resilience of tropical rainforests to CO2-induced climate change. Nature Geoscience, 6, 268-273.

Jackson ST (2013) Natural, potential and actual vegetation in North America. Journal of Vegetation Science, 24, 772-776.

Jiang Y, Zhuang Q, Schaphoff S et al. (2012) Uncertainty analysis of vegetation distribution in the northern high latitudes during the 21st century with a dynamic vegetation model. Ecology and Evolution, 2,

593-614.

Jiang YY, Zhuang QL, Sitch S et al. (2016) Importance of soil thermal regime in terrestrial ecosystem carbon dynamics in the circumpolar north. Global and Planetary Change, 142, 28-40.

Jolly WM, Cochrane MA, Freeborn PH et al. (2015) Climate-induced variations in global wildfire danger from 1979 to 2013. Nature Communications, 6, 7537.

Josefsson T, Hornberg G, Ostlund L (2009) Long-Term Human Impact and Vegetation Changes in a Boreal Forest Reserve: Implications for the Use of Protected Areas as Ecological References. Ecosystems, 12, 1017-1036.

Jung M, Reichstein M, Schwalm CR et al. (2017) Compensatory water effects link yearly global land CO2 sink changes to temperature. Nature, 541, 516-520.

Justice CO, Giglio L, Korontzi S et al. (2002) The MODIS fire products. Remote Sensing of Environment, 83, 244-262.

Kalnay E, Kanamitsu M, Kistler R et al. (1996) The NCEP/NCAR 40-Year Reanalysis Project. Bulletin of the American Meteorological Society, 77, 437-472.

Karhu K, Fritze H, Hamalainen K et al. (2010) Temperature sensitivity of soil carbon fractions in boreal forest soil. Ecology, 91, 370-376.

Kc S, Lutz W (2017) The human core of the shared socioeconomic pathways: Population scenarios by age, sex and level of education for all countries to 2100. Global Environmental Change, 42, 181-192.

Khvostikov S, Venevsky S, Bartalev S (2015) Regional adaptation of a dynamic global vegetation model using a remote sensing data derived

land cover map of Russia. Environmental Research Letters, 10, 125007.

Kloster S, Lasslop G (2017) Historical and future fire occurrence (1850 to 2100) simulated in CMIP5 Earth System Models. Global and Planetary Change, 150, 58-69.

Knapp AK, Seastedt TR (1986) Detritus Accumulation Limits Productivity of Tallgrass Prairie. Bioscience, 36, 662-668.

Knorr W, Arneth A, Jiang L (2016) Demographic controls of future global fire risk. Nature Climate Change, 6, 781-785.

Knorr W, Kaminski T, Arneth A et al. (2014) Impact of human population density on fire frequency at the global scale. Biogeosciences, 11, 1085-1102.

Krawchuk MA, Moritz MA, Parisien MA et al. (2009) Global pyrogeography: the current and future distribution of wildfire. PloS One, 4, e5102.

Lasslop G, Thonicke K, Kloster S (2014) SPITFIRE within the MPI Earth system model: Model development and evaluation. Journal of Advances in Modeling Earth Systems, 6, 740-755.

Lehsten V, Tansey K, Balzter H et al. (2009) Estimating carbon emissions from African wildfires. Biogeosciences, 6, 349-360.

Lenihan JM, Bachelet D (2015) Historical Climate and Suppression Effects on Simulated Fire and Carbon Dynamics in the Conterminous United States. In: Global Vegetation Dynamics. pp Page., John Wiley & Sons, Inc.

Lewis SL (2006) Tropical forests and the changing earth system. Philosophical Transactions of the Royal Society of London. Series B: Biological Sciences, 361, 195-210.

Li F, Levis S, Ward DS (2013) Quantifying the role of fire in the Earth system - Part 1: Improved global fire modeling in the Community Earth System Model (CESM1). Biogeosciences, 10, 2293-2314.

Liu Y, Phinn SR (2003) Modelling urban development with cellular automata incorporating fuzzy-set approaches. Computers, Environment and Urban Systems, 27, 637-658.

Liu Z, Ballantyne AP, Cooper LA (2019) Biophysical feedback of global forest fires on surface temperature. Nature Communications, 10, 214.

Liu ZH, Yang J, Chang Y et al. (2012) Spatial patterns and drivers of fire occurrence and its future trend under climate change in a boreal forest of Northeast China. Global Change Biology, 18, 2041-2056.

Magnani F, Mencuccini M, Borghetti M et al. (2007) The human footprint in the carbon cycle of temperate and boreal forests. Nature, 447, 848-850.

Mccullough DG, Werner RA, Neumann D (1998) Fire and insects in northern and boreal forest ecosystems of North America. Annual Review of Entomology, 43, 107-127.

Meehl GA, Teng H, Arblaster JM (2014) Climate model simulations of the observed early-2000s hiatus of global warming. Nature Climate Change, 4, 898-902.

Meinshausen M, Smith SJ, Calvin K et al. (2011) The RCP greenhouse gas concentrations and their extensions from 1765 to 2300. Climatic Change, 109, 213-241.

Mills AJ, Rogers KH, Stalmans M et al. (2006) A framework for exploring the determinants of savanna and grassland distribution. Bioscience, 56, 579-589.

Millward H (2005) Rural population change in Nova Scotia, 1991–2001: bivariate and multivariate analysis of key drivers. Canadian Geographer / Le Géographe canadien, 49, 180-197.

Mitchell RM, Bakker JD, Vincent JB et al. (2017) Relative importance of abiotic, biotic, and disturbance drivers of plant community structure in the sagebrush steppe. Ecological Applications, 27, 756-768.

Moritz MA, Batllori E, Bradstock RA et al. (2014) Learning to coexist with wildfire. Nature, 515, 58-66.

Moritz MA, Parisien MA, Batllori E et al. (2012) Climate change and disruptions to global fire activity. Ecosphere, 3, 1-22.

Moss RH, Edmonds JA, Hibbard KA et al. (2010) The next generation of scenarios for climate change research and assessment. Nature, 463, 747-756.

Murphy BP, Bowman DM (2012) What controls the distribution of tropical forest and savanna? Ecology Letters, 15, 748-758.

Nemani RR, Keeling CD, Hashimoto H et al. (2003) Climate-driven increases in global terrestrial net primary production from 1982 to 1999. Science, 300, 1560-1563.

New M, Hulme M, Jones P (2000) Representing twentieth-century space-time climate variability. Part II: Development of 1901-96 monthly grids of terrestrial surface climate. Journal of Climate, 13, 2217-2238.

Pan Y, Birdsey RA, Fang J et al. (2011) A large and persistent carbon sink in the world's forests. Science, 333, 988-993.

Parmesan C, Root TL, Willig MR (2000) Impacts of extreme weather and climate on terrestrial biota. Bulletin of the American Meteorological Society, 81, 443-450.

Parmesan C, Yohe G (2003) A globally coherent fingerprint of climate change impacts across natural systems. Nature, 421, 37-42.

Pechony O, Shindell DT (2009) Fire parameterization on a global scale. Journal of Geophysical Research-Atmospheres, 114, D16115.

Pechony O, Shindell DT (2010) Driving forces of global wildfires over the past millennium and the forthcoming century. Proceedings of the National Academy of Sciences of the United States of America, 107, 19167-19170.

Pellegrini AFA, Ahlstrom A, Hobbie SE et al. (2018) Fire frequency drives decadal changes in soil carbon and nitrogen and ecosystem productivity. Nature, 553, 194-198.

Pereira JMC, Oom D, Pereira P et al. (2015) Religious Affiliation Modulates Weekly Cycles of Cropland Burning in Sub-Saharan Africa. PloS One, 10, e0139189.

Pfeiffer M, Spessa A, Kaplan JO (2013) A model for global biomass burning in preindustrial time: LPJ-LMfire (v1.0). Geoscientific Model Development, 6, 643-685.

Piao S, Ciais P, Friedlingstein P et al. (2008) Net carbon dioxide losses of northern ecosystems in response to autumn warming. Nature, 451, 49-52.

Piao S, Huang M, Liu Z et al. (2018) Lower land-use emissions responsible for increased net land carbon sink during the slow warming period. Nature Geoscience, 11, 739-743.

Poulter B, Ciais P, Hodson E et al. (2011) Plant functional type mapping for earth system models. Geoscientific Model Development, 4, 993-1010.

Prentice IC, Cowling SA (2013) Dynamic Global Vegetation Models. In: Encyclopedia of Biodiversity (Second Edition). (ed Levin SA) pp Page. Waltham, Academic Press.

Rabin SS, Ward DS, Malyshev SL et al. (2018) A fire model with distinct crop, pasture, and non-agricultural burning: use of new data and a model-fitting algorithm for FINAL.1. Geoscientific Model Development, 11, 815-842.

Raich JW, Schlesinger WH (1992) The Global Carbon-Dioxide Flux in Soil Respiration and Its Relationship to Vegetation and Climate. Tellus Series B-Chemical and Physical Meteorology, 44, 81-99.

Ramankutty N, Foley JA (1999) Estimating historical changes in global land cover: Croplands from 1700 to 1992. Global Biogeochemical Cycles, 13, 997-1027.

Ran YH, Li X, Cheng GD et al. (2012) Distribution of Permafrost in China: An Overview of Existing Permafrost Maps. Permafrost and Periglacial Processes, 23, 322-333.

Randerson JT, Chen Y, Van Der Werf GR et al. (2012) Global burned area and biomass burning emissions from small fires. Journal of Geophysical Research-Biogeosciences, 117, G04012.

Randerson JT, Liu H, Flanner MG et al. (2006) The impact of boreal forest fire on climate warming. Science, 314, 1130-1132.

Reich PB, Peterson DW, Wedin DA et al. (2001) Fire and vegetation effects on productivity and nitrogen cycling across a forest–grassland continuum. Ecology, 82, 1703-1719.

Riahi K, Grübler A, Nakicenovic N (2007) Scenarios of long-term socio-economic and environmental development under climate stabilization.

Technological Forecasting and Social Change, 74, 887-935.

Riahi K, Van Vuuren DP, Kriegler E et al. (2017) The Shared Socioeconomic Pathways and their energy, land use, and greenhouse gas emissions implications: An overview. Global Environmental Change-Human and Policy Dimensions, 42, 153-168.

Rogers BM, Soja AJ, Goulden ML et al. (2015) Influence of tree species on continental differences in boreal fires and climate feedbacks. Nature Geoscience, 8, 228-234.

Roy DP, Boschetti L, Justice CO et al. (2008) The collection 5 MODIS burned area product - Global evaluation by comparison with the MODIS active fire product. Remote Sensing of Environment, 112, 3690-3707.

RStudio. (2015) RStudio: integrated development environment for R. Version 0.99.489. RStudio, Boston, Massachusetts, USA.

Scheffer M, Hirota M, Holmgren M et al. (2012) Thresholds for boreal biome transitions. Proceedings of the National Academy of Sciences of the United States of America, 109, 21384-21389.

Scheiter S, Higgins SI (2009) Impacts of climate change on the vegetation of Africa: an adaptive dynamic vegetation modelling approach. Global Change Biology, 15, 2224-2246.

Scheiter S, Higgins SI, Beringer J et al. (2015) Climate change and long-term fire management impacts on Australian savannas. New Phytologist, 205, 1211-1226.

Scheiter S, Langan L, Higgins SI (2013) Next-generation dynamic global vegetation models: learning from community ecology. New Phytologist, 198, 957-969.

Scholze M, Knorr W, Arnell NW et al. (2006) A climate-change risk analysis for world ecosystems. Proceedings of the National Academy of Sciences of the United States of America, 103, 13116-13120.

Seiler C, Hutjes RWA, Kruijt B et al. (2014) Modeling forest dynamics along climate gradients in Bolivia. Journal of Geophysical Research-Biogeosciences, 119, 758-775.

Seto KC, Guneralp B, Hutyra LR (2012) Global forecasts of urban expansion to 2030 and direct impacts on biodiversity and carbon pools. Proceedings of the National Academy of Sciences of the United States of America, 109, 16083-16088.

Sitch S, Friedlingstein P, Gruber N et al. (2015) Recent trends and drivers of regional sources and sinks of carbon dioxide. Biogeosciences, 12, 653-679.

Sitch S, Huntingford C, Gedney N et al. (2008) Evaluation of the terrestrial carbon cycle, future plant geography and climate-carbon cycle feedbacks using five Dynamic Global Vegetation Models (DGVMs). Global Change Biology, 14, 2015-2039.

Sitch S, Smith B, Prentice IC et al. (2003) Evaluation of ecosystem dynamics, plant geography and terrestrial carbon cycling in the LPJ dynamic global vegetation model. Global Change Biology, 9, 161-185.

Soja AJ, Tchebakova NM, French NHF et al. (2007) Climate-induced boreal forest change: Predictions versus current observations. Global and Planetary Change, 56, 274-296.

Steffen W, Richardson K, Rockstrom J et al. (2015) Sustainability. Planetary boundaries: guiding human development on a changing planet. Science, 347, 1259855.

Stephenson NL (1990) Climatic Control of Vegetation Distribution - the Role of the Water-Balance. American Naturalist, 135, 649-670.

Syphard AD, Keeley JE, Pfaff AH et al. (2017) Human presence diminishes the importance of climate in driving fire activity across the United States. Proceedings of the National Academy of Sciences of the United States of America, 114, 13750-13755.

Syphard AD, Radeloff VC, Keeley JE et al. (2007) Human influence on California fire regimes. Ecological Applications, 17, 1388-1402.

Tan K, Piao S, Peng C et al. (2007) Satellite-based estimation of biomass carbon stocks for northeast China's forests between 1982 and 1999. Forest ecology and management, 240, 114-121.

Tao FL, Yokozawa M, Xu YL et al. (2006) Climate changes and trends in phenology and yields of field crops in China, 1981-2000. Agricultural and Forest Meteorology, 138, 82-92.

Thonicke K, Spessa A, Prentice IC et al. (2010) The influence of vegetation, fire spread and fire behaviour on biomass burning and trace gas emissions: results from a process-based model. Biogeosciences, 7, 1991-2011.

Thonicke K, Venevsky S, Sitch S et al. (2001) The role of fire disturbance for global vegetation dynamics: coupling fire into a Dynamic Global Vegetation Model. Global Ecology and Biogeography, 10, 661-677.

Tjoelker MG, Oleksyn J, Reich PB (2001) Modelling respiration of vegetation: evidence for a general temperature-dependent Q10. Global Change Biology, 7, 223-230.

Turetsky MR, Kane ES, Harden JW et al. (2011) Recent acceleration of biomass burning and carbon losses in Alaskan forests and peatlands.

Nature Geoscience, 4, 27-31.

Van Der Werf GR, Randerson JT, Giglio L et al. (2017) Global fire emissions estimates during 1997–2016. Earth System Science Data, 9, 697-720.

Van Vuuren DP, Edmonds J, Kainuma M et al. (2011) The representative concentration pathways: an overview. Climatic Change, 109, 5-31.

Venevsky S, Le Page Y, Pereira JMC et al. (2019) Analysis fire patterns and drivers with a global SEVER-FIRE v1.0 model incorporated into dynamic global vegetation model and satellite and on-ground observations. Geoscientific Model Development, 12, 89-110.

Venevsky S, Maksyutov S (2007) SEVER: A modification of the LPJ global dynamic vegetation model for daily time step and parallel computation. Environmental Modelling & Software, 22, 104-109.

Venevsky S, Thonicke K, Sitch S et al. (2002) Simulating fire regimes in human-dominated ecosystems: Iberian Peninsula case study. Global Change Biology, 8, 984-998.

Veraverbeke S, Rogers BM, Goulden ML et al. (2017) Lightning as a major driver of recent large fire years in North American boreal forests. Nature Climate Change, 7, 529-534.

Verheijen LM, Aerts R, Brovkin V et al. (2015) Inclusion of ecologically based trait variation in plant functional types reduces the projected land carbon sink in an earth system model. Global Change Biology, 21, 3074-3086.

Volney WJA, Fleming RA (2000) Climate change and impacts of boreal forest insects. Agriculture Ecosystems & Environment, 82, 283-294.

Wan S, Hui D, Luo Y (2001) Fire effects on nitrogen pools and dynamics

in terrestrial ecosystems: a meta-analysis. Ecological Applications, 11, 1349-1365.

Ward DS, Kloster S, Mahowald NM et al. (2012) The changing radiative forcing of fires: global model estimates for past, present and future. Atmospheric Chemistry and Physics, 12, 10857-10886.

Wu C, Venevsky S, Sitch S et al. (2017) Present-day and future contribution of climate and fires to vegetation composition in the boreal forest of China. Ecosphere, 8, e01917.

Wu MC, Knorr W, Thonicke K et al. (2015) Sensitivity of burned area in Europe to climate change, atmospheric CO2 levels, and demography: A comparison of two fire-vegetation models. Journal of Geophysical Research-Biogeosciences, 120, 2256-2272.

Xiao X, Boles S, Liu J et al. (2002) Characterization of forest types in Northeastern China, using multi-temporal SPOT-4 VEGETATION sensor data. Remote Sensing of Environment, 82, 335-348.

Yue C, Ciais P, Cadule P et al. (2014) Modelling the role of fires in the terrestrial carbon balance by incorporating SPITFIRE into the global vegetation model ORCHIDEE - Part 1: simulating historical global burned area and fire regimes. Geoscientific Model Development, 7, 2747-2767.

Yue X, Unger N (2018) Fire air pollution reduces global terrestrial productivity. Nature Communications, 9, 5413.

Zelazowski P, Huntingford C, Mercado LM et al. (2018) Climate pattern-scaling set for an ensemble of 22 GCMs – adding uncertainty to the IMOGEN version 2.0 impact system. Geoscientific Model Development, 11, 541-560.

Zhang LJ, Jiang LQ, Zhang XZ (2015) Spatially precise reconstruction of cropland areas in Heilongjiang Province, northeast China during 1900-1910. Journal of Geographical Sciences, 25, 592-602.

Zhu ZC, Piao SL, Myneni RB et al. (2016) Greening of the Earth and its drivers. Nature Climate Change, 6, 791-795.